CENTENNIAL-RESOLUTION PALAEOCEANOGRAPHY OF THE AEGEAN SEA; 15,000 BP – PRESENT

JAMES S. L. CASFORD

Submitted in partial fulfillment of the requirements for the Degree of Doctor of Philosophy

GRADUATE SCHOOL OF THE

SOUTHAMPTON OCEANOGRAPHY CENTRE

This PhD dissertation by

James Sebastian Lee Casford

has been produced under the supervision of the following persons

Supervisor/s

Dr. Eelco Rohling
Dr. John Thomson
Dr. Andrew Roberts
Dr. Ian Croudace

Chair of Advisory Panel

Dr. Andrew Roberts

Member/s of Advisory Panel

Dr. Eelco Rohling
Dr. John Thomson
Dr. Andrew Roberts
Dr. Ian Croudace
Dr. Rachel Mills

TABLE OF CONTENTS

ABSTRACT

This thesis provides detailed multi-proxy records from six sediment cores in the Aegean Sea and Levantine Basin, including high-resolution (1 cm to 0.5 cm) faunal records of planktonic foraminifera; stable isotope data for oxygen and carbon based on the same samples; and inorganic geochemistry records. The study interprets changes in palaeo-circulation as the result of climatic change, acting on several different time scales. This approach combines glacial inter-glacial warming, procession driven monsoon variation and cooling events acting on the 1450 year and 2300 year cycles.

It investigates longer-term variability during the Late Glacial and Holocene, in particular that associated with the deposition of the early Holocene dysoxic/anoxic sapropel S1. Concentrating on the onset of sapropel-forming conditions we identify the start of 'seasonal' stratification and highlight a lag in $\delta^{18}O$ response of the planktonic foraminifer *N.pachyderma* to Termination T1b as identified in the $\delta^{18}O$ record of *G.ruber*. By use of a simple model, it is determined that this offset cannot be a function of bioturbation effects. The lag is in the order of 1 kyr and suggests that isolation of intermediate/ deep-water preceded the start of sapropel formation by up to 1.5 kyr. Using this discovery, the author proposes an explanation for the major unresolved problem in sapropel studies, namely the source of nutrient supply required for export productivity to reach levels needed for sustained sapropel deposition. It is suggested that nutrients had been accumulating in a stagnant basin for 1 - 1.5 kyr and that these accumulated resources were utilized during the deposition of S1. In addition, the study provides a first quantitative estimate of the diffusive (1/e) mixing time scale for the eastern Mediterranean in its "stratified" sapropel mode, which is of the order of 450 years.

Using four high sedimentation-rate marine cores with suppressed bioturbation effects, recovered along the northern margin of the eastern Mediterranean. It is demonstrated that the study region, central to the development of modern civilisation, was substantially affected throughout the Holocene by a distinct cycle of cooling events on the order of 2 C-degrees. In the best-preserved cases the onset of these events appears particularly abrupt, within less than a century. The cooling events typically lasted several centuries, and there are compelling indications that they were associated with

increased aridity in the Levantine/NE African sector [Rossignol-Strick, 1995; 1998; Alley et al., 1997; Hassan, 1986; 1996; 1997a,b; McKimMalville et al., 1998]. Several of these episodes appear coincident with cultural reorganisations, with indigenous developments (eg. cattle domestication, new technologies) and population migrations and fusion of peoples and ideas [Hassan, 1986; 1996; 1997a,b; McKim Malville, 1998]. It is infered that climatic events of a likely high-latitude origin [O'Brien et al., 1995; Bond et al., 1997; Mayewski et al., 1997; Alley et al., 1997] caused cooling and aridity in and around the eastern Mediterranean via a direct atmospheric link, and therefore played an important role in the development of modern civilisation.

Comparing paleoclimate proxy records from central Greenland and the Aegean Sea the study offers new insights into the causes, timing, and mechanisms of Holocene atmosphere-ocean interactions. A direct atmospheric link is revealed between Aegean sea surface temperature (SST) and high latitude climate. The major Holocene events in our proxies of Aegean SST and winter/spring intensity of the Siberian High (GISP2 K+ record) follow an ~2300 year spacing, recognised also in the Δ14C record and in worldwide Holocene glacier advance phases, suggesting a solar modulation of climate. It is argued that the primary atmospheric response involved decadal-centennial fluctuations in the meridional pressure gradient, driving Aegean SST events via changes in the strength, duration, and/or frequency of northerly polar/continental air outbreaks over the basin. The observed natural variability should be accounted for in predictions of future climate change, and our timeframe for the Aegean climate events in addition provides an independent chronostratigraphic argument to Middle Eastern archaeological studies.

Using this data a method is developed to determine and optimise the confidence levels in marine, radiocarbon-based chronostratigraphies. A multi-parameter event stratigraphy dated by AMS ^{14}C, is developed based on highly resolved (centimetre to sub-centimetre) multi-proxy data. The applicability of this framework to the published, lower resolution records from the Aegean Sea is assessed. Subsequently the comparison is extended into the wider Eastern Mediterranean, using new and previously published high-resolution data from the N.E. Levantine and Adriatic cores. The study quantitatively determines that the magnitude of uncertainties in the intercore comparison of AMS datings based on planktonic foraminifera, to be of the order of ± 250 years in radiocarbon convention

ages. These uncertainties are related to syn- and post- sedimentary processes that affect the materials dated (e.g. bioturbation, re-deposition and resuspension). This study also offers a background age-control that allows for vital refinements to radiocarbon-based chronostratigraphy in the Eastern Mediterranean, with the potential for similar frameworks to be developed for any other well-studied region. This should lead to a significant advance in constraining the confidence limits in marine radiocarbon-based chronostratigraphies.

CHAPTER 1

1.INTRODUCTION

1.1 RATIONALE

1.2 AIMS

1.3 GEOGRAPHICAL SETTING

1.4 RESEARCH AREA AND CORE LOCATION

1.1 RATIONALE

Hopkins (1978) notes that the Aegean is the third major sea of the Mediterranean, with a volume of 7.4×10^4 km^3. While around a factor of ten smaller than the Levantine Basin, it is both deeper and larger than the Adriatic Sea. Despite this, the Aegean's palaeoceanographic history has received less attention than the rest of the Mediterranean. Recent climate driven changes in eastern Mediterranean deep-water circulation (Roether et al 1996) have highlighted the role of Aegean Deep Water (AeDW) and dramatically revised our understanding of the regions hydrology. In light of this the need to correct this omission has become increasingly obvious.

The sedimentary record in the Aegean Sea is particularly well suited for a high-resolution palaeoceanographic investigation. The high sedimentation rates give a detailed record and the small basin volume provides a rapid response to the climatic forcing. This provides an amplified amplitude proxy record, with high signal to noise ratio. The occurrence of the sapropel S1, characterized by darker sediment color and the near or total absence of benthos, further reduces the signal noise for this interval. The sapropel has also been recognized as a period of significantly differing hydrology and hence is ideally suited to the study of changing circulation.

This study looks at the signature of circulation patterns in the sedimentary record, during the last 15 ka BP and in particular at the onset of the S1 sapropel (Chapter 2). It identifies a sequence of millennial scale cool arid events during the Holocene (Chapter 3 and 4) and highlights the possible effects of these climatic variations on human populations and the development of modern civilization. A highly detailed chronostratigraphic model is developed for the Aegean Sea over the last 15 ka BP. This is highly applicable outside of the Aegean and subsequently used to determine confidence limits for marine AMS ^{14}C dating in the study region (chapter 5). Finally a synthesis is presented (chapter 6) highlighting the advances made in this investigation, providing an overview of palaeoceanographic development of the Aegean Sea from 15ka B.P. until the present, and proposing the direction for future study.

1.2 AIMS

- To develop a time stratigraphic framework for the Late Glacial to Holocene in the Aegean Sea
- Complete a high-resolution study of climatic change and palaeoceanography from marine cores.
- Assess the influence of early diagenetic processes on marine sediments in the study region.

1.3 GEOGRAPHICAL SETTING

The Aegean Sea (FIGURE 1.1) is one of the most complicated topographical areas of the Mediterranean (Maley and Johnson 1971). A peripheral basin, it is located to the North East of the Mediterranean Sea, between the Turkish Coast in the East, the Greek mainland to the North and West and by Crete to the South. It is connected to the larger Mediterranean via a number of passages between the Greek Mainland, the Peloponnesos, Crete, Rhodes and the Turkish coast. It is also linked northwards with the Sea of Marmara via the Dardanelles and thence to the Black Sea via the Bosporus.

The Aegean Sea itself consists of a series of basins separated by shallower plateau areas. These plateaux are normally associated with island arcs. The Cyclades Island Plateau for example, separates the Cretan Basin in the Southern Aegean from the Northern Aegean. All of the major basins of the Aegean are inter linked at a depth of at least 400m.

In addition much of the Mediterranean and the whole of the Aegean is tectonically active (Camerlenghi and Cita 1987), with both the Cyclades and the Cretan island arcs being volcanic in origin. The North Aegean Trough forms an extension of the Anatolian fault system (Lybéris 1984). Regular volcanic activity gives rise to a well-developed tephrachronology. This provides both additional dating and

synchronous correlatable horizons in some cores.

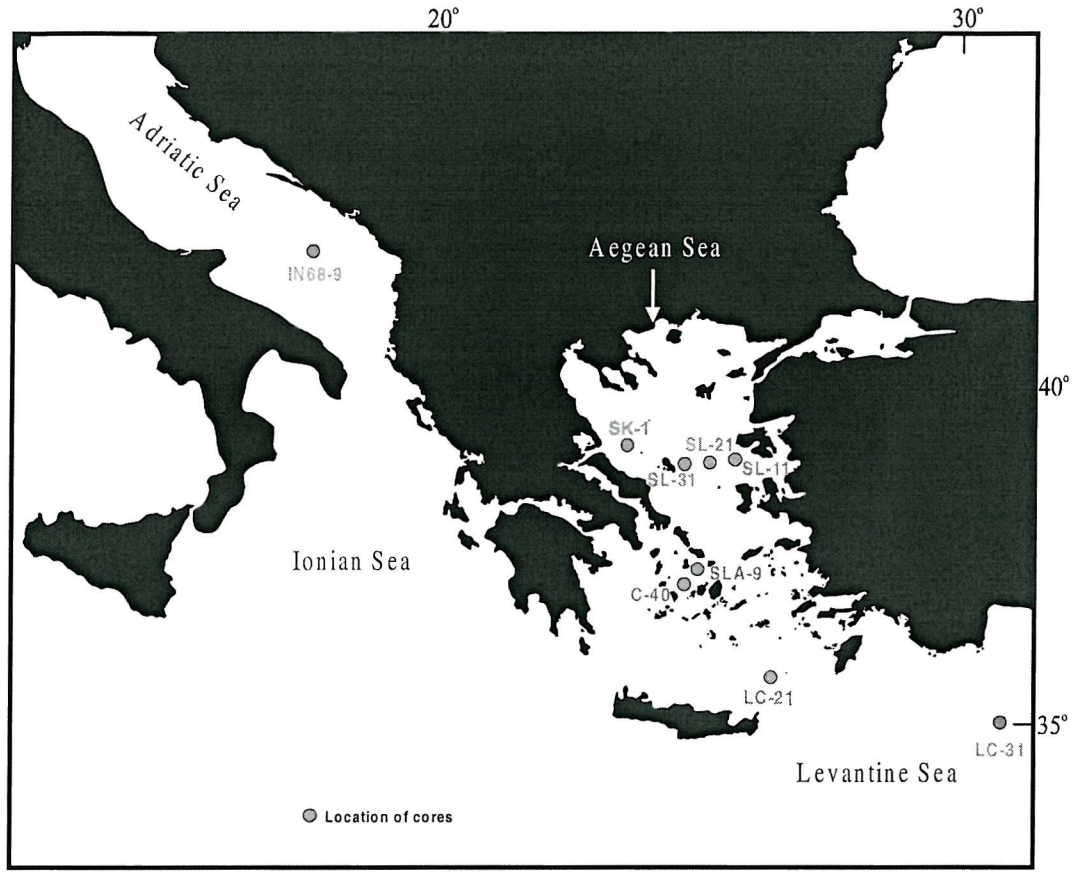

FIGURE 1.1 Mediterranean Map showing spatial distribution of cores in this study, LC-21 is shown [after Rohling et al.1999, Hayes et al. 1999].

1.4 RESEARCH AREA AND CORE LOCATION

This investigation is limited to the period from the Last Glacial Maximum to the Present. Considerable attention is paid to the interval representing the early Holocene sapropel (S1). The study comprises data collected from eight sediment cores (see TABLE 1.1.), for which summary graphic logs are shown in FIGURE 1.2. Material was collected from the Aegean Sea on two separate cruises by R.V. Aegeo in May 1998 and April 1999, the latter as part of the E.C. MATER project. R.V. Marion

Dufresne Cruise 81 recovered the longer piston cores (LC) from the Levantine basin and the Cretan Sea, 17th January - 9th February 1995 as part of the EC-MAST2 program PALAEOFLUX. Core LC-21 from the Cretan Sea was previously studied by Hayes et al. [1999], De Rijk et al [1999], Mercone et al. [2000, 2001].

CORE	Type of Core	Length (cm)	Depth below sea level (m)	Co-ordinates
LC-21‡	Piston	-	1522 m	35°40'N, 26°35'E
LC-31	Piston	-	2298 m	34°60'N, 31°10'E
SL-11	Gravity	209 cm	258 m	39°06'N, 25°48'E
SL-21	Gravity	273 cm	317 m	39°01'N, 25°25'E
SL-31	Gravity	251 cm	430 m	38°56'N, 25°00'E
SLA-9	Gravity	286 cm	260 m	37°31'N, 24°33'E
MNB-3	Gravity	392 cm	798 m	39°13'N, 24°59'E
SPR-3	Gravity	96 cm	374 m	39.04°N, 23.94°E

TABLE 1.1 Core Location and type. ‡[Hayes et al. 1999, De Rijk et al 1999, Mercone et al. 2000, Mercone et al. 2001, Casford et al. 2001b, and Rohling et al. 2001].

The studied cores consist predominantly of light gray-brown hemipelagic sediments with intercalated dark olive gray sapropel sediments. All of these sediments are rich in micro- and nanno-fossils. The data presented in this thesis while predominately the work of the author, is the result of a multi-proxy study involving several team members. Details of the analyses undertaken and by whom, is presented in TABLE 1.2

Core	planktonic fauna	stable isotopes	XRF	ICP	Palaeo magnetism
LC-21	AH	AH/CDF/JSLC	-	DM	-
LC-31	JSLC	JSLC	JSLC	-	-
MNB-3	-	-	-	JT	JSLC
SL-31	RHAZ	RHAZ/JSLC	-	JT	JSLC
SL-21	JSLC	JSLC	-	-	JSLC
SL-11	JSLC	JSLC	-	-	JSLC
SPR-3	-	-	-	-	JSLC
SLA-9	CF/JSLC	CF	-	JT	JSLC

AH = A. Hayes CDF = C. deFries CF = C. Fontanier
JT = J. Thomson RHAZ = R. Abu-Zied JSLC = the author (J. Casford)

TABLE 1.2 Analyses preformed by core and researcher.

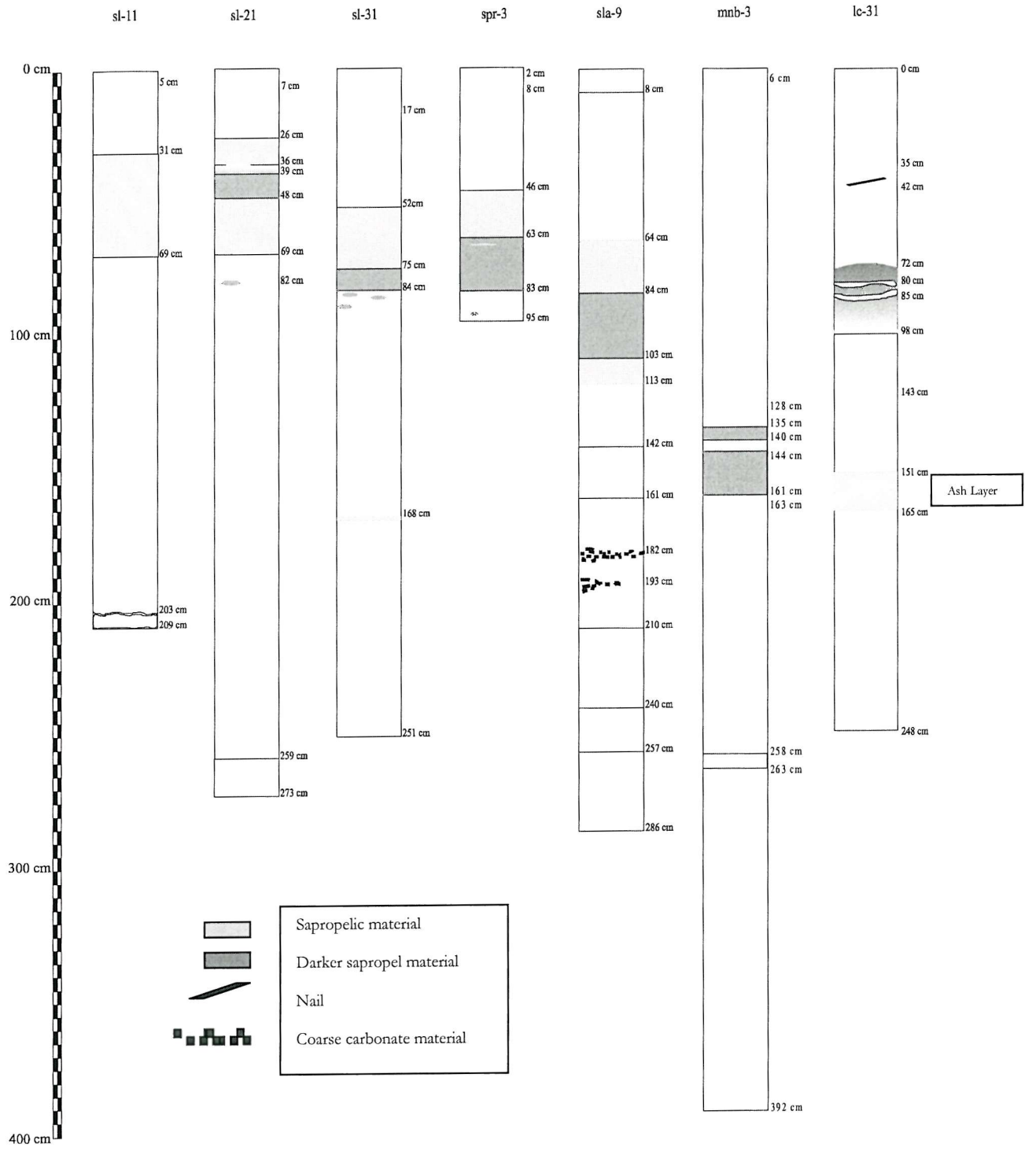

FIGURE 1.2 graphic log of cores in the study. Taken from original log made on opening cores, showing visual boundaries. Solid lines indicate a sharp boundary, with dotted line the approximate position of more gradual changes. Core LC-31 represents the top two sections of a longer piston core. Shaded areas represent darker coloured material, and show the extent of the visible sapropel. Details for core LC-21 are available in Hayes et al. [2000]. See appendix for individual logs.

CHAPTER 2

IN PRESS, PALEOCEANOGRAPHY (2001). AUTHORED BY

Casford[1].J.S.L., Rohling[1] E.J., Abu-Zied[1] R., Cooke[1] S., Fontanier[2] C., Leng M[3]., and Lykousis[4] V..

[1] *School of Ocean and Earth Science, Southampton University, Southampton Oceanography Centre, European Way, Southampton, SO14 3ZH, UK.*

[2] *Department of Geology and Oceanography, Bordeaux University, UMR 58-05, Avenue des Facultes, 33405 Talence cedex, France.*

[3] *Natural Environment Research Council Isotope Geoscience Laboratory, Keyworth, UK..*

[4] *National Centre for Marine Research, Athens, Greece.*

2. CIRCULATION CHANGES AND NUTRIENT CONCENTRATIONS IN THE LATE QUATERNARY AEGEAN SEA:

A NON-STEADY STATE CONCEPT FOR SAPROPEL FORMATION.

2.1 ABSTRACT

The Modern Aegean Sea is an important source of deep-water for the Eastern Mediterranean. Its contribution to deep-water ventilation is known to fluctuate in response to climatic variation on a decadal time scale. This study uses marine micropalaeontological and stable isotope data to investigate longer-term variability during the Late Glacial and Holocene, in particular that associated with the deposition of the early Holocene dysoxic/anoxic sapropel S1. Concentrating on the onset of sapropel-forming conditions we identify the start of 'seasonal' stratification and highlight a lag in $\delta^{18}O$ response of the planktonic foraminifer *N. pachyderma* to Termination T1b as identified in the $\delta^{18}O$ record of *G. ruber*. By use of a simple model, we determine that this offset cannot be a function of bioturbation effects. The lag is in the order of 1 kyr and suggests that isolation of intermediate/ deep-water preceded the start of sapropel formation by up to 1.5 kyr. Using this discovery, we propose an explanation for the major unresolved problem in sapropel studies, namely the source of nutrient supply required for export productivity to reach levels needed for sustained sapropel deposition. We suggest that nutrients had been accumulating in a stagnant basin for 1 - 1.5 kyr and that these accumulated resources were utilized during the deposition of S1. In addition, we provide a first quantitative estimate of the diffusive (1/e) mixing time scale for the eastern Mediterranean in its "stratified" sapropel mode, which is of the order of 450 years.

2.2 INTRODUCTION

The present day Aegean Sea (figure 1) is an important source of deep water for the Eastern Mediterranean [Lacombe et al. 1958, Miller 1963, Roether et al 1996 and Lascaratos et al. 1999]. Aegean Intermediate Water (AeIW) is derived from Levantine Intermediate Water (LIW), with its source in the Rhodes Gyre. As this travels north along the Turkish Coast, prevailing offshore winds allow upwelling of the intermediate water to the surface [Lascaratos 1989, Yüce 1995]. In these shallow eastern shelf areas, the AeIW consequently forms a single uniform water-mass from the surface to the sea floor. As the upwelled AeIW progresses northwards, its salinity continues to increase due to evaporation. Winter winds across the Athos Basin (Figure 1) in the far north

further enhance the salinity of AeIW and this together with winter cooling, increase its density. This buoyancy loss drives the formation of Aegean Deep-Water (AeDW) [Bruce and Charnock 1965, Burman and Oren 1969, Theocharis 1989, Yüce 1995]. Today AeDW settles in the deeper parts of the Aegean Basin, below 300m. Traditionally AeDW formation was considered of minor importance to the deep-water ventilation of the open Eastern Mediterranean [Wüst 1961]. However, recent studies show that specific (cold) climatic forcing over the Aegean has throughout the 1990s caused AeDW to replace Adriatic Deep Water (ADW) as the main deep water in the open Eastern Mediterranean [Roether et al. 1996, Samuel et al. 1999]. The Aegean's rapid response to atmospheric forcing makes it an ideal case study for the analysis of deep-water formation and its relationship with climatic change.

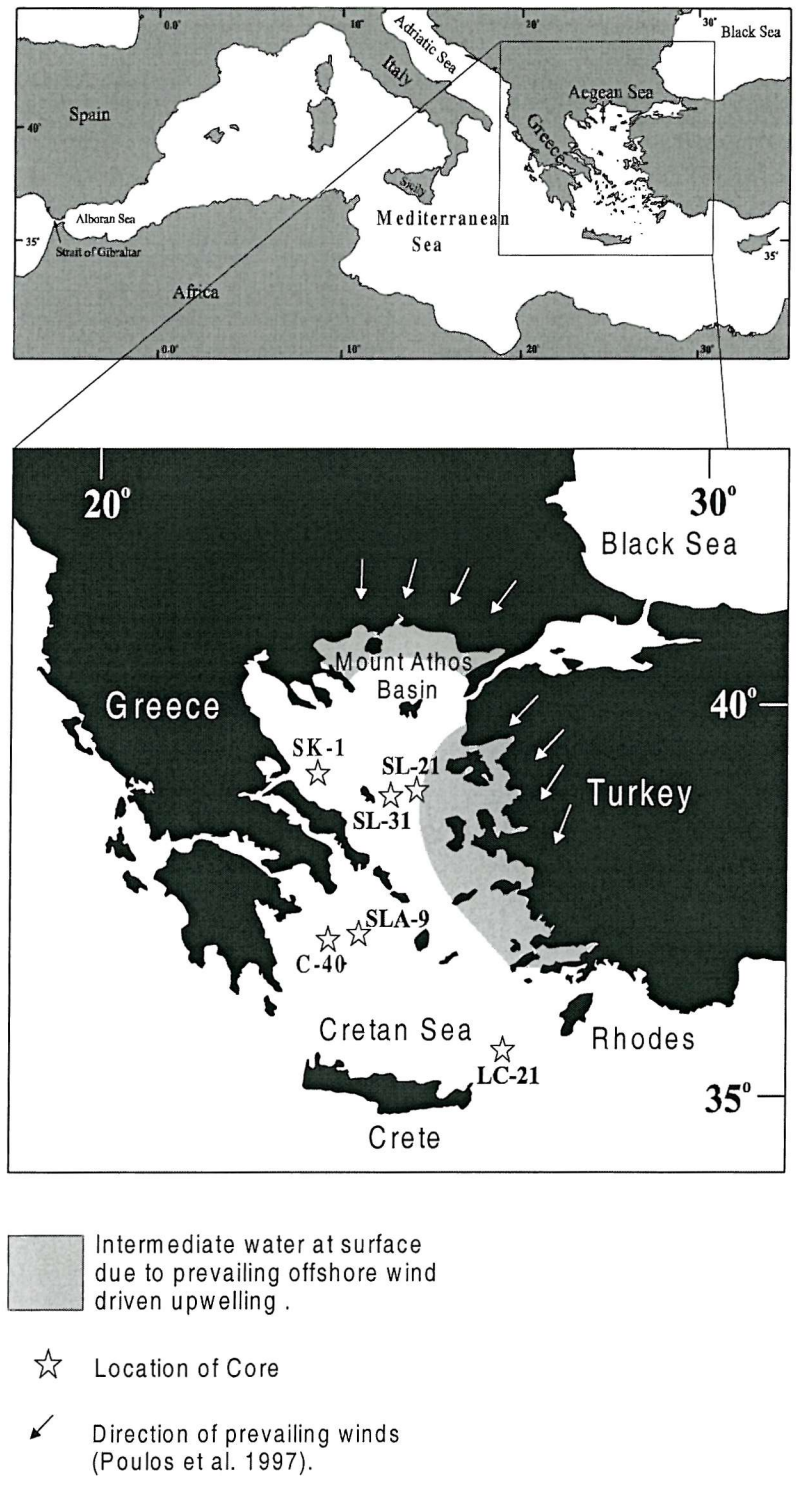

Figure 1. Location map illustrating the core positions for SL-31 (water depth 430 m), SL-21 (317 m), SLA-9 (250 m), and LC-21 (1520 m). The hatched area represents the approximate area of AeIW upwelling to the surface. This water-mass extends from the surface to ~200m depth in the shallow shelf areas off the Turkish coast (Theocharis 1989, Yuce 1995, Poulos et al. 1997].

Dramatic deep-water ventilation changes, on longer time scales, are also witnessed in the sedimentary record of the Mediterranean, by the presence of sapropels. These dark organic-rich layers are found throughout the Eastern Mediterranean. Sapropel formation is related to slow-down of deep-water ventilation in response to climate related reductions in buoyancy loss [Rossignol-Strick et al. 1982, Jenkins and Williams 1983, Rossignol-Strick 1983, 1985,1987, Parisi 1987, Cramp and Collins 1988, Cramp et al. 1988, Perissoratis and Piper 1992, Rohling 1994]. These reductions are thought to be caused by changes to much wetter climatic conditions at times of increased Northern Hemisphere insolation (precession cycle minima) [Rossignol-Strick et al. 1982, Rossignol-Strick 1983, 1985, Rohling and Hilgen 1991, Hilgen 1991, Lourens et al. 1996]. In addition to suppression of deep-water production, sapropel formation has also been associated with increases in export productivity [Rohling and Gieskes 1989, De Lange et al. 1990, Rohling 1991, 1994, Thomson et al. 1995, Cramp and O'Sullivan 1999].

Modeling of circulation during deposition of the most recent, Holocene, sapropel (S1) has suggested that relatively small increases in surface buoyancy can lead to suppression of deep-water circulation in the E. Mediterranean. An increase of 20-30% in the freshwater budget is thought to be enough to allow interruption of deep-water production [Myers et al.1998, Rohling and De Rijk 1999, Rohling et al. 1999b]. Using the Myers [Myers et al. 1998] circulation model, the biogeochemical implications of sapropel formation have been assessed [Stratford et al. 2000]. Preserving the anti-estuarine circulation of the eastern Mediterranean, and using a three fold increase in river inputs [after Kallel et al. 1997], organic fluxes in coastal regions and marginal basins were found to approach the required levels for sapropel deposition [Stratford et al 2000].

The model of Stratford et al [2000] highlights a common problem recognized in all current models for sapropel formation, with emphasis on the much studied and well-dated S1: "Where did the nutrients come from to sustain organic matter burial over the ~3 kyr of S1 deposition in the eastern Mediterranean?" It appears that steady-state models cannot import sufficient nutrients into the basin, outside of the coastal regions and marginal seas, to sustain this accumulation. The steady-state models assume that nutrients lost via Corg burial are continuously balanced by fluvial/aeolian influxes. We here present evidence to suggest that the steady-state approach is seriously flawed, in

that a significant period of potential nutrient accumulation in a stagnant basin may have preceded the actual sapropel deposition

We use abundance variations of planktonic foraminifera together with species-specific oxygen and carbon stable isotope ratios in these forams to derive a picture of the oceanographic processes leading up to, during and after the most recent sapropel deposition in the Aegean. We observe a conspicuous change in hydrography, starting ~6 kyr prior to S1. We validate our observations with a simple bioturbation model and use the validated records to suggest that long-term (1.5 kyr) storage of nutrients may have occurred in the Aegean basin. When this reservoir became available for production, the formation of S1 commenced.

2.3 METHODS AND MATERIALS

We present results for two gravity cores from the Northern Aegean Basin (SL-21 and SL-31) and an additional gravity core (SLA-9) together with one piston core (LC-21) from the Southern Aegean (figure 1). All four cores are comprised of microfossil-rich hemipelagic ooze, with a clearly defined darker band of sapropelic material.

Each core was sampled in a continuous sequence, SL-21, SL-31 and SLA-9 at 0.5cm intervals and LC-21 at 1cm intervals. The samples were freeze dried, weighed and selected (weighed) sub-samples were disaggregated and wet sieved using de-mineralized water. The sieved fractions were collected on 600, 150, 125 and 63μm mesh sizes. The >150μm fractions were sub-divided using a random splitter to provide an aliquot of about 200 individual planktonic foraminifera. These were then determined and sorted on Chapman slides, and counted. Results were obtained as numbers g^{-1} and as percentages (Figure 2).

Several AMS radiocarbon dates were obtained for cores LC-21, SLA-9 and SL-31 using only hand-picked clean planktonic foraminiferal tests with no evidence of pyritisation or overgrowth. The samples were too small for monospecific dating, but no systematic differences would be expected for such dates relative to our results [cf.

Jorissen et al. 1993 comparison of planktonic versus benthic dating). The picked material was submitted for analysis at the NERC radiocarbon laboratory at SURRC (LC-21) and at the Leibniz AMS Laboratory at Kiel (Germany) (SLA-9, SL-31). Radiocarbon convention ages obtained were calibrated using the marine mode of the program Calib 4.2 [Stuiver and Reimer 1993]. A reservoir-age correction of 149 ± 30 years for the Aegean was used [Facorellis et al. 1998]. The results are listed in Table 1. All ages in this paper are reported in calibrated ka BP unless otherwise stated.

	Sample code	median depth	conventional Age	+/-	cal yrs BC	cal yrs BP	+/- σ
LC-21	CAM-41314	50	3370	60	1070	3020	100
	CAM-41313	95.5	4290	60	2260	4210	100
	CAM-41311	137.5	5590	60	3890	5840	90
	CAM-41315	161.5	7480	60	5830	7780	70
	CAM-41312	174.25	8120	60	6450	8400	60
	AA-30364	179.5	9085	65	7590	9540	320
	AA-30365	209	11765	80	11190	13140	370
	CAM-41316	242.5	14450	60	14610	16560	240
SL-31	KIA9467	51.75	6515	45	4870	6820	70
	KIA9468	65.75	7950	60	6330	8280	80
	KIA9469	84.25	9330	60	7870	9820	150
	KIA9470	91	9990	55	8650	10600	380
	KIA9471	126.25	14650	80	14840	16790	250
SLA-9	KIA9472	60.5	5950	45	4260	6210	50
	KIA9473	71.5	6445	55	4790	6740	70
	KIA9474	83.25	7900	45	6240	8190	70
	KIA9475	99.5	8400	50	6820	8770	120
	KIA9476	120.5	11910	70	11220	13170	350

Table 1. Dating calibration. Dating on LC-21 is after Mercone et al. (2000]. Samples with codes starting CAM were prepared as graphite targets at the NERC radiocarbon laboratory and analysed at the Lawrence Livermore National Laboratory AMS facility. Sample codes AA were prepared at Scottish Universities Reactor Research Centre at East Kilbride and analysed at the Arizona Radiocarbon Facility. KIA sample codes indicate the Leibniz AMS Laboratory at Kiel. Radiocarbon dating was calibrated using CALIB 4.2 after Stuiver and Reimer (1993] and using the marine data set (Stuiver et al.1998]. A reservoir age correction (ΔR) of 149 ± 30 years was used (Facorellis et al. 1998].

Detailed stable oxygen and carbon isotope records have been constructed for individual planktonic foraminiferal species in cores LC-21, SLA-9, SL-21 and SL-31, with resolutions in the order of 1cm (Figure 3). The species chosen were; the very shallow, surface dwelling *Globigerinoides ruber*; the deeper dwelling *Globorotalia inflata* associated with deep (winter) mixing; and the deep living species *Neogloboquadrina pachyderma* which has been associated with the Deep Chlorophyll Maximum at the base of the euphotic layer. This selection follows global and specific Mediterranean habitat descriptions in [Hemleben et al 1989, Pujol and Vergnaud-Grazzini 1995, Rohling et al. 1993a, 1995, 1997, De Rijk et al. 1999 and Hayes et al. 1999]. The analyses were performed at two separate inter-calibrated facilities; the Europa Geo 20-20, with individual acid bath preparation, at the Southampton Oceanography Centre (SOC); and the VG-Optima with a common acid bath preparation, at NERC Isotope Geoscience Laboratory (NIGL), Keyworth. Isotope results are reported as ‰, standardized to Vienna Pee Dee Belemnite. Machine error is in the order of < 0.06 ‰(std).

2.4 RESULTS

PLANKTONIC FORAMINIFERA

Five distinct assemblages were identified in this study (figure 2). The main boundaries equate well with the previously identified biozonal boundary II/III, and biozonal boundary I/II [Jorissen et al 1993] and this nomenclature is used. The three remaining assemblages consist of sub-divisions of biozone I of Jorissen et al. [1993]. Relevant Mediterranean habitat characteristics have been summarized in Rohling et al. [1993a,b, 1995,], Pujol and Vernaud-Grazzini [1995], De Rijk et al. [1999] and Hayes et al. [1999]. From old to young we identify the following five assemblages:

III). An assemblage dominated by *N.pachyderma* and *Turborotalita quinqueloba*, with lower densities of *Globorotalia scitula* and *Globigerinita glutinata*, and a generally low to very low abundance of *G.ruber*. This fauna dominates the cool "glacial" intervals.

II) An intermediate assemblage characterized by presence of *T. quinqueloba*, somewhat enhanced numbers of *N. pachyderma* and *G. glutinata* especially in the central Aegean cores, and the presence of *G. ruber* and *G. inflata.*

I) An assemblage dominated by the warm subtropical species *G.ruber* and the SPRUDTS group (including but not requiring *Globigerinella **s**iphonifera, Hastigerina **p**elagica* (absent in the Aegean), *Globoturborotalita **r**ubescens, Orbulina **u**niversa, Globigerinella **d**igitata, Globoturborotalita **t**enella* and *Globigerinoides **s**acculifer*, cf. Rohling et al. 1993a,b]. In addition it includes abundant *Globigerina bulloides* and somewhat increased *T. quinqueloba* compared with the preceding assemblage *II. Ic)* is characterized by elevated absolute and relative abundances of the pink morphotype, *G. ruber* rosa. A peak in *G. inflata* is also present at the base of this assemblage, followed by a marked absence in this species in the remainder of *Ic.* Core LC-21 shows an interruption in assemblage *Ic* with a return to a fauna resembling assemblage *II*, which corresponds to an "interruption" of the darker coloured sapropel [Hayes et al.1999, DeRijk et al. 1999, Mercone et al. 2000]. *Ib* and *Ia* are diverse assemblages dominated by *G.ruber* and *G.bulloides*, with SPRUDTS, *G. inflata* and *G. glutinata. Ib)* is characterized by elevated numbers of *G.inflata* and appears to be of short duration. *Ia)* shows a fauna similar to that seen in the present-day Mediterranean [core top data Thunell 1978]. Assemblage *Ia* shows slightly lower abundances of "warm" preferring species than assemblage *Ic.*

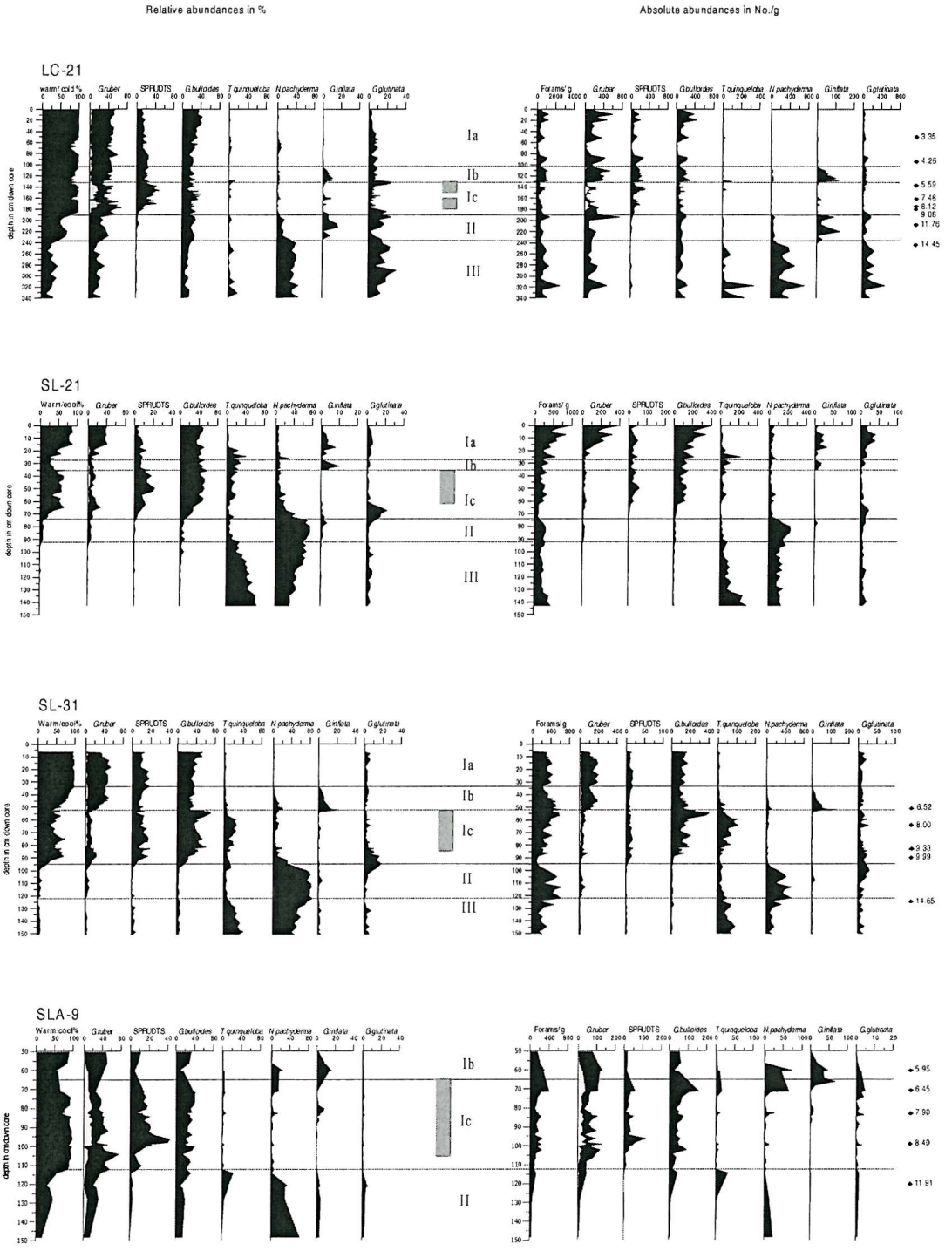

Figure 2. Relative and absolute abundances of planktonic foraminifera in cores SLA-9, SL-21, SL-31 and LC-21. The vertical gray box indicates the extent of the benthic sapropel, identified from the presence of low oxygen tolerant benthic foraminifera and/or total absence of benthic fauna that is equated with truly anoxic bottom waters (Fontanier 2000]. Warm/cold plots are %warm species /(%warm + % cold), following the method of Rohling et al. (1997]. The previously defined biozonal boundaries *I/II* and *II/III* are also shown (Jorissen et al.1993]. White curve under *G. ruber* gives abundances of *G. ruber* rosa. All dates in this figure are expressed as uncalibrated radiocarbon convention ages (ka BP), uncorrected for reservoir effect, detailed in table 1.

STABLE ISOTOPES

Combination plots of the mono-specific isotopic profiles of $\delta^{18}O_{ruber}$, $\delta^{18}O_{inflata}$ and $\delta^{18}O_{pachyderma}$ (figure 3) show several distinct, previously unreported features:

Oxygen isotopes initially show a high degree of synchronicity, being similar in value and variation. This is followed by a depletion in $\delta^{18}O_{ruber}$ that separates it from the unaffected signal of *N. pachyderma.* This first separation between $\delta^{18}O_{ruber}$ and $\delta^{18}O_{pachyderma}$ coincides with the biozonal boundary *III/II* and corresponds in age with glacial termination T1a. After a short interval of little change $\delta^{18}O_{ruber}$ shows a second rapid depletion to its typical Holocene values while $\delta^{18}O_{pachyderma}$ remains at pre-Holocene values or even shows an enrichment. This enrichment, while generally small is well within the sensitivity of our equipment and must be regarded as real. It is most obvious in cores SLA-9 (0.8‰ over 5 samples), SL-21 (0.5‰ over 10 samples) and SL-31 (0.4‰ over 4 samples), while the available resolution leaves the signal in LC-21 inconclusive in this respect. The $\delta^{18}O$ signal of *G.inflata* shows an inflection to lighter values at the same time as this second depletion in $\delta^{18}O_{ruber}$, while the absolute $\delta^{18}O_{inflata}$ values remain intermediate between those of $\delta^{18}O_{ruber}$ and $\delta^{18}O_{pachyderma}$. This second sharp depletion in $\delta^{18}O_{ruber}$ equates with termination T1b. Finally after a period in the order of ~1kyr the values of $\delta^{18}O_{pachyderma}$ also start depleting to this species' Holocene values.

Shortly after the start of the depletion in $\delta^{18}O_{pachyderma}$ to Holocene values, we observe a general depletion in $\delta^{13}C$. The $\delta^{13}C$ records show an initial synchronous drop in both $\delta^{13}C_{ruber}$ and $\delta^{13}C_{pachyderma}$, which is followed in SL-21, SL-31 and SLA-9 by a separation of values as $\delta^{13}C_{pachyderma}$ continues to deplete after $\delta^{13}C_{ruber}$ has leveled out. This separation in the $\delta^{13}C$ records coincides with the onset of sapropel deposition.

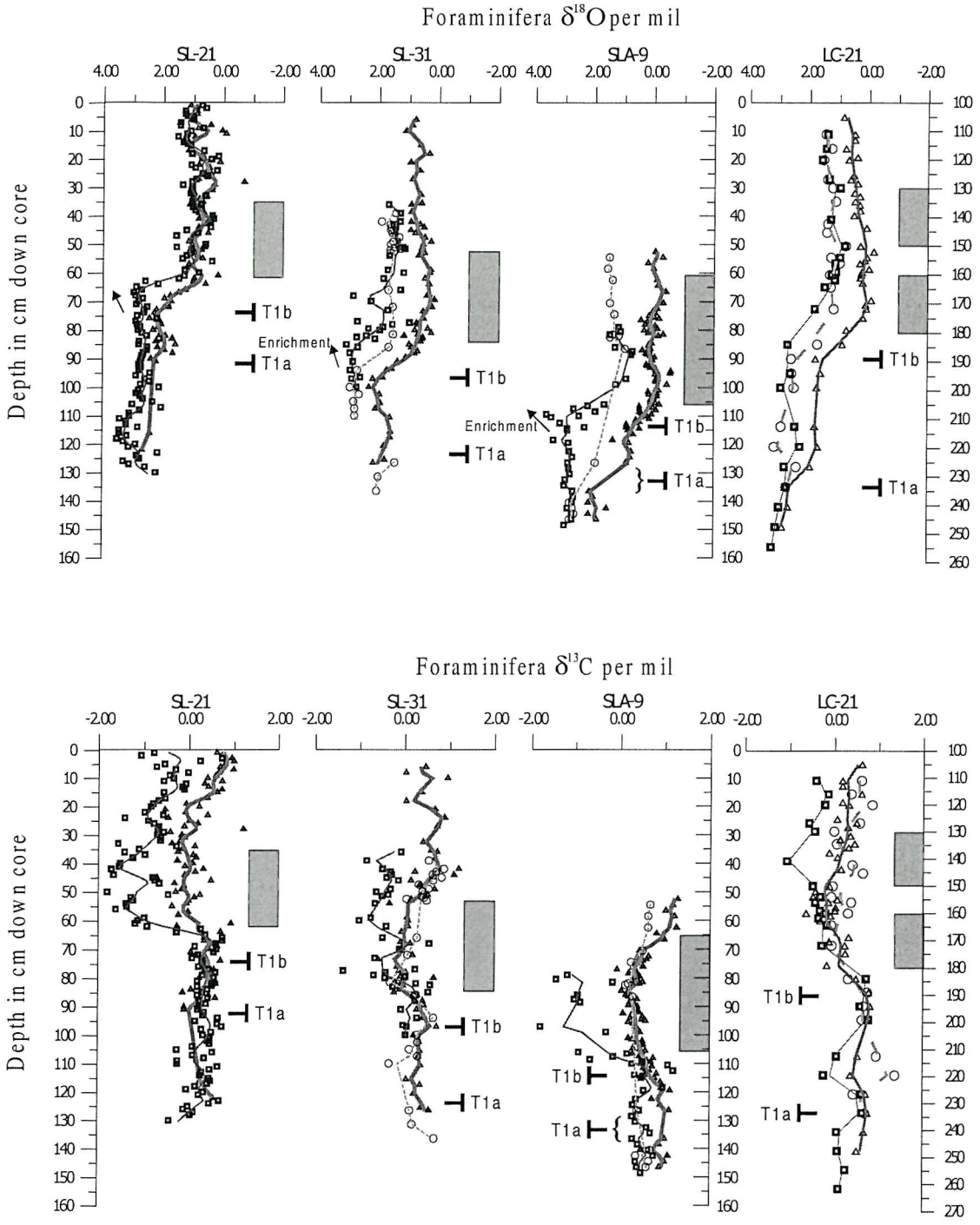

Figure 3. Stable isotope data, showing $\delta^{18}O$ and $\delta^{13}C$ versus depth, for *G.ruber* (heavy gray line with triangles), *N.pachyderma* (lighter black line with squares) and *G.inflata* (dashed line with circles) in cores SLA-9, SL-21, SL-31 and LC-21. The superimposed lines represent a 10cm running gaussian smoothing of the data. The gray shaded boxes represent the extent of the sapropel as defined by the switch from oxygen requiring benthic foraminifera, to the presence of low oxygen fauna or in the case of LC-21, the total absence of benthic forams. Glacial terminations T1a and T1b are also shown. Arrows on $\delta^{18}O$ plots of SL-21, SL-31 and SLA-9 indicate enrichment trends in $\delta^{18}O_{pachyderma}$. All values are in per mil, versus Vienna Pee Dee Belemnite (‰VPDB) and calibrated with standards NBS18 and 19.

2.5 BIOTURBATION MODEL

The offset in the isotopic responses for $\delta^{18}O_{ruber}$ and $\delta^{18}O_{pachyderma}$ around T1b is conspicuous and we need to assess whether this is a genuine feature or the result of bioturbation. Due to the rapid fall in numbers of *N.pachyderma* before the depletion, bioturbation might mix a relatively large proportion of undepleted foraminifera with the comparatively few depleted forams. This could potentially shift the resultant isotopic composition to less depleted values. To test whether such processes could explain the observed trends we developed a simple model, which assumes a hypothetical step change in the isotopic compositions of both *G.ruber* and *N.pachyderma* at the same point in time. The model then simulates a progressive homogenization (bioturbation) of each successive 0.5cm of deposited sediment with the previous 5cm or 10cm (separate model runs). Two versions of this simulation were run. An extreme version based on a large step-change in numbers, of both *G.ruber* and *N.pachyderma* at the same point as the isotopic shift and a run based on the actual numbers observed for these species. The results of the bioturbation model are shown in figure 4.

All simulations smoothed the imposed step-like $\delta^{18}O$ change into more gradual depletions similar to those seen in the sedimentary record, with differences in the profiles for the two species. However, in all cases the inflection point for the $\delta^{18}O$ values of both species is the same, with both values start to deplete at the same point. This differs markedly from the observed data with a separation in the inflection points of these species by upto >15cm. Only in our most-extreme scenario do we approach the real data, with a lag in the order of 5-10 cm, although even here the infection points appear synchronous on closer observation. The models also totally failed to reproduce the enrichment trend in *N.pachyderma* (5-10 data points) that is seen in the actual data, during the major depletion in *G.ruber* (this is most clearly seen in cores SL-21, SL-31 and SLA-9).

The bioturbation model leads us to suggest that the actual $\delta^{18}O$ depletion may have been more step-like than is preserved in the sedimentary record. We also deduce that the

offset in inflection points seen in our cores reflects a real change in isotopic gradients within the water column during this period.

Interestingly the signal from *G.inflata* does appear to parallel the *N.pachyderma* signal shape seen in our model. It too sees a marked decline in numbers over the period of isotopic depletion. This signal may therefore provide an indication of the strength of bioturbation below the sapropel, suggesting that homogenization of foraminiferal sized particles due to bioturbation was less than 5cm. This would agree with observations in the faunal counts where species *N.pachyderma*, *G.inflata* and *G.glutinata* fall abruptly to zero in between consecutive samples at 2.5cm spacing.

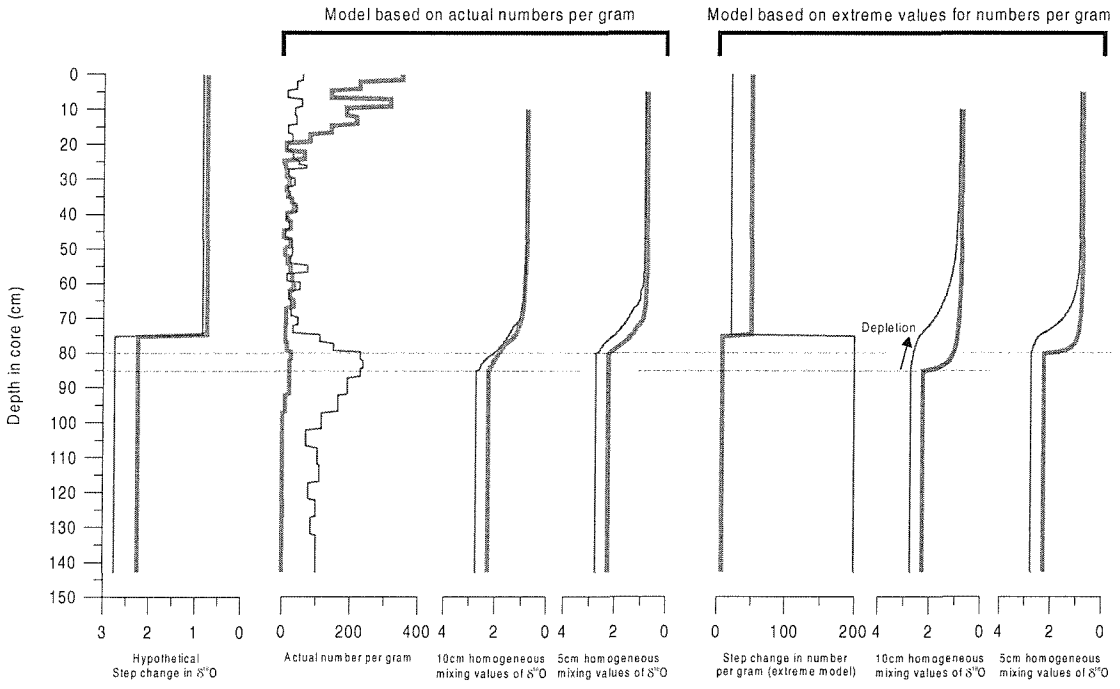

Figure 4. The Bioturbation model illustrates the smoothing of a hypothetical stepped change in isotopic values (left panel) with a progressive homogenisation to simulate bioturbation effects. This includes two runs of the model. 1) Based on the actual numbers per gram of *G.ruber* (heavy gray line) and *N.pachyderma* (lighter black line) found in core SL-21. 2) Based on an hypothetical extreme step-change in numbers per gram, with this change, taking place at the same point as the step-change in isotopic value. Each version was run with a 5cm and a 10cm homogenisation and these are plotted adjacent to each other for comparison. The horizontal tie lines (dotted) highlight the timing of the inflections in the derived $\delta^{18}O$ records.

2.6 DISCUSSION

Changes in stable isotope composition have led to considerable speculation on the variability of Mediterranean fresh-water budgets [Huang and Stanley 1972, Cita et al. 1977, Ryan and Cita 1977, Williams et al. 1978, Rossignol-Strick et al. 1982, Thunell et al. 1989, Kallel et al 1997, Rohling and De Rijk 1999]. Recent work points out that oxygen isotopic ratios from planktonic foraminifera cannot be used to determine absolute salinities in any straightforward way, on geological time scales. Rather they show responses to hydrographic changes that may be several times greater than the corresponding changes in conservative properties, i.e. salinity [Rohling and De Rijk 1999, Rohling 1999a,b]. Such problems associated with temporal gradients are avoided in comparisons of isotopic compositions of different species within an individual sample, since foraminifera are then analysed from an area in a single hydrological regime. Thus, differences in the signal between species will reflect real, contemporaneous differences between their preferred habitats.

We propose that our multi-proxy records are best interpreted in combination with the foraminiferal abundance records, as a series of successive changing, climatically driven, dynamic regimes. These are illustrated as a series of transitory states together with a schematic summary of the main isotopic and faunal changes recognised in our Aegean records (figures 5,6). Each state represents a single point in time, which may be considered typical of the particular climatic/circulation regime. These transitory states are described in detail below.

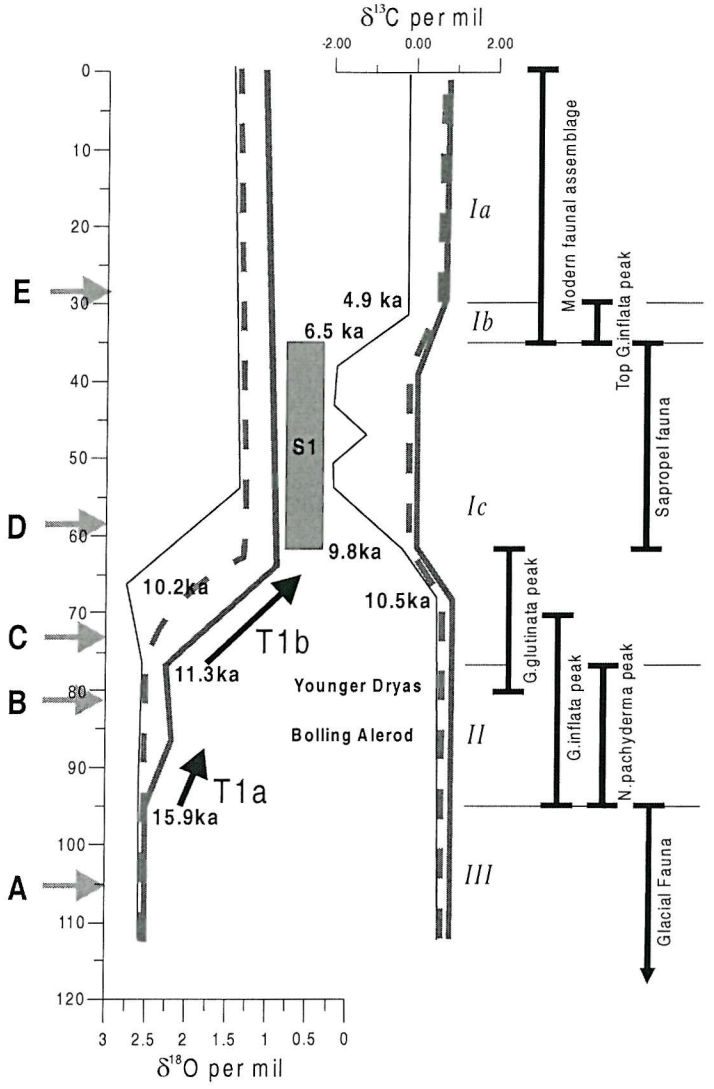

Figure 5. Summary of major changes in isotopic signals $\delta^{18}O$ and $\delta^{13}C$. The heavy gray line indicates $\delta^{18}O_{ruber}$, lighter black line $\delta^{18}O_{pachyderma}$ and the dashed line $\delta^{18}O_{inflata}$. Depth scale is based on core SL-21 and the vertical gray box indicates the extent of the benthic foraminiferal defined sapropel. Bold letters refer to state summaries in Figure 5. All dates are expressed as calibrated radiocarbon convention ages, corrected for reservoir effect (ka BP) and derived from average ages for the event from cores in this study (Table 2). The hatched area of dysoxic water may be truly anoxic at greater depths (eg LC-21 1500m). The positions of the Younger Dryas and the Bölling Alerød are also indicated.

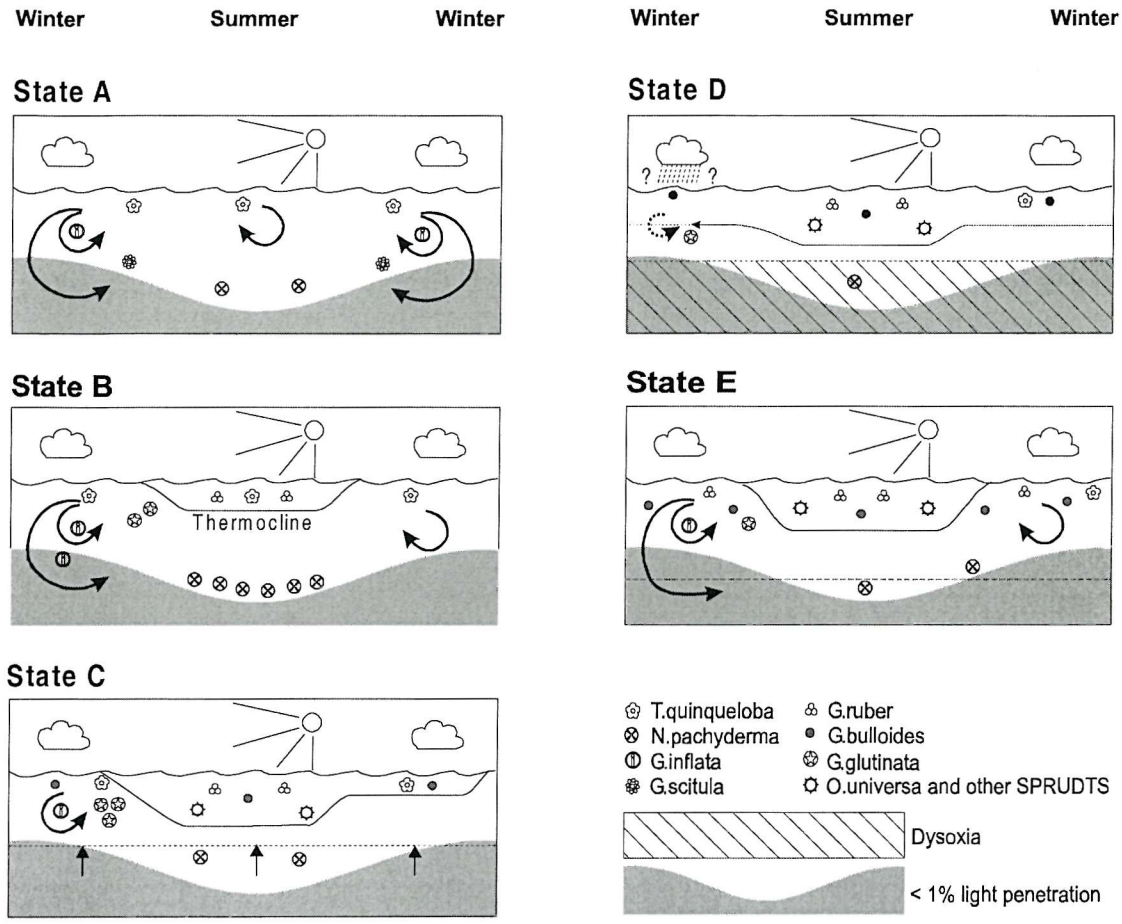

Figure 6. Schematic reconstruction of the history of Aegean circulation. The states illustrated are transitory and this schematic represents the typical changes in deep-water mixing and faunal distribution in the Aegean, since the last glaciation. The timing of these transitions and placement of these typical assemblages is summarized in Figure 5

STATE A

State A is interpreted as typical of the glacial Aegean Sea. This state is characterised by the absence of warm mixed-layer species. We observe coinciding values of $\delta^{18}O_{ruber}$ and $\delta^{18}O_{pachyderma}$, as well as $\delta^{13}C_{ruber}$ and $\delta^{13}C_{pachyderma}$ suggesting that there were no isotopic gradients between these shallow and sub-surface living species. Thus it is deduced that the water column during state A comprised of a single homogenised water mass, with intermediate water undistinguished from surface water. The presence of *G.inflata* is regarded as indicative of deep seasonal mixing and is hence shown in association with

winter mixing [Hemleben et al. 1989, Rohling et al. 1995 and Pujol and Vergnaud-Grazzini 1995; summarised in Rohling et al. 1993a and Reiss et al.2000]. The faunal assemblage comprised of predominantly cool-water species, with only very rare occurrences of the warm dweller *G.ruber*. *T.quinqueloba* is shown as the principal surface dweller [cf. Rohling et al 1993]. *G.scitula* and *N.pachyderma* are shown living at depth. *N.pachyderma* is known to thrive at or just above the base of the euphotic zone and generally prefers stable stratified environments [Hemleben et al. 1989, Rohling and Gieskes 1989, Rohling et al.1993a, 1995, Reiss et al.2000]. *G.scitula* in particular is tolerant of low temperatures [Hemleben et al. 1989] and we therefore show it as present exclusively in winter, although we cannot exclude its possible presence from other seasons on the basis of the data available.

STATE B

This state is typical of the regime we believe marks the appearance of distinct seasonal stratification in the post-glacial Aegean. The earliest depletion in $\delta^{18}O_{ruber}$ represents Termination 1a. The onset of a separation between the $\delta^{18}O_{ruber}$ and $\delta^{18}O_{pachyderma}$ records suggests that *G.ruber* lived in an isotopically different water-mass than *N.pachyderma*. Where available the $\delta^{18}O_{inflata}$ values clearly follow the $\delta^{18}O_{pachyderma}$ record. Therefore we show these two species in State B as inhabiting the same water mass; *G.inflata* in the deep winter-mixed season and *N.pachyderma* below the seasonal thermocline in the previous winter's water. The increased abundance of *G.ruber* over Termination 1a itself also indicates the development of seasonal stratification with a warm mixed layer, since *G.ruber* has a minimum temperature requirement of ~14°C [Hemleben et al. 1989, Bijma et al. 1990a,b, Reiss et al.2000]. Hence, we infer that Termination 1a was associated with significant development/strengthening of the summer thermocline. This is further corroborated by the increase in *N.pachyderma* abundances, since this species is known to prevail in stable stratified settings with a well developed Deep Chlorophyll Maximum [Hemleben et al. 1989, Rohling and Gieskes 1989, Rohling et al.1993, Reiss et al.2000]. Plankton tows from the modern NW Mediterranean clearly illustrate *N.pachyderma's* preference for such hydrographic conditions [Rohling et al. 1995]. The continued presence of *G.inflata* and its peak in

abundance towards the end of Biozone *II* strongly suggests the persistence of seasonal mixing to considerable depth. The shallower living (~75m) species *G.glutinata* [Reiss et al. 1999] also occurs in State B. This species is a specialist diatom feeder [Hemleben et al. 1989] and is normally associated with the spring bloom, triggered by the newly available nutrients at the end of winter mixing and increased solar irradiation. Thus, we interpret the overall evidence for state B as indicative of seasonal, thermal stratification, alternating with vigorous seasonal overturn of the water column in the colder months.

STATE C

State C in particular represents a transitory phase, marking a "snapshot" within the changing conditions from the start of Termination 1b to the onset of sapropel production. This regime sees the first occurrence of *O.universa* and other members of the SPRUDTS group These taxa prefer warm conditions and are shown in figure 5 above the thermocline. *O.universa* lives in a temperature range of 12-31°C and although its photosynthetic symbionts show a dominant habitat in shallower waters, with sufficient light penetration it can be found down to 250m, [Hemleben et al.1989]. We interpret the increase in SPRUDTS and *G.ruber* as indicative of an increase in depth and extent of the thermocline. The regime in state C is also characterised by the distinct de-coupling of the $\delta^{18}O_{ruber}$ and $\delta^{18}O_{pachyderma}$ signals at the biozone *I/II* boundary, marking an increasing (isotopic) isolation of intermediate/bottom waters from the surface system. There is a synchronous onset of depletions in $\delta^{18}O_{ruber}$ and $\delta^{18}O_{inflata}$, but $\delta^{18}O_{pachyderma}$ on the contrary responds initially with a small enrichment. As $\delta^{18}O_{inflata}$ inflects with $\delta^{18}O_{ruber}$, we deduce that the winter water ($\delta^{18}O_{inflata}$) responded to the same climatic trend as the summer water ($\delta^{18}O_{ruber}$). This is what would be expected for a substantial perturbation: the effect is seen first and strongest in the shallow summer mixed layer and subsequently passed on to the more voluminous winter mixed layer. Any species living below the summer mixed layer effectively lives in the previous year's winter water, and hence even subsurface summer species should reflect the main isotopic change. However as $\delta^{18}O_{pachyderma}$ shows a completely independent and opposite response, we infer that *N.pachyderma* lived in a water mass "isolated" from the surface water system. For this reason, we indicate *N.pachyderma* in an intermediate water mass (IW) that was strongly differentiated from

the surface system, with the mixing indicators restricted to levels above the IW boundary. Such a condition could have resulted from an invasion of intermediate water from a remote source. Despite the presence of a physically stable environment for *N.pachyderma* we see a rapid reduction in this species' abundance, suggesting that its habitat underwent rapid deterioration. This would fit with our proposal of remotely derived intermediate water, since an increase in the pathway from its source relative to the previous locally produced AeIW would result in poorer oxygenation for intermediate water masses in the Aegean. State C also shows a marked reduction in numbers of *G.inflata*, implying that seasonal water column homogenization became inhibited. Shortly following State C, *G.inflata* numbers dwindle into insignificance. The only species showing a real increase is *G.glutinata*. *G.glutinata* may require less dramatic vertical mixing and may hence have replaced *G.inflata*. However, as *G.glutinata* has a short reproductive cycle [Hemleben et al.1989] its occurrence may also be an opportunistic response to any increase in nutrient availability. We also identify an increase in numbers of the eutrophic species *G.bulloides*. Based on its year-round occurrence in the area today [Pujol and Vergnaud-Grazzini 1995], we have represented it with a year-round occurrence. State C therefore represents a progressive warming of climate and a resulting reduction in local Intermediate and Deep-Water production. This allows the increasing isolation of the intermediate water, which in turn allows the mineralisation products resultant from surface productivity to accumulate in more or less isolated deeper waters.

STATE D

This represents the deposition of sapropel S1 and is the culmination of the sequence of changes that started with Termination 1b. Roughly 1 kyr after the start of the T1b depletion in $\delta^{18}O_{ruber}$ a similar depletion begins to show up in $\delta^{18}O_{pachyderma}$. The long time lag suggests that diffusive mixing was the major mechanism for transfer of the isotopic depletion from the surface (*G.ruber*) to the deeper environments (*N.pachyderma*), since convective mixing would have caused a virtually instantaneous response between the two species (see for example the coincidence between the onsets of depletion in $\delta^{18}O_{ruber}$ and $\delta^{18}O_{inflata}$). The anomalous response of $\delta^{18}O_{pachyderma}$ led us to conclude that it was living subsurface in a water-mass unaffected by the local seasonal homogenisation (see state

C). The $\delta^{13}C_{pachyderma}$ in state D becomes strongly depleted relative to $\delta^{13}C_{inflata}$ and $\delta^{13}C_{ruber}$, suggesting that the strongly reduced *N.pachyderma* population that could survive, did so subsurface, in an "isolated" poorly ventilated water mass with accumulation of ^{12}C-rich remineralisation products. We therefore contend that the eventual depletion in $\delta^{18}O_{pachyderma}$ resulted from a slow diffusive mixing process. Our inference of a halt in convective mixing is supported by the presence of dysoxic indicators in the benthic foraminiferal fauna within S1, since a lack of convective overturn results in poor ventilation and consequent dysoxia in bottom waters. For some intervals, at depth (LC-21, 1500m), no benthic species survive at all, suggesting that bottom waters became totally anoxic. In the planktonic foraminifera, assemblage *Ic* dominates, which consists of predominately warm-water species with a notable absence of fall/winter/spring mixing indicators. Hence, we infer that there was a strongly developed, possibly year-round, thermo-/halocline. During this regime we see depletion in $\delta^{13}C$ for all species recorded. This may be the effect of influx of terrestrial Dissolved Organic Carbon (DOC) [Asku et al. 1999], since this period is known to coincide with a wide spread increase in humidity. This is also evidenced by high N. African lake levels; high abundance of humidity markers in the local palynological records; and the isotopic anomalies in speleothem data [Rossignol-Strick 1995, Edmunds et al. 1999, Bar-Matthews et al.1999, Tzedakis 1999 and de Menocal et al. 2000]. The resultant increase in fresh-water input is schematically represented by a rainfall symbol in State D, even though much of the fresh water would have arrived in the form of river run-off rather than direct precipitation [Jenkins and Williams 1983, Shaw and Evans 1984, Thunell and Williams 1987, Rohling and Hilgen 1991, Rohling 1994, Rohling 1999]. As mentioned previously $\delta^{13}C_{pachyderma}$ depletes more than $\delta^{13}C_{ruber}$ and $\delta^{13}C_{inflata}$, which suggests that any DOC explanation needs to be combined with the concept that *N.pachyderma* survived in an aging water mass. With the intermediate water isolated and (virtually) stagnating, it would accumulate an excess of ^{12}C from remineralisation. In contrast, the shallow $\delta^{13}C_{ruber}$ signal is continually being equilibrated by contact with the atmosphere. Note that the separation in $\delta^{13}C$ signals coincides with the onset of sapropel formation, and therefore with the appearance of benthic markers for very poor bottom-water oxygenation, suggesting a culmination of

subsurface/deep-water stagnation.

STATE E

Here we recognise the establishment of a modern circulation regime. The $\delta^{18}O_{pachyderma}$ and $\delta^{18}O_{inflata}$ signals have come back together, suggesting that both live in isotopically undifferentiated winter water. The $\delta^{18}O_{ruber}$ is also similar to $\delta^{18}O_{pachyderma}$ and $\delta^{18}O_{inflata}$ in SL-21, but is slightly more depleted in the remaining cores. This suggests that intermediate and surface waters in this area are once again very similar, which implies direct local communication between these water masses. This may indicate that 1) intermediate waters are upwelling to the surface, and/or 2) surface waters directly contribute to intermediate water formation. Slight $\delta^{13}C$ differentiation between *N.pachyderma* and *G.ruber/G.inflata* suggests that *N.pachyderma* continued to live subsurface at levels more affected by remineralisation than the surface/mixed layer environments preferred by *G.ruber* and *G.inflata.* The return of deep mixing indicator *G.inflata* and the presence of the spring bloom indicator *G.glutinata* suggests that seasonal mixing is again well developed. In addition we see a dominance of *G.bulloides,* giving an overall faunal aspect that is very similar to that seen in modern records [Thunell 1978, Pujol and Vergnaud-Grazzini 1995].

DEDUCTIONS ON MECHANISM AND TIMING OF CIRCULATION CHANGE.

Having identified a general trend of reduced potential for deep overturn in the circulatory system during the 6 kyr leading up to sapropel production, we now consider the mechanism and timing of these changes. The trend starts from a glacial environment characterised by a single well-mixed water mass with strong accordance between isotopic signals in all species analysed. This suggests little density contrast in the water column, while the presence of deep mixing species like *G.inflata* points to regular homogenisation/overturn. We have interpreted this as indicative of year-round mixing. This glacial circulation appears to alter with the start of termination 1a. At that time, a shift in environment is clearly indicated in both the fauna and the isotopic data. Our interpolated dates suggest the onset of this change at ~15.9 ka BP (Table 2). This change

associated with T1a appears to have occurred very rapidly, within a few hundred years.

The subsequent regime is characterised by the start/strengthening of summer stratification. We believe this change in circulation was driven by the combination of climatic warming and rising sea levels at the onset of the Bölling-Allerød. During that interval we see the first substantial occurrence of warm mixed-layer species, suggesting a general sea surface warming. Together with the increase in *N.pachyderma*, this leads us to suggest the development/strengthening of a stable summer thermocline in a generally well-oxygenated environment. Studies of African lake levels and aeolian dust influxes [Edmunds et al. 1999, de Menocal et al. 2000] suggest that this period also saw the start of a regional humidity increase (African Humid Phase AHP). Any increase in fresh water budget would have increased surface buoyancy, helping to establish (seasonal) stratification. This state persisted until the onset of the Younger Dryas (YD) at ~12.5 ka BP

In common with many Mediterranean records, the YD is represented in this study by a plateau in the $\delta^{18}O$ records. The fauna shows increases in the mixing indicator *G.inflata* and a decrease in relative abundance of the warm mixed layer species. This suggests a strengthening of winter convection during this period. The YD has also been identified as an interruption in the AHP [deMenocal et al. 2000], and probably represented a cool arid climatic event [Rossignol-Strick 1993,1995,1999]. The YD conditions continue until the start of Termination 1b marked at ~11.3 ka BP in our records.

The start of T1b marks a clear dissociation between $\delta^{18}O_{pachyderma}$ and $\delta^{18}O_{ruber}$ /$\delta^{18}O_{inflata}$, from which we deduce that the (intermediate) water mass in which *N.pachyderma* lived was no longer locally connected to the surface system. In addition, we argue that the major source region of intermediate water at this time was somewhere outside of the Aegean. Adriatic intermediate water would be one possible source of our proposed "foreign" intermediate water in the Aegean. This agrees with suggestions of Myers et al [1998] that the Adriatic Sea was a major source of intermediate water to the eastern Mediterranean during sapropel formation, and that this under certain circumstances could enter the Aegean Sea [Myers and Rohling 2000]. This introduction of foreign intermediate water also has implications for the dating of foraminiferal

material, a proportion of which will be living in this older water. Correlation between the LC-21 timescale and the GISP II data suggests we see the start of a 350 year offset in LC-21 dates from the start of the anoxic phase [Rohling et al. 2001]. T1b marked the end of the peak in *G.inflata* abundance and a shift towards the dominance of the shallower living species *G.glutinata* and of warm mixed-layer species. This signals the inhibition of deep mixing and the isolation of intermediate waters, corroborating our interpretation of the separation between $\delta^{18}O_{ruber}$ and $\delta^{18}O_{pachyderma}$. From this point on remineralisation products were able to build up in the sub-surface to deep waters.

With the ending of the Younger Dryas, the AHP recommenced and persisted until 5.5 ka BP [deMenocal et al.2000]. In the Aegean cores, we note a depletion in $\delta^{13}C$ for all species analysed, starting at ~10.5 ka BP, which we interpret as possibly the result of increasing humidity in the Aegean Sea. Coinciding with this depletion in $\delta^{13}C$, *G.glutinata* replaces *G.inflata*. This may be tentatively explained in terms of increased fresh water input, which reduced surface buoyancy loss and hence suppressed mixing.

With the suppression of convective mixing in the Aegean, diffusion-type processes become the main driver for property exchange through the water column. At ~10.2 ka BP, we identify an inflection in $\delta^{18}O_{pachyderma}$, which seems to mark the start of the conveyance of the Termination 1b signal to the isolated intermediate water. This allows us to determine a time scale of diffusive mixing. By assessing the time between the maximum $\delta^{18}O_{ruber}$ - $\delta^{18}O_{pachyderma}$ gradient and its 1/e-fold reduction, we can roughly estimate the diffusive time scale for the basin in its stratified sapropel mode. We calculate this to be ~450 years (Table 2).

Event	LC-21 Depth 1520m	SL-31 Depth 430m	SK-1	Geraga et al. (2000)	SLA-9 Depth 250m	Mean age (cal.ka BP)	Youngest age (cal.ka BP)	± (Range/2)
Start of $\delta^{18}O_{ruber}$ depletion T1a	15.7	16.0	-	-	15.9	15.9	15.7	±0.2
III-II	15.8	16.1	15.4	14.8	-	15.5	14.8	±0.6
Start of $\delta^{18}O_{ruber}$ depletion T1b	10.9	11.5	-	-	11.6	11.3	10.9	±0.4
II-Ic	10.9	11.6	11.4	11.1	11.5	11.3	10.9	±0.4
Start $\delta^{13}C$ depletion	10.4	10.3	-	-	10.7	10.5	10.3	±0.2
Start $\delta^{18}O_{pachyderma}$ depletion	10.1	10.2	-	-	10.4	10.2	10.1	±0.2
Age of max $\delta^{18}O_{ruber}$ - $\delta^{18}O_{pachyderma}$ difference	10.1	10.2	-	-	10.4	10.2	-	±0.2
Age of level $1/e(\delta^{18}O_{ruber} - \delta^{18}O_{pachyderma})$	9.85	9.9	-	-	9.55	9.75	-	±0.2
Benthic sapropel	9.5	9.8	-	-	10.1	9.8	9.5	±0.3
End of benthic Sapropel	6.1	6.9	-	-	6.4	6.5	6.1	±0.4
Ic-Ib	5.6 (6.1)	6.9	7.1	6.8	6.4	6.6 (6.7)	5.6 (6.1)	±0.8 (±0.5)
Ib-Ia	4.6	5.1	6.1	5.1	-	5.2	4.6	±0.8

Table 2. Timing of events. This table details the interpolated starting ages of important horizons in core LC-21, SL-31 and SLA-9. All ages are expressed as calibrated ka BP and are derived by linear interpolation between bracketing dated horizons. The mean age of each event is given in the final row with the range between cores expressed as an error. Additional dates are given after Zachariasse et al (1997] for core SK1 and Geraga et al. (2000] for core C40. The number in brackets, in the first column, gives the interpolated age of the start of *G.glutinata* increase in LC-21. This also corresponds with the start of benthic re-ventilation as indicated by an initial reoccurrence of *G.orbicularis*. This point corresponds with an increase of *G.ruber* and a decrease in *T.quinqueloba* and *G.inflata*. We suggest (see text) that the *G.glutinata* increase in the more open setting of LC-21 correlates with the *G.inflata* increase in the more continental settings of the N.Aegean cores.

By ~9.8 ka BP, deposition of sapropel S1 has commenced (Table 2). This is ~400 years after the total suppression of mixing inferred from the start of the overall $\delta^{13}C$ depletion, and the faunal shift to a virtually complete dominance of mixed-layer species. The start of sapropel production also occurs ~1500 years after the isolation of the deep/intermediate waters, inferred from the separation of $\delta^{18}O_{ruber}$ and $\delta^{18}O_{pachyderma}$. The isolation of subsurface waters would have allowed subsurface accumulation of remineralisation products over a period of up to 1.5 kyr, before these products became available for production in the euphotic zone. We suggest that this long-term accumulation provided a major source of excess nutrients that could sustain enhanced productivity during sapropel deposition.

Based on benthic foraminiferal indicators, S1 persisted until 6.5 ka BP (Table 2). At its termination, the return of *G.inflata* indicates the re-start of seasonal mixing. The warm/cold plots (figure 2) suggest this may have been a cooling event. In LC-21 the end of the sapropel is marked in the planktonic record by the occurrence of *G.glutinata* first rather than *G.inflata.* This may be related to the proximity of the Northern Aegean cores (SL-21, SL-31) to the area of deep-water production in the Athos Basin [Yüce 1995]. While, the more remote position of LC-21 from the region of water column overturn would have resulted in a more gradual increase in seasonal mixing, with a correspondingly different progression in the fauna. The general $\delta^{13}C$ depletion may reflect terrestrial DOC influx due to increased humidity persisted until ~4.9 ka BP. However, the timing of the $\delta^{13}C$ depletion, some 400 years after suppression of mixing, is of the same order as our e-fold diffusive time-scale, suggesting that the carbon depletion maybe in part due to the upward advective-diffusive transport of ^{13}C-depleted dissolved inorganic carbon (DIC). This DIC would be supplied from deeper waters, depleted in ^{13}C by remineralisation. Around that time the fauna also settled into its modern abundance distributions (*Ib – Ia* transition, Table 2).

2.7 CONCLUSIONS

There is a clear link between the Aegean hydrographic regime and the global deglaciation phases. Seasonal stratification is weak to non-existent before the onset of termination 1a, while intermediate water was virtually indistinguishable from shallow waters. After the onset of termination 1a, we identify a distinct seasonal stratification alternating with vigorous overturning seasons. This resulted in a winter mixed layer of similar characteristics to the intermediate water and a summer mixed layer that was distinguished from this by a marked seasonal thermocline. T1b marks the next distinct hydrographic change when intermediate water became dissociated from the summer/winter mixed layers in the study area. This non-communication between the surface and intermediate system indicates reduced/curtailed ventilation of intermediate and deeper waters. This implies that property exchanges would have become dominated by slow (diffusive) mixing and we estimate a 1/e-fold diffusive mixing time scale of ~450 years. This gives the first ever observation-based quantitative estimate of this time scale in the stratified (sapropel mode) Mediterranean.

Furthermore, the dissociation of surface and intermediate systems allowed remineralisation products to accumulate in intermediate and deep-waters, over a period of up to ~1.5 kyr prior to sapropel deposition. Meanwhile the isolated intermediate water would have become progressively more dysoxic, a process augmented by the observed increase in (year-round?) stratification. The sapropel, therefore, appears to represent the culmination of a dynamic non-steady state process. This has important consequences for the current, accepted, steady state approach to circulation and property budget calculations for the eastern Mediterranean in sapropel mode.

The sapropel mode ended with the reoccurrence of winter mixing indicative species at ~ 6.5 ka BP, while the return to a modern faunal assemblage was completed by ~4.9 ka BP.

ACKNOWLEDGEMENTS

We thank: Frans Jorissen and John Thomson for their constructive comments and discussion; Hilary Sloane for her help with isotopic analysis of cores SL-21 and SL-31, at the NERC Isotope Geoscience Laboratory at Keyworth, UK and; Connie de Vries for her efforts with the stable isotopes of LC-21 at the SOC isotope facility. LC-21 was recovered within EC-MAST2 programme PALAEOFLUX and is held at the BOSCOR repository in Southampton. Aegean cores were collected with the aid of NCMR in Athens, Greece. Data from this paper has been lodged with the NOAA-NGDC website.

CHAPTER 3

IN PRESS, MEDITERRANEAN MARINE SCIENCE (2001). AUTHORED BY

Casford[1] J.S.L., Abu-Zied[1] R., Rohling[1] E.J., Cooke[1] S., Boessenkool[2], C., Brinkhuis[2], H., De Vries[2], C., Wefer[3], G., Geraga[4], M., Papatheodorou[4], G., Croudace[1], I., Thomson[1], J., and Lykousis[5] V..

[1] *School of Ocean and Earth Science, Southampton University, Southampton Oceanography Centre, European Way, Southampton, SO14 3ZH, UK.*

[2] *Laboratory for Paleobotany and Palynology, Utrecht University, 3584CD Utrecht, NL*

[3] *Fachbereich Geowissenschaften, Universität Bremen, D*

[4] *Department of Geology, University of Patras, G*

[5] *National Centre for Marine Research, Athens, Greece.*

3. MEDITERRANEAN CLIMATE VARIABILITY DURING THE HOLOCENE

3.1 ABSTRACT

We present a study on four high sedimentation-rate marine cores with suppressed bioturbation effects, recovered along the northern margin of the eastern Mediterranean. We demonstrate that this region, central to the development of modern civilisation, was substantially affected throughout the Holocene by a distinct cycle of cooling events on the order of 2° C-degrees. In the best-preserved cases the onset of these events appears particularly abrupt, within less than a century. The cooling events typically lasted several centuries, and there are compelling indications that they were associated with increased aridity in the Levantine/NE African sector [Rossignol-Strick, 1995; 1998; Alley et al., 1997; Hassan, 1986; 1996; 1997a,b; McKimMalville et al., 1998]. Several of these episodes appear coincident with cultural reorganisations, with indigenous developments (eg. cattle domestication, new technologies) and population migrations and fusion of peoples and ideas [Hassan, 1986; 1996; 1997a,b; McKim Malville, 1998]. We infer that climatic events of a likely high-latitude origin [O'Brien et al., 1995; Bond et al., 1997; Mayewski et al., 1997; Alley et al., 1997] caused cooling and aridity in and around the eastern Mediterranean via a direct atmospheric link, and therefore played an important role in the development of modern civilisation.

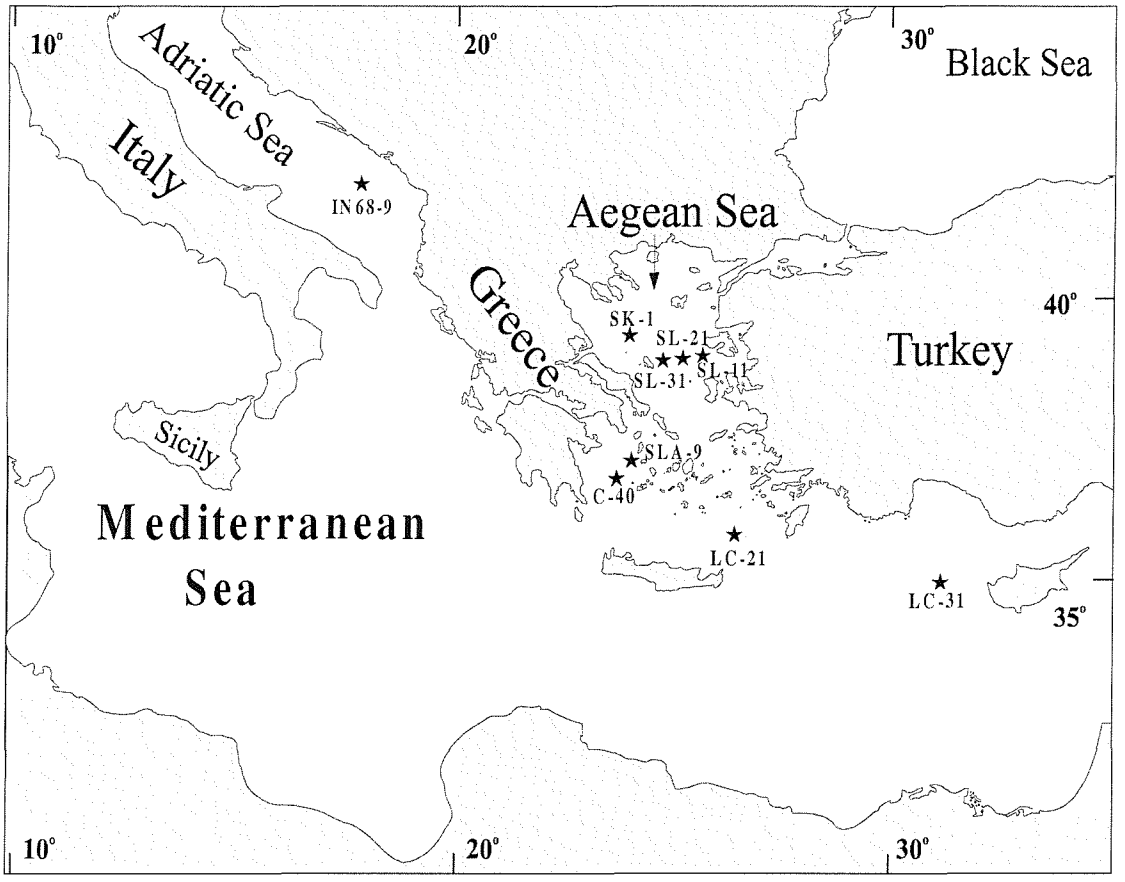

Figure 1. Map of Eastern Mediterranean, showing locations of cores used in this study.

3.2 INTRODUCTION

The Holocene is customarily regarded as a period of climate stability, but recently a distinct millenium-scale repetition of Holocene cold events has been recognised [O'Brien et al., 1995; Bond et al., 1997; Campbell et al., 1998; Bianchi and McCave, 1999]. This climatic variability may have driven migratory patterns and settlement behaviour in early societies [Hassan, 1986; 1996; 1997a,b], but it remains to be established how high-latitude Holocene climate variability affected the near/middle East region. One measure of such climatic variability are fluctuations in past sea surface temperature (SST) estimated from marine planktonic microfossil records [Cita 1977; Thunell 1977; Rohling et al., 1993; Pflaumann et al., 1996; Kallel et al., 1997; Ortiz and Mix, 1997; Rohling et al., 1997; Targarona, 1997; Hayes et al., 1999]. We assess the Late Glacial-Holocene SST changes

from planktonic foraminiferal abundance variations in four cores (Table 1). IN68-9 from the S Adriatic Sea; C40 from the SW Aegean Sea; LC21 from the SE Aegean Sea; and LC31 from W of Cyprus (Fig. 1), using a simple *a-priori* grouping of warm versus cool species (expressed as %warm species/(%warm + %cool species), Table 2; Fig. 2 and 3). Similar groupings are found from multivariate statistical analyses of Mediterranean records[Cita 1977; Thunell 1977; Rohling et al., 1993; Hayes et al., 1999]. In subtropical waters, the species of the 'warm' group predominate within the shallow, warm, and nutrient-depleted summer mixed layer. Many are spinose and contain photosynthetic symbionts. Species of the 'cool' group are mostly present in winter, when SST is reduced and the mixed layer has considerably deepened (> 100 m) and become enriched in nutrients. Despite an obvious overprint of the degree of eutrophication related to the development of the seasonal thermocline, recent modern analogue studies show that such groupings provide useful first-order information on SST fluctuations[Pflaumann et al., 1996; Kallel et al., 1997; Ortiz and Mix, 1997]. In corroboration of the SST fluctuations based on planktonic foraminifera (zooplankton), we include a similar warm and cool water grouping for core IN68-9 of selected organic walled cyst species derived from autotrophic dinoflagellates (phytoplankton) that generally preserve well (Table 2). Both qualitative records differ in detail due to the effects of productivity and preservation constraints, but the basic patterns in intervals with comparable sampling resolution are quite similar (Fig.3).

Core	Location	Depth
LC-21	35° 39.71' N 26° 34.96' E	1522 m
LC-31	34° 59.76' N 31° 09.81' E	2298 m
IN68-9	41° 47.5' N 17° 54.5' E	1234 m
C-40	36° 56.12' N 24° 04.69' E	852 m

Table 1. Core characteristics

Planktonic foraminifera (zooplankton)	
Warm group	Cool group
Globigerinoides ruber	*Globorotalia scitula*
Globigerinoides sacculifer	*Turborotalita quinqueloba*
Hastigerina pelagica	*Globorotalia inflata*
Globoturborotalita rubescens	*Neogloboquadrina pachyderma*
Orbulina universa	
Globigerinella digitata	
Globoturborotalita tenella	
Globigerinella siphonifera	

Selected autotrophic dinoflagellate cyst species (phytoplankton)	
Warm group	Cool group
Impagidinium aculeatum	*Bitectatodinium tepikiense*
Impagidinium strialatum	*Spiniferites elongatus*
Impagidinium paradoxum	*Impagidinium pallidum*
Spiniferites mirabilis	

Table 2. Composition of species-groups used in planktonic foraminiferal and dinoflagellate warm-cold plots.

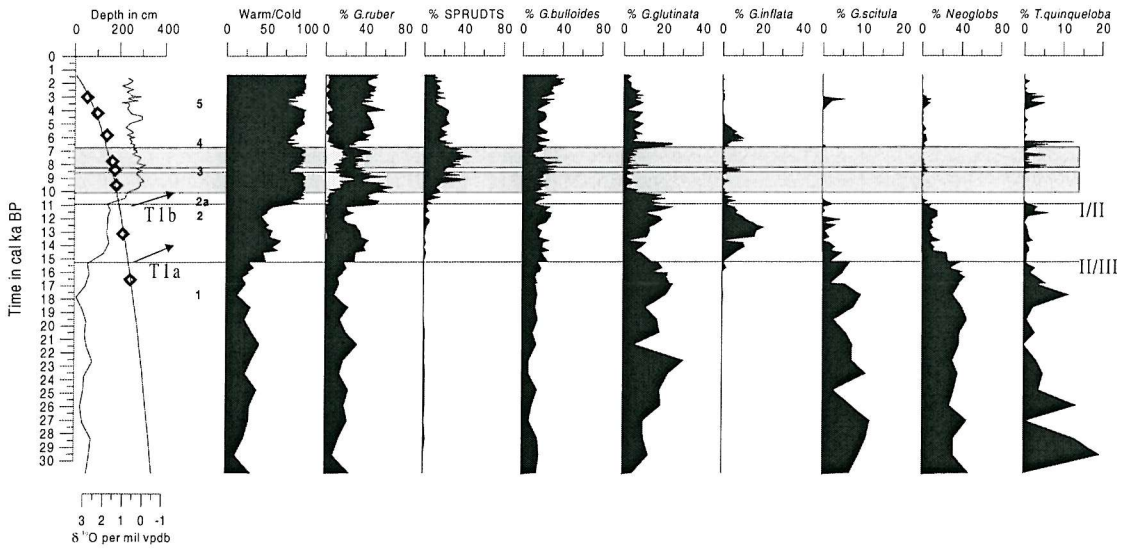

Figure 2. Time-stratigraphic framework of the core LC-21, using a second order polynomial fit through age-control points given in Table 3. The $\delta^{18}O$ plot is based on measurements of the foraminiferal species *G.ruber* and is expressed in per mil (VPDB). Bold arrows indicate the extent of the isotopic depletions associated with terminations T1a and T1b. The bold numbers indicate the position of cooling events identified in LC-21 primarily from warm/cold faunal plots. Relative abundances of key planktonic foraminifera species are also shown together with the biozonal boundaries I/II and II/III [Jorissen et al., 1993]

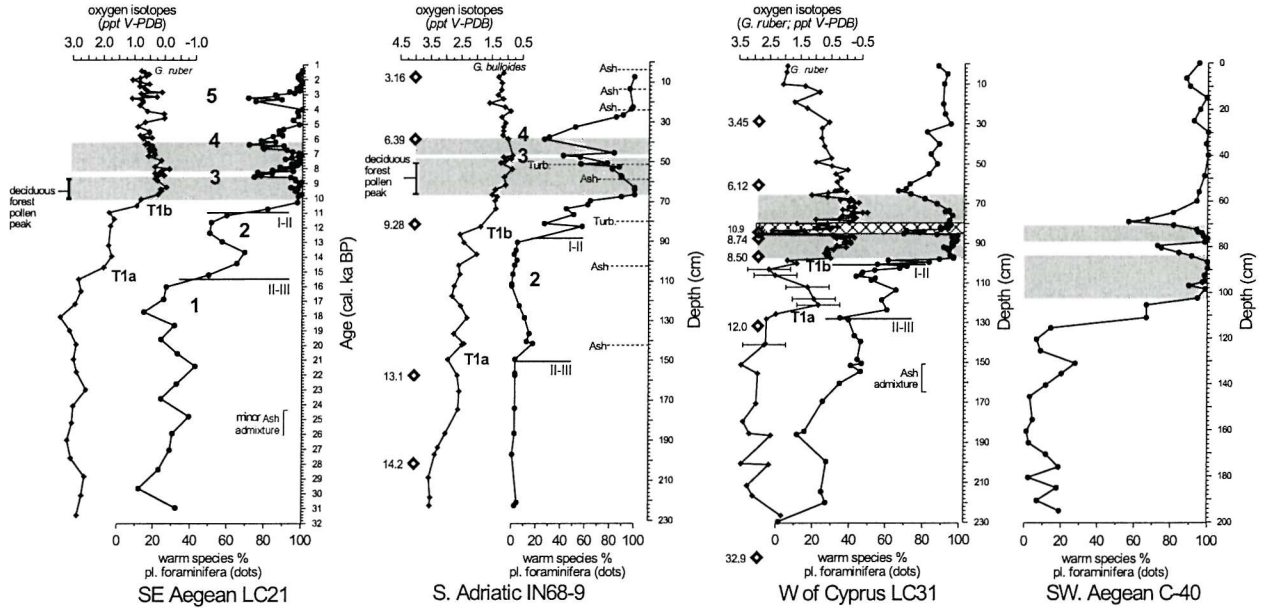

Figure 3. Records of warm versus cold planktonic foraminiferal species as discussed in the text. LC-21 is plotted versus time, plots of IN68-9 for clarity show depth subtracting thicknesses of turbidites and ash-layers, and for LC31 and C40 versus true depth. Planktonic foraminiferal biozone boundaries after Jorissen et al.[1993]. Cooling intervals are numbered sequentially in bold. Main cooling events in the dinoflagellate-based warm-cold record (see text) for IN68-9 are numbered sequentially in bold italics, with the prefix *d.* In LC21, the dinoflagellate-based temperature record is near 100% throughout the Holocene, and is compromised by low cyst abundances outside the sapropelic intervals; levels where minor cooling events were found are marked *d*---. Grey bands represent sapropelic intervals. The crosshatched interval within the sapropel in LC31 represents a slump (see Table 3). Oxygen isotope stratigraphies are based on *G. bulloides* for IN68-9 and *G. ruber* for LC21 and LC31, from the 250-350 μm size-window. Error-bars in LC31 represent range of variability observed in replicate analyses, for analyses added at the S.O.C. isotope facility to an originally less detailed record analysed at Bremen. The two facilities were intercalibrated by exchange of laboratory standards and replicate sample analyses. Bold lines indicate the two main deglaciation steps: Terminations T1a and T1b. Within the basal sapropel unit, relatively small effects of temperature change on $\delta^{18}O$ are overwhelmed by those of the dramatic summer rainfall increase witnessed by a peak in deciduous forest pollen in both IN68-9 [Targarona, 1997] and LC21 (preliminary record; not shown). Warm-cold record for C40 excludes *Turborotalita quinqueloba*, a small-size species that is over represented in this >120 μm study, relative to the other three >150 μm studied

3.3 TIME-STRATIGRAPHIC FRAMEWORK

The chronostratigraphy is determined by several AMS14C analyses in each of cores IN68-9, LC21, LC31 and C40, all performed on hand-picked clean planktonic foraminiferal tests (Table 3). A calendar age of 3.578 ka BP[Kuniholm et al., 1996] is used for the Santorini ash layer at 81-91 cm in LC21, and 33-36 cm in C40. We calibrate all radiocarbon convention ages using the marine mode of the Calib3.03 programme[Stuiver and Reimer, 1993]. It is immediately obvious that some of the AMS14C datings tend towards older ages than expected from the well-established ages of the biozonal boundaries and the Santorini ash layer (Table 3; Fig. 3). This tendency is mostly minor (e.g. the ages around the Santorini ash in LC21), but in some cases a substantial offset is seen. For example, the age immediately below the 5 cm thick slump within the sapropel in LC31 appears about 1000 years too old. This is probably due to the immediate proximity of the mass-transport layer, which itself is about 3000 years older than surrounding sediments. Offsets towards older radiocarbon ages are potentially caused by addition of an uncertain component of older tests to the material analysed, which seems possible in view of the high accumulation rates of the cores and their proximity to the continental slopes. Calibrated ages for LC21 are then plotted versus depth subtracting the thicknesses of the interbedded Santorini ash layer and turbidites. As LC21 has the highest resolution of the four cores in the study and appears to be the most complete record, it is used as a master chronology in the following discussion (Fig. 2). All ages are reported as calibrated AMS 14C years BP unless otherwise stated.

Bio-stratigraphic control also provides two well-dated correlation horizons, the biozone I-II and II-III boundaries, as defined on the basis of 11 central Mediterranean marine records with a total of 50 AMS14C ages [Jorissen et al., 1993]. Subsequent studies emphasised Mediterranean-wide applicability and synchroneity of both boundaries [Capotondi et al., 1999; Hayes et al., 1999]. This includes the Aegean Sea [Zachariasse et al., 1997], as is shown also by the results of core C40 presented here. The II/III biozonal boundary in the Adriatic however, does not appear to be entirely synchronous with the corresponding faunal break in our other cores. The chronostratigraphy of Adriatic core IN68-9 gives ages for the zone I-II and II-III boundaries of 10.5 cal ka BP and 14.5 cal ka BP, respectively [Jorissen et al., 1993; Rohling et al., 1993, 1997]. We note that IN68-9

presents a date almost 1000 years younger for the II/III boundary than that observed in their other cores [Jorissen et al., 1993] or in the cores presented here. As yet, there is no satisfactory explanation but it is possible that a small hiatus is present in IN68-9 over the II/III boundary

True depth (cm)	Corrected depth (cm)	AMS lab. code	Uncorrected AMS^{14}C age from direct dating or dated horizon (ka BP)	cal. age (ka BP)	cal. age range (1σ) (ka BP)
IN68-9					
11.5	7.5	UTC-500	3.16±0.12	2.93	2.78-3.10
54.5	38.5	UTC-1607	6.39±0.06	6.85	6.77-6.90
157.25	81.25	UTC-501	9.28±0.18	9.93	9.80-10.08
241.5	157.5	UTC-502	13.10±0.20	14.95	14.61-15.30
322.5	201.5	UTC-503	14.20±0.30	16.55	16.15-16.92
510.5	247.5	UTC-504	17.20±0.30	19.82	19.40-20.30
LC-21					
50	50	CAMS-41314	3.35±0.06	3.20	3.11-3.27
95.5	85.5	CAMS-41313	4.29±0.06	4.40	4.32-4.45
137.75	127.75	CAMS-41311	5.59±0.06	5.95	5.90-6.03
161.5	151.5	CAMS-41315	7.48±0.06	7.90	7.94-7.84
174.25	164.25	CAMS-41312	8.12±0.06	8.52	8.59-8.44
179.5	169.5	AA-30364	9.01±0.07	9.54	9.22-9.86
209	199	AA-30365	11.77±0.08	13.14	12.77-13.51
252.5	242.5	CAMS-41316	14.45±0.06	16.85	16.96-16.74
81-91	81		Santorini	3.578	
LC-31					
28.5	28.5	CAMS-45864	3.45±0.05	3.33	3.26-3.36
60.5	60.5	CAMS-45863	6.12±0.05	6.54	6.47-6.62
84.25	81 (slump)	AA-30367	10.90±0.10	12.42	12.27-12.55
87.5	82.5	CAMS-45861	8.74±0.05	9.38	9.34-9.43
96.5	91.5	CAMS-45862	8.50±0.05	9.06	8.98-9.19
131.5	126.5	CAMS-45860	12.04±0.05	13.57	13.47-13.69
247.5	242.5	CAMS-45859	32.96±0.05	35.96 (simple 3 kyr addition)	
C-40					
73.5	73.5	Beta-110420	6.83±0.11	7.30	7.20-7.39
82.5	82.5	Beta-110419	7.83±0.14	8.26	8.10-8.38
131	131	Beta-110418	12.35±0.16	13.93	13.72-14.16
33-36	33-36		Santorini	3.578	

Table 3. Age control-points used in the present study, with true depths in the cores, and corrected depths (subtracting thicknesses of turbidites and ash-layers). I-II and II-III are planktonic foraminiferal biozone boundaries [Jorissen et al., 1993]. Radiocarbon convention ages calibrated using marine mode of programme Calib3.03 [Stuiver and Reimer, 1993]. Santorini age after Kuniholm et al.[1996] . Core LC-31 dates include a local ΔR correction of 149±39 years after Facorellis et al.,[1998]. Dates in LC-21 are after Mercone et al., [1999] and in C-40 after Geraga et al., [2000].

3.4 COOLING EVENTS

We identify several cooling events, these are sequentially numbered (in bold), noting their positions relative to the biozonal boundaries, ash layers, and sapropelic units (Fig. 2 and 3). Events 1 and 6 are less accurately timed because of their occurrence near the limits of the investigated records where resolution is lowest. The 2a event (9.6-9.8 ka BP) is only identified positively from core IN68-9 with limited support from the other cores outside the Adriatic. The 1a event (13.4-13.6 ka BP) is only identified in the base of core LC-31, and needs to be considered with caution. The age-ranges determined for the NE Mediterranean cooling events are 1.5-2.0, 3.6-4.0, 5.8-6.2, 8.2-8.6, 9.6-9.8, 11.4-12.4, 13.4-13.6, and 17.0-18.5 ka BP, similar to ages reported for high-latitude N. Atlantic cold events in the Holocene (Table 4)[O'Brien et al., 1995; Bond et al., 1997].

The magnitude of the 8 ka BP event (our event 3) in IN68-9 has been estimated in the order of 2°C [Rohling et al., 1997]. For a full glacial-interglacial temperature difference in the Aegean Sea of about 6°C [Rohling and De Rijk, 1999], comparison of the magnitudes of the cooling events with the full glacial-interglacial amplitude of change in the warm/cold plot of LC21 (Fig. 3) also suggests effects of the order of 2 C-degrees.

The rapidity of the onset of the cooling events is best illustrated using the 8 ka BP event (event 3), since it follows the deposition of the unbioturbated (abenthic) lower sapropelic unit. In LC21, this event starts from one sample to the next. Due to the high accumulation rate in this core we infer that the period of onset for this event was less than a century (Fig. 2). The cooling events typically last several centuries, and appear to be repeated at regular intervals.

3.5 DISCUSSION

Together, the timing of the events and the apparent rapidity of changes in the eastern Mediterranean suggest a direct atmospheric link between high latitudes and the NE Mediterranean. Regionally delimited expressions of cold Atlantic Heinrich events in the glacial Gulf of Lions (NW Mediterranean) also suggest an efficient atmospheric teleconnection between that area and the high latitudes [Rohling et al., 1998]. Today, high latitude Arctic/N.Atlantic perturbations are rapidly transmitted to the northern edge

of the Mediterranean via orographically channelled winter outbreaks of cold and dry air from high latitudes over the NW Mediterranean, the Adriatic and the Aegean Sea [Leaman and Schott 1991; Mariopoulos, 1961; Poulos et al., 1997]. An increased duration and/or intensity of these atmospheric outbreaks would cause not only cooling, but also aridity. Palaeobotanical records around the Aegean Sea [Rossignol-Strick, 1995], and the $\delta^{18}O$ and $\delta^{13}C$ profiles of Soreq Cave (Israel)[Bar Matthews et al., 1999] both suggest notable cooling and aridity during the Younger Dryas and around 8 ka BP. Moreover, overviews of continental palaeoclimate and archaeological records from the Levant and NE Africa show arid spells of similar age to our Adriatic/Aegean cooling events (Table 4), coinciding with important reorganisations in settlement patterns and agricultural behaviour of early societies [Hassan, 1997a,b; McKim Malville et al., 1998]. For example, "droughts ... between 8.3 and 7.7 ka BP encouraged movements of nomadic cattle keepers from the Egyptian Sahara and bands possessing sheep/goats and wheat/barley from Southwest Asia to the banks of the Nile Valley and Nile Delta. This event was crucial for the agricultural developments in the Nile Valley" [Hassan, 1998] (our event 3). In addition, "It was during the 7th and 6th millennium bp episodes of severe droughts that dwellers of the desert drifted towards the Nile Valley, and elsewhere, in search of water, food, and fodder" [Hassan 1997], (our event 4, see table 4). We infer that the development of modern civilisation was punctuated by abrupt cooling/aridity events due to an atmospheric teleconnection between the 'cradle of modern civilisation' and the high latitudes. We propose that this connection operates through significant increases in winter northerly air flow over the eastern Mediterranean.

The observed temporal spacing of these cooling events appears (Table 4) similar to that of planet-induced sun-tide cycles [Lamb, 1972]. Ice-core 14C residual series indicate this periodicity to be around 1450 years, suggesting that fluctuations in solar forcing may indeed have affected glacial and Holocene climate on these time-scales [Mayewski et al., 1997]. However, any external forcing would likely drive internal oscillations within the earth's ocean/climate system, such as the recently invoked 'oceanic oscillator', a fluctuation in the global thermohaline circulation, the nature of which remains to be determined [Bianchi and McCave, 1999]. We tentatively propose that the Mediterranean may form part of the 'oceanic oscillator'. Although the Mediterranean appears to behave initially as a passive response-basin to high-latitude cold events, resultant increases in buoyancy loss would increase its saline outflow flux into the Atlantic. Mediterranean salt today contributes to the water-column destabilisation needed for North Atlantic Deep

Water (NADW) formation eg [Reid, 1979; Hill and Mitchelson-Jacob, 1993]. If the Mediterranean salt flux into the Atlantic were sufficiently increased to trigger enhanced NADW formation (for assessment of current hypotheses, see Bryden and Webb, [1998]), then consequent increases in heat-advection to high latitudes could have contributed to termination of high-latitude cold events. This possibility merits consideration, particularly in view of the anthropogenic impact on Mediterranean deep-water properties and the recently observed and rapid major salt redistribution within the eastern Mediterranean [Bethoux et al., 1990; Leaman and Schott, 1991; Rohling and Bryden, 1992; Bethoux and Gentilli, 1996; Roether, 1996].

This paper	Bond et al.,1997	Hassan 1997a,b	McKim.. et al., 1998	Gasse et al., 1996	O'Brien et al., 1995	Event
--	--	--	--	0.7	0.0-0.6	--
~1.5	1.2-1.7	1.5-2.0	--	1.3-2.1	--	6?
3.2-4.0	2.5-3.1	--	--	--	2.4-3.1	5
--	4.1-4.8	4.0-4.4	--	<3.9	--	
5.8-6.2	5.6-6.3	5.5-6.7*	<5.8 arid	5.7-6.3	5.0-6.1	4
8.2-8.6	7.6-8.5	7.7-8.3	7.4-8.1***	7.7-8.2	7.8-8.8	3
9.6-9.8	9.4-9.7	9.2-9.5	--	9.6-9.9	--	2a‡
11.4-12.4	10.7-12.6**	--	--	--	>11.3	2
13.4-13.6	13.0-13.4	13.4-14.0	--	--	--	1a‡‡
--	14.6-15.0	--	--	--	--	--
17.0-18.5						1

Table 4. Comparison of ages of abrupt climate events. This paper: planktonic foraminifera-based cooling events in the Adriatic and Aegean/NE Levantine Seas. Bond et al. [1997]: high latitude N. Atlantic cold events from marine records compared with GISP2 ice record. Hassan et al [1997a,b] and McKim Malville et al. [1998]: NE African arid/cold spells and impact on early societies. Gasse et al. [1996]: aridity in the Lake Bangong area (W. Tibet). O'Brien et al. [1995]: cold events with increased meridional atmospheric circulation affecting the Greenland Ice Sheet. Last column: mean ages based on boundaries of discrete events listed in the table, with standard error of the mean (cal. ka BP).
* Onset of major drought and cold conditions around 6.7 ka BP, culminating around 5.5 ka BP with shift of societies into active Nile channels[Hassan 1997b].
** Their event 8 and Y.D. combined[Bond et al., 1997].
*** Combination of two separately reported events (7.4-7.5 and 7.9-8.1)[McKim Malville et al., 1998].
‡ Only weakly supported outside of Adriatic.
‡‡Identified in LC-31 only, to be treated with caution.

ACKNOWLEDGEMENTS.

This paper represents a joint effort of EC-MAST3 programmes: Climatic variability of the Mediterranean palaeo-circulation and; Sapropels and palaeoproductivity. Cores LC21 and LC31 were recovered within EC-MAST2 programme PALAEOFLUX and are held at the BOSCOR repository in Southampton. We thank M. Segl at the isotope laboratory in Bremen, F. Hassan, M. Rossignol-Strick, F.J. Jorissen, and J. Targarona for valuable discussions, the NERC laboratory for AMS radiocarbon analyses, the Egyptian Government for support to RA-Z, K.A.F. Zonneveld and J. Targarona for analysis and synthesis of the dinoflagellate and pollen records of IN68-9, and J. Kallmeyer for his contribution to study of LC31.

CHAPTER 4

IN PRESS, CLIMATE DYNAMICS (2001). AUTHORED BY

Eelco J. Rohling[1], Paul A. Mayewski[2], Ramadan H. Abu-Zied[1], James S. L. Casford[1], and Angela Hayes[1]

1 School of Ocean and Earth Science, Southampton University, Southampton Oceanography Centre, European Way, Southampton, SO14 3ZH, UK.

2 Climate Studies Centre, Institute for Quaternary Studies and Department of Geological Sciences, University of Maine, Orono, Maine 04469, USA

4. HOLOCENE ATMOSPHERE-OCEAN INTERACTIONS: RECORDS FROM GREENLAND AND THE AEGEAN SEA

4.1 ABSTRACT

We compare paleoclimate proxy records from central Greenland and the Aegean Sea to offer new insights into the causes, timing, and mechanisms of Holocene atmosphere-ocean interactions. A direct atmospheric link is revealed between Aegean sea surface temperature (SST) and high latitude climate. The major Holocene events in our proxies of Aegean SST and winter/spring intensity of the Siberian High (GISP2 K+ record) follow an ~2300 year spacing, recognised also in the Δ14C record and in worldwide Holocene glacier advance phases, suggesting a solar modulation of climate. We argue that the primary atmospheric response involved decadal-centennial fluctuations in the meridional pressure gradient, driving Aegean SST events via changes in the strength, duration, and/or frequency of northerly polar/continental air outbreaks over the basin. The observed natural variability should be accounted for in predictions of future climate change, and our timeframe for the Aegean climate events in addition provides an independent chronostratigraphic argument to Middle Eastern archaeological studies.

4.2 INTRODUCTION

Study of the Holocene (current interglacial, last ~11,500 years) allows assessment of climatic variability through the early to fully developed interglacial state during which modern climatic and geographic boundary conditions have evolved. To assess direct atmosphere-ocean interactions during the Holocene, we compare the excellently dated record of atmospheric chemistry from the Greenland summit GISP2 ice core (72.6°N, 38.5°W; +3200 m) with an SST proxy record from an Aegean Sea (NE Mediterranean) sediment core (35.66°N, 26.58°E; -1522 m). This focus on the Aegean Sea is driven by the fact that it is a marginal sea with virtually no direct forcing by the North Atlantic thermohaline circulation (THC), and which is unaffected by sea-ice related complications (eg., insolation, albedo effects). Due to its small volume, the Aegean lacks the inertia of larger ocean basins, allowing direct rather than lagged responses to forcing and well-developed signal amplitudes. Strong winter cooling due to orographically channelled northerly outbreaks of polar/continental air forms a dominant characteristic of the Aegean SST regime [Theocharis and Georgopoulos, 1993; Poulos et al., 1997]. This process is related to the vigour and southward extent of (sub)polar climate conditions

over the Eurasian continent, and hence to the intensity of the Siberian High. Therefore, a direct relationship is expected between our Aegean SST proxy and the GISP2 K^+ series, which we argue to be a reliable proxy for winter/spring intensity of the Siberian High. The Aegean Sea therefore provides an ideal natural laboratory for assessment of direct hydrographic responses to high-latitude climate variability, for comparison with more complex fluctuations in THC- and ice-dominated regions.

4.3 Material And Methods

The GISP2 K^+ proxy for intensity of the Siberian High (Fig. 1f) is based on the identification of strong relationships (summarised below, after Meeker and Mayewski, in press] between high-resolution glaciochemical time series from central Greenland [Mayewski et al., 1997], and 1899–1987 AD instrumental records of atmospheric sea level pressure (SLP) over the North Atlantic and Asia [Trenberth and Paolino, 1980]. Given their seasonal deposition patterns in Greenland snow (eg., winter/spring K^+ maxima; Legrand and Mayewski, 1997] annual ion concentration values are strongly influenced by variations in seasonal atmospheric circulation. Relative to years of low K^+ deposition, years with high K^+ deposition are associated with winter/spring strengthening of the high over Siberia, the coldest air mass in the northern hemisphere; the K^+ and Siberian High series are positively correlated, sharing 58% of their variance [Meeker and Mayewski, in press]. Potassium is transported in the finest range of Asian dust [Zhang et al., 1993], which enables long distance transport to Greenland [Biscaye et al., 1997].

The time-stratigraphic framework for the relevant interval of our SE Aegean core LC21 (Fig. 1a) represents a best fit through eight calibrated AMS^{14}C datings [Mercone et al., 2000] (calibration details in the caption of Fig. 1a). It is corroborated by three further calibrated AMS^{14}C datings, correlated into LC21 from nearby core SL31 on the basis of high-resolution foraminiferal records (available on request). Refinement is possible using the established age-range of 3.57±0.08 ka BP for the Minoan eruption of Santorini [Bruins and Van der Plicht, 1996; Kuniholm et al., 1996], and signal-correlation with the GISP2 K+ series (see tie-lines between Figs. 1e and f, and discussion below).

The record of relative SST changes in LC21 (Fig. 1d) is based on planktonic foraminiferal abundance data with an average Holocene resolution of ~125 years. It represents a relative abundance (%) plot of "warm" versus "cool" species [cf. Rohling et al., 1997; De Rijk et al., 1999], based on modern habitat characteristics discussed in Hemleben et al. [1989], Rohling et al. [1993], Pujol and Vergnaud-Grazzini [1995], and Reiss et al. [2000]. The "warm" group consists of the photosynthetic symbiont-bearing spinose species *Globigerinoides ruber* (pink+white), *Orbulina universa*, *Globigerinoides sacculifer*, *Globigerinella siphonifera*, *Globoturborotalita rubescens*, and *Globorotalita tenella*, with traces of *Hastigerina pelagica* and *Globigerinella digitata*. Today, this association dominates warm and oligotrophic summer mixed layers in subtropical regions, including the easternmost Mediterranean. The "cool" group comprises the non-spinose species *Globorotalia scitula*, *Turborotalita quinqueloba*, *Globorotalia inflata*, and *Neogloboquadrina pachyderma* (right-coiling). These lack symbionts, show a herbivorous feeding preference, and thrive in the cool, more eutrophic conditions fuelled by upmixing of regenerated nutrients in winter mixed layers (*G. scitula*, *T. quinqueloba*, *G. inflata*), or in the previous winters' water below the summer thermocline (*N. pachyderma*). Due to small available sample volumes and very low post~6 ka BP organic carbon contents, there is no supporting alkenone SST record for LC21. However, previous studies support the validity of relative SST trends from our basic faunal proxy, showing similar trends in records based on elaborate statistical transformations, dinoflagellate abundance data, and Uk'37 [Rohling et al., 1993; Targarona et al., 1997; Cacho et al., 1999, 2000, 2001; De Rijk et al., 1999; Hayes et al., 1999; Paterne et al., 1999].

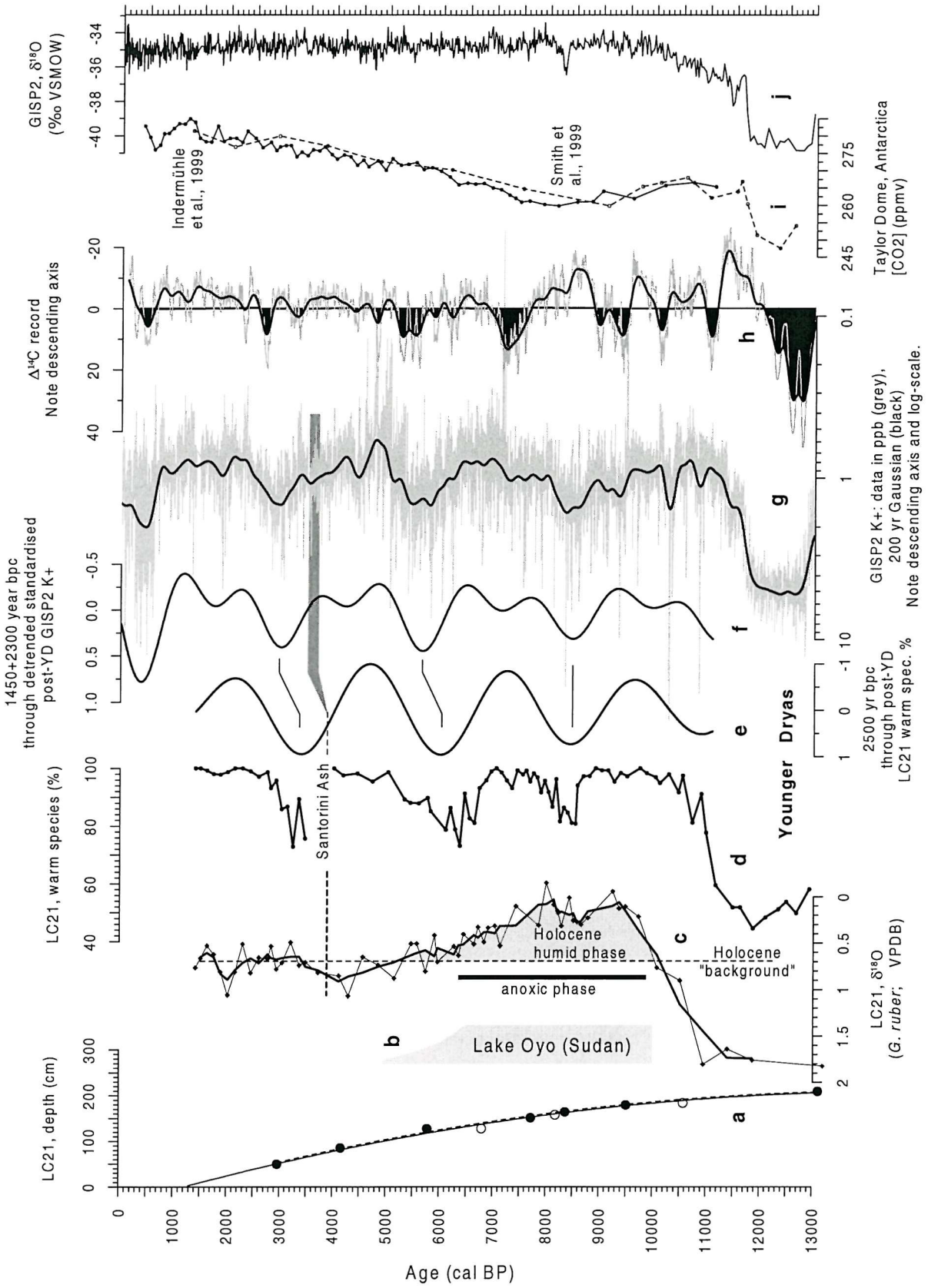
GISP2, δ18O (‰ VSMOW)
-40 -38 -36 -34
Indermühle et al., 1999
Smith et al., 1999
j
i
Taylor Dome, Antarctica [CO2] (ppmv)
245 260 275
Δ14C record Note descending axis
-20 0 20 40
h
0.1 1 10
GISP2 K+: data in ppb (grey), 200 yr Gaussian (black) Note descending axis and log-scale.
g
1450+2300 year bpc through detrended standardised post-YD GISP2 K+
1.0 0.5 0.0 -0.5
f
e
2500 yr bpc through post-YD LC21 warm spec. %
1 0 -1
Younger Dryas
Santorini Ash
LC21, warm species (%)
40 60 80 100
d
Holocene humid phase
Holocene "background"
anoxic phase
c
LC21, δ18O (G. ruber; VPDB)
2 1.5 1 0.5 0
b
Lake Oyo (Sudan)
LC21, depth (cm)
0 100 200 300
a
0 1000 2000 3000 4000 5000 6000 7000 8000 9000 10000 11000 12000 13000
Age (cal BP)

Figure 1. (**a**) Time-stratigraphic framework for Aegean core LC21. Depth scale adjusted for the 10 cm thickness of the ash layer from the Minoan eruption of Santorini. Solid line is 2nd order polynomial fit through all dots, dashed line through filled dots only. Filled dots represent the seven youngest calibrated AMS^{14}C datings of clean handpicked planktonic foraminifera from LC21 (Mercone et al., 2000). The framework presented here also uses a further dating for LC21, at 242.5 cm (Mercone et al., 2000), with a calibrated value of 16.66 ka BP. Open dots are similar datings for nearby core SL31, correlated into LC21 on the basis of high-resolution foraminiferal records for both cores. All datings were calibrated with Calib 4.1, the web-based updated version of the radiocarbon calibration program originally presented by Stuiver and Reimer (1993). An Aegean reservoir age correction of 150 years is applied (Facorellis et al., 1998). Note that the chronostratigraphic frameworks for the two options (one including, one excluding ages from SL31) are virtually identical; (**b**) Interval of presence of a lake in Oyo depression (NW Sudan), marking the early Holocene monsoonal maximum. Tapered end schematically represents the gradual aridification of Oyo Lake (Ritchie et al., 1985); (**c**) Oxygen isotope record for the summer mixed-layer dweller *Globigerinoides ruber* in LC21 (in ‰ VPDB). Bold line represents 3-point moving average that reduces noise. The Holocene background level is approximated at about the mean value of the last 2 kyr covered by the record. An excess depletion (grey) marks the enhanced freshwater flux into the Mediterranean during the monsoonal maximum (cf. Rohling, 1999). Black bar indicates the extent of anoxic sedimentation in LC21 that corresponds to a widespread early Holocene phase of eastern Mediterranean deep water stagnation (eg. Rohling et al., 1993, 1997; Myers et al., 1998; De Rijk et al., 1999; Hayes et al., 1999; Myers and Rohling, 2000; Mercone et al., 2000; 2001); (**d**) Warm-cold plot for LC21, showing Holocene cool events representing relative winter SST reductions of the order of 2-4°C (see text); (**e**) 2500±250 year bandpass filtering component through the linearly detrended Holocene portion of the record shown in (d). Between (e) and (f), tie-lines are indicated that relate peak 'cold events' in the bandpass components for the LC21 warm-cold plot and the GISP2 K^+ series. The inferred offsets are corroborated by the (grey band) tie-line for the Minoan eruption of Santorini (Bruins and Van der Plicht, 1996; Kuniholm et al., 1996; NB. the strong 1623±36 BC sulphate peak in GISP2 cannot further constrain this correlation, since associated ash-shards are non-Minoan (Zielinski and Germani, 1998)). (**f**) Composite of 1450 and 2300 (±10%) year bandpass components through the detrended Holocene portion of the GISP2 K^+ record (solid line) (for frequency analysis, see Mayewski et al., 1997); (**g**) GISP2 K^+ ion series (log-scale). The concentration axis is printed in reverse for consistency with the other records presented. Grey shows the data in ppb, black a 200yr moving Gaussian for main trends; (**h**) Global $\Delta^{14}C$ record (grey; Stuiver et al., 1998), with definition of long-term trends by means of a 200-year moving Gaussian (heavy black line). Long-term positive excursions are highlighted in black. (**i**) Atmospheric CO_2 concentrations from analyses on Taylor Dome ice core, Antarctica (Indermühle et al., 1999; Smith et al., 1999); (**j**) GISP2 ice $\delta^{18}O$ record (Stuiver et al., 1995).

Absolute calibration of faunal SST proxies remains controversial because of the potential impacts of additional physico-chemical influences on abundance patterns (eg., food availability). In fact the ratio used here would be more aptly described as a reflection of the prevalence of summer stratification, but since this is intimately linked to temperature, the ratio can be used to obtain first-order estimates of SST change. The bulk of the warm, oligotropic, eastern Mediterranean shows very high values above 90%, but certain limited regions show lower values, down to ~70%. Such values are attained in regions of pronounced winter cooling, with deeper and more intensive winter overturn than in most of the eastern Mediterranean, and the northern Aegean is such a region. Figure 2 illustrates that the gradient in warm species percentage values observed in core-top sediments [Thunell, 1978; 1979] closely relates to the present-day winter SST gradient in the Aegean Sea [Poulos et al., 1997]. Core LC21's location at the present-day boundary between the cooler Aegean regime and the warmer Levantine conditions assures a sensitive response in the SST proxy.

We contend that the Holocene alternation between intervals with ~100% and intervals with ~80% scores on our faunal proxy (Fig. 1d) allows a sufficiently accurate first-order reconstruction of relative changes in winter temperature/hydrographic conditions. We simply consider that ~100% intervals were characterised by temperature/hydrographic conditions similar to those in nearby modern areas where such scores are attained (the Levantine Basin), and that intervals with scores ~80% were characterised by temperature/ hydrographic conditions found in nearby modern areas with such values in the faunal proxy (the northernmost Aegean) (Fig. 2).

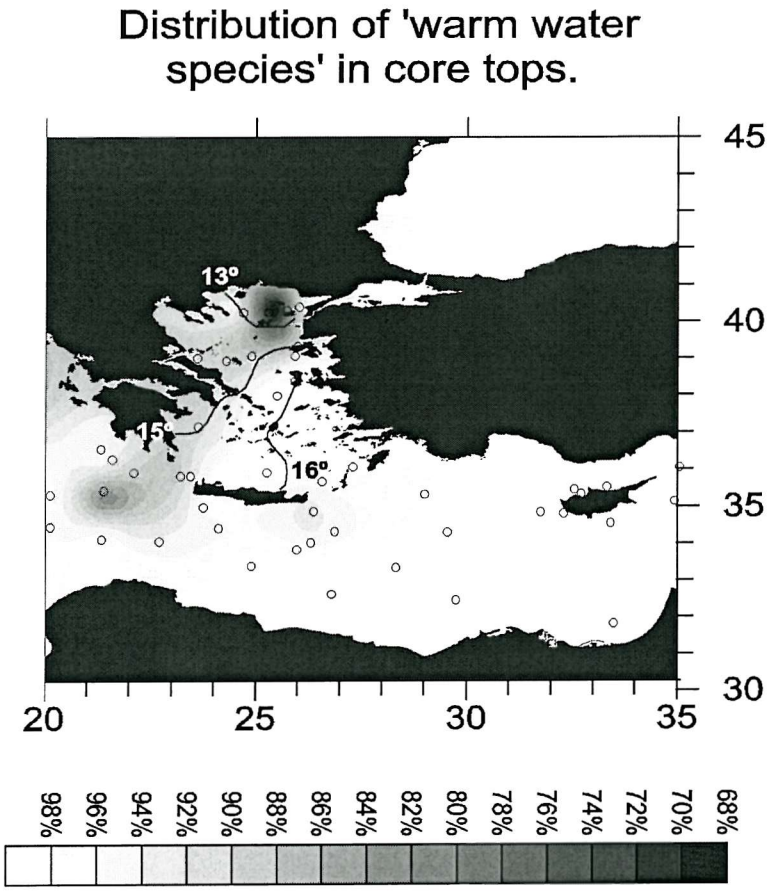

Figure 2. Map of the Aegean Sea and adjacent Levantine Sea, with warm species percentage scores following the method discussed in the text, based on the core-top faunal descriptions of Thunell (1978, 1979). Solid black lines indicate the positions of the present-day 13, 15, and 16°C surface water isotherms in winter (Poulos et al., 1997).

Frequency analysis for the Holocene part of the GISP2 K^+ series was discussed extensively in Mayewski et al. [1997], and the bandpass components (bpc) of 1450 and 2300 years detected in that study are presented in Figure 1f. We here present a similar analysis for the Holocene Aegean SST proxy. First we linearly interpolated the record, to read values at evenly spaced intervals of one decade. Next, we linearly detrended the decadally interpolated data. This was followed by calculation of a maximum entropy spectrum from the autocorrelation matrix as determined over N/4 lags. The results were considered in a logarithmic plot of variance density, and confidence limits determined using the χ^2 distribution. A broad peak was observed at 0.4 cycles kyr^{-1}. Being based on only three effective cycles, the spectral analysis is not entirely conclusive for this frequency. In validation, the spacing of the significant correlation maxima in a complete autocorrelation series was considered (mean spacing: 262 decadal lags between three highly significant correlation maxima). The bandpass component (bpc) presented in Figure 1e is based on a Blackman-type bandpass filter using a window of 0.4±0.04 cycles kyr^{-1}.

4.4 Nature Of Aegean Cooling Events

The ~100% warm fauna in core LC21 resembles that found today in the southeast Mediterranean Levantine basin, where minimum SST remains above 16°C [Hecht, 1992; Pujol and Vergnaud-Grazzini, 1995; Reiss et al., 2000]. In contrast, the faunas in the cool intervals are rather similar to those in the present-day northernmost Aegean (Fig. 2), and tend towards those commonly observed in winter in the western Mediterranean Provençal and Catalan basins where temperatures range between 12.5 and 14°C [Pujol and Vergnaud-Grazzini, 1995; Rohling et al., 1995]. Winter conditions in the Aegean Sea are strongly affected by northerly outbreaks of cold and dry polar/continental air over the basin, funnelled through the valleys of the rivers Axios (Vardar zone), Strimon, and Evros, causing minimum temperatures of 12-14°C in the north to ~16°C in the southerly site of core LC21 [Theocharis and Georgopoulos, 1993; Poulos et al., 1997].

We interpret the Holocene cool events in LC21 (Fig. 1d) in terms of long-term (multi-decadal) periods of increased intensity, duration, and/or frequency of the winter-time northerly air outbreaks, causing winter conditions that today are restricted to the northern sector of the basin to intensify and expand southward over the Aegean Sea. As a consequence, the northerly "Aegean type" regime significantly affected the SE Aegean site of LC21 during the cool events, while episodes with ~100% warm fauna in LC21 reflect a strong dominance of southerly "Levantine type" conditions. This reconstruction implies that the Holocene cool events were characterised by 2-4 °C winter SST reductions throughout the Aegean. The inferred magnitude of the Holocene cooling events compares favourably with that found with the Uk'37 method for the western Mediterranean [Cacho et al., 1999; 2000, 2001]. Note that those studies also related the western Mediterranean cooling events to intensified orographically channelled northerly air outbreaks, supporting the initial identification of this mechanism's importance for intense NW Mediterranean cooling during Atlantic Heinrich events [Rohling et al., 1998].

Our inference that the Aegean cooling events were predominantly winter phenomena is corroborated by the very muted responses in the stable oxygen isotope record of the summer mixed-layer dweller *G. ruber* (Fig. 1c). Short-lived winter cooling events would leave negligible residual signals in the strongly heated summer mixed layer, and, in general, the isotope record through the early-mid Holocene is strongly dominated by changes in the basin's hydrological constraints [cf. Rohling, 1999]. We emphasise that both observations in the modern Aegean Sea [Roether et al., 1996; Klein et al., 1999], and numerical simulations of eastern Mediterranean palaeocirculation [Myers and Rohling, 2000], show that even minor winter SST decreases would have profound impacts on the local hydrography, driving increased rates of local deep-water formation that impact on ventilation of the entire eastern Mediterranean.

4.5 Temporal Relationship Between LC21 And GISP2

Before possible climatic relationships can be discussed, the event timing and structure of the Aegean SST proxy record needs to be compared carefully with that of the GISP2 K^+ proxy for winter/spring intensity of the Siberian High (Fig. 1d-g). The structure of the bandpass components (Figs. 1e,f) suggests in-phase behaviour of the

main Holocene variability (2.3-2.5 kyr cycle) in the early Holocene portion of the two records, but shows a 300 to 400 year offset in the middle to late Holocene that would suggest a minor phase lag (tie-lines between Figs. 1e and f). However, we argue that these offsets are *not* real phase differences, but instead result from minor inconsistencies in the chronostratigraphic framework of LC21. This is clearly witnessed by the fact that the age of the Minoan ash layer in LC21 (~3.9 ka BP) appears too old by the same 300-400 year difference, relative to its actual age of 3.57±0.08 ka BP [Bruins and Van der Plicht, 1996; Kuniholm et al., 1996] (dashed line to grey band through Figs 1c-g). Since the core has been adequately dated in the interval in question, and since the dating technique's analytical precision is an order of magnitude more accurate than the apparent offsets, other processes must be considered that could have introduced a bias of up to several centuries in the datings.

The limiting factor on the quality of AMS^{14}C datings of foraminiferal shells from sediment samples is not analytical precision, but the nature of the material dated. Several processes may introduce bias, such as syn-sedimentary admixture of older shells (eg., eroded from the basin's extensive shelf/slope areas), poorly constrained reservoir-age corrections, or bioturbational admixture of previously deposited material with more recently deposited material. We infer that bioturbation effects were particularly important in causing the 300 to 400 year offset in the younger part of LC21 (around the Minoan ash; see above), since there is no such offset for the event centered at ~8.4 ka BP, which resides within an interval of severe bottom-water dysoxia (sapropel S1) that impeded benthic life and so suppressed bioturbation [Mercone et al., 2001]. The actual data (Fig. 1d,g), rather than the bandpass components, suggest a greatest apparent offset between LC21 and GISP2 of ~500 years for the event centered on 5.5 ka BP in GISP2. The equivalent event in LC21 marks the eastern Mediterranean reventilation after the S1 stagnant/anoxic deep-water episode [cf. Rohling et al., 1997; Myers et al., 1998; De Rijk et al., 1999; Hayes et al., 1999; Mercone et al., 2000; 2001] that corresponded to the early Holocene monsoon maximum (Fig. 1b,c). Dated carbonates from this interval are likely to reflect some admixture of old carbon from previously stagnant parts of the water column (ie., the reservoir age was higher than we have assumed).

The above arguments, with particular emphasis on the discrepancy in the age of the Minoan ash, leads us to conclude (1) that the apparent age offsets between the

Aegean and GISP2 records are *not* genuine phase lags but the result of minor complications in the radiocarbon framework of LC21, and (2) that the main variability in the Aegean record highlighted by the bpc consequently shows a high degree of correspondence in both event timing and structure with that of the GISP2 K^+ proxy for winter/spring intensity of the Siberian High (Fig. 1e,f).

4.6 Discussion And Conclusions

The ~1450 year quasi-cyclicity that strongly dominates the glacial part of the GISP2 K+ record is only weakly represented in the Holocene [Mayewski et al., 1997]. The Holocene section shows a much more powerful ~2300 year cycle (Fig. 1f,g), which is also present in the Δ14C residual series [Stuiver and Braziunas, 1993; Mayewski et al., 1997]. We find a basic periodicity in the Holocene Aegean SST proxy record around 2500 year (Fig. 1e). The Aegean record offers no evidence for a pervasive ~1450 year periodicity such as that described from Glacial and Holocene ice rafted debris records in the North Atlantic [Bond et al., 1997; 1999], and from Holocene drift deposits in the North Atlantic Deep Water overflow region [Bianchi and McCave, 1999]. We consider the widespread dominance of the ~1450 year cyclicity in palaeoclimate proxy records of the last glacial cycle [overviews in Boyle, 1997; Broecker, 2000; and references therein] to be suggestive of amplified environmental responses, involving the thermohaline circulation (THC), in a world bound by glacial boundary conditions. Coral records show that the northern hemisphere was only deglaciated to its present extent by ~7 ka BP [Blanchon and Shaw, 1995], and the associated deceleration of sea level change is corroborated by widespread delta initiation around that time [Stanley and Hait, 2000]. The disappearance of the glacial ice would have minimised ice-related feedback processes responsible for amplified expression of the ~1450 year cycle, so that only North Atlantic sites directly affected by the THC and any remaining continental ice (Greenland) continued to record its weak influence through the Holocene [Bond et al., 1997; 1999; Bianchi and McCave, 1999]. Virtually isolated from the influences of the THC and remaining ice, the Aegean experienced no residual ~1450 year variability during the Holocene, but instead recorded some fundamental ~2300 to 2500 year cycle (Fig. 1d,e).

What is the nature of this roughly 2300 year cycle observed in both the GISP2 K+ and Aegean SST series? It is very similar to the ~2500 year global cooling cycle illustrated by Holocene glacier advances in Europe, N America, New Zealand [Denton and Karlen, 1973] and central Asia [summary in Zhang et al., 2000]. It obviously is not related to any systematic variability in the atmospheric CO_2 record [Indermühle et al., 1999; Smith et al., 1999; Fig. 1i). Within the interval since 7 ka BP (ie., since completion of the deglaciation), however, there is a good match of each of the ~2300 year spaced events in our records with longer-term peaks in the Δ14C residual series, which are associated with so-called triplet Δ14C episodes [Stuiver and Braziunas, 1989, 1993; O'Brien et al., 1995; Stuiver et al., 1998; Fig., 1h]. This correspondence cannot be explained in terms of THC variability since THC-intensity proxies are considered to show variability not of ~2300 years but of ~1500 years [Bianchi and McCave, 1999]. During the early Holocene prior to 7 ka BP, our records suggest a completely different phase-relationship with the Δ14C series than after 7 ka BP. We tentatively suggest that this might be a function of stronger northern hemisphere ice dynamics and associated THC variability prior to 7 ka BP. We refrain from further speculations in view of the limited amount of global information that is available about the Holocene intensity and/or structure of ocean circulation.

Even within the post-7ka BP interval, the match of the Δ14C anomalies and the atmospheric circulation changes reflected in the GISP2 K+ series is not unequivocal when considered in detail (Fig. 1h,g). There either are small offsets in the age-models for these two proxies, or changes in the mixing between the various carbon reservoirs within the circulation/climate system contributed significantly to the Δ14C signals (see also Magny, 1993]. The latter contribution cannot be resolved until a truly global synthesis of Holocene ocean/climate variability is generated, but Bianchi and McCave's [1999] recent insight into North Atlantic THC variability suggests that at least the involvement of that major system can be discounted. Combining our findings with a previous assessment [Van Geel, 1999], and considering the striking agreement that exists between the 10Be [Finkel and Nishiizumi, 1997] and Δ14C records, we suggest that the global ~2300 year cycle in the Holocene reflects a primary forcing mechanism, which could be anchored in solar variability. Our results suggest that this forcing affected the physical environment via reorganisation in the atmospheric circulation, conducive to long-term (multi-decadal) enhancement of winter conditions over the Eurasian continent, with consistently

enhanced pressure in the winter/spring Siberian High over decades to centuries and enhanced polar/continental air outbreaks over the Aegean Sea.

In view of the above, we call for an in-depth multi-disciplinary assessment of the potential for solar modulation of climate on centennial scales. Potential mechanisms for transmission of solar variability to climate change were discussed by Van Geel et al. [1999] and Beer et al. [2000]. Moreover, a climate model suggested that in/decreases in stratospheric ozone production – due to in/decreases in UV radiation – would lead to warming/cooling of the lower stratosphere, which in turn would affect the meridional extent of atmospheric cells [Haig, 1996]. Since this is exactly the type of reorganisation in the climate system that was inferred previously to explain the GISP2 ion series (ie., the Polar Circulation Index for strength and extent of the polar vortex; Mayewski et al., 1997] and which is further supported in the present study, we consider that targeted investigations of Haig's [1996] mechanism are particularly relevant. As stated also by Magny [1993], extrapolation of the observed natural variability into the future suggests a high probability for a distinct natural warming trend over the next few centuries that would intensify any anthropogenic greenhouse effects.

Finally, we note that our reconstruction (a) signals the importance of the incorporation of appropriate modes and time scales of natural climate variability in models for future climate predictions, and (b) offers narrow constraints to the timing and sequence of major Holocene climate events near the Middle East that may help in constraining the chronologies of archaeological records from this region.

ACKNOWLEDGEMENTS.

We thank: the two anonymous reviewers for valuable suggestions; I. Cacho, J. Thomson and F.J. Jorissen for stimulating discussions; M. Sarnthein and J. Kennett for organising the February 2000 SCOR-IMAGES workshop in Trins (Austria) where we first compared the records presented here; and Steve Cooke and Connie de Vries for their efforts concerning the stable isotope analyses of LC21 at the SOC stable isotope facility. Datings for LC21 [after Mercone et al., 2000] and for SL31 [after Casford et al., in press], as well as foraminiferal relative abundance data for both cores, may be requested from E.Rohling@ soc.soton.ac.uk. Data for Figs.1g-j are held at the National Snow and Ice Data Center, University of Colorado at Boulder, and the WDC-A for Paleoclimatology, National Geophysical Data Center, Boulder, Colorado.

CHAPTER 5

SUBMITTED TO MARINE GEOLOGY. AUTHORED BY

Casford[1] J.S.L., E.J. Rohling[1], R. Abu-Zied[1], S. Cooke[1], C. Fontanier[2], M. Leng[3], and J. Thomson[1]

[1] *School of Ocean and Earth Science, Southampton University, Southampton Oceanography Centre, European Way, Southampton, SO14 3ZH, UK.*

[2] *Department of Geology and Oceanography, Bordeaux University, UMR 58-05, Avenue des Facultes, 33405 Talence cedex, France.*

[3] *Natural Environment Research Council Isotope Geoscience Laboratory, Keyworth, UK..*

5. ERROR REDUCTIONS IN A RADIOCARBON-BASED MULTI-PROXY, CHRONOSTRATIGRAPHY

5.1 ABSTRACT

A method is presented to determine and optimise the confidence levels in marine, radiocarbon-based chronostratigraphies, using the Late Glacial to Holocene Aegean Sea as an example. A multi-parameter event stratigraphy dated by AMS ^{14}C, is developed based on highly resolved (centimetre to sub-centimetre) multi-proxy data from four gravity cores. The applicability of this framework to the published, lower resolution records from the Aegean Sea is assessed. Subsequently the comparison is extended into the wider Eastern Mediterranean, using new and previously published high-resolution data from the N.E. Levantine and Adriatic cores. We quantitatively determine that the magnitude of uncertainties in the intercore comparison of AMS datings based on planktonic foraminifera, to be of the order of ± 250 years in radiocarbon convention ages. These uncertainties are related to syn- and post- sedimentary processes that affect the materials dated (e.g. bioturbation, re-deposition and resuspension). This study also offers a background age-control that allows for vital refinements to radiocarbon-based chronostratigraphy in the Eastern Mediterranean, with the potential for similar frameworks to be developed for any other well-studied region. This should lead to a significant advance in constraining the confidence limits in marine radiocarbon-based chronostratigraphies.

5.2 INTRODUCTION

The Aegean Sea and the wider Mediterranean are of particular importance to palaeoceanography, as their limited volumes allow these marginal basins to respond rapidly to climatic change. Due to the restricted communication with the open ocean, responses are also amplified in comparison with the oceanic signal. Generally enhanced sediment accumulation rates in marginal basins allow detailed records of change to be preserved and facilitates high-resolution sampling. As a consequence, detailed investigation of the mechanisms and processes by which these basins respond to climatic forcing is possible [Bethoux et al., 1999]. To accurately interpret this wealth of information, good dating constraints are essential [Sarnthein et al., 2000].

Unfortunately, high accumulation rates commonly increased the probability of sediment reworking. It has been suggested that much of the sediment in the Mediterranean is re-deposited, with some estimates ranging as high as 75% [Stanley 1985]. Another pervasive problem in detailed chronostratigraphic assessment of marine cores is bioturbation, which re-mixes older and more recent material. Hence, individual AMS dating results are not as reproducible as one would wish. Careful sample selection can increase the accuracy of individual datings, but even small amounts of allochthonous carbon, which is normally impossible to detect when picking the material, may cause significant anomalies, which normally biases results toward older ages.

Jorissen et al., [1993] reported a wide dating range for the timing of the I/II and II/III biozonal boundaries in the Mediterranean, reporting ranges spanning 950 and 1270 years, respectively. The association of these boundaries with the global glacial Termination 1a and 1b in their records suggests that the dating range is not real, but an artefact due to dating uncertainties. Jorissen et al., [1993] also note offsets in the radiocarbon ages for a number of evident lithological horizons between two Adriatic cores, IN68-9 and IN68-5 (only 100km apart), with offsets non-systematically varying between 300 and 1400 years, again suggesting dating uncertainties. Moreover dating within a single core may also highlight uncertainties. For example, Jorissen et al., shows several instances of dating "reversals" within individual cores. Core KET 8216 from the Adriatic shows an 800 year difference in the closely-spaced datings from either side of the sapropel (S1) base [Fontugne et al., 1989]. These datings are only 3 cm apart and the

suggested separation would require an almost 3-fold reduction in the average sedimentation rate of the core. KET 8216 also displays an offset between the dating of the Tuff de Agnano tephra layer (9.76 ka B.P.) and its apparent radiocarbon age (9.99 ± 0.16 ka B.P.), which appears at least 250 years too old [Fontugne et al., 1989]. Where individual datings may be offset from "true" age by uncertainties in the reservoir age, this is unlikely to explain substantial dating reversals or large age differences between narrowly space samples. Those offsets are more likely to have resulted from sedimentary processes that affect the dated material.

The main sedimentary processes concerned involve remobilization and redeposition of previously deposited materials and/or bioturbational mixing. Bioturbation effects have been recently discussed, in general [Bard 2001] and for the specific example of *Zoophycos* burrows [Löwemark and Werner 2001]. The latter emphasises that there can be considerable difficulty in recognising *Zoophycos* traces in unconsolidated sediments, and suggest that such burrows may cause age falsifications of as much as 1110-2525 years. These effects are not limited to the remobilization of older material by burrowing, but may also include the pushing of younger material down into older sediments by up to 1m. Fortunately *Zoophycos* appears rare in the Mediterranean [Löwemark and Werner 2001], but it is evident that other burrows if not identified may create similar problems, albeit of smaller magnitudes.

It seems safe to state that the real limitations to age accuracy are not instrumental but are determined by the nature of the dated materials and its sedimentary history. It would appear then that datings on a single horizon are best viewed as individual samples from a probability function, which we aim to quantify here. Previous work (see above) suggests that in this basin, margins of "error" might be expected in the order of ± 800 years. However, these high-resolution Aegean records provide a unique opportunity to constrain the Aegean regional, chronostratigraphic framework, by comparing and contrasting detailed stratigraphic and AMS ^{14}C data. Given the Aegean's limited area it is expected that events occurring here would appear to be synchronous across the basin and the occurrence of the sapropel S1 provides an interval with suppressed bioturbation. We use a multi-proxy approach to reduce parameter-specific bias, such as: regional asynchroneity or patchiness in faunal records; post depositional re-oxygenation of sapropel tops [Higgs et al., 1994; Thomson et al., 1995]; or more general signal

disturbances by, for example, bioturbation and reworking. An event-based stratigraphy enables the assembling of dates from several cores into a "master" stratigraphic framework with the potential to assess the error in any one individual dating. This approach allows insight into both temporal and spatial gradients. This event stratigraphic framework may provide further studies with a means to assess chronostratigraphy in considerable detail and hence, to provide guidance for targeting new AMS radiocarbon datings.

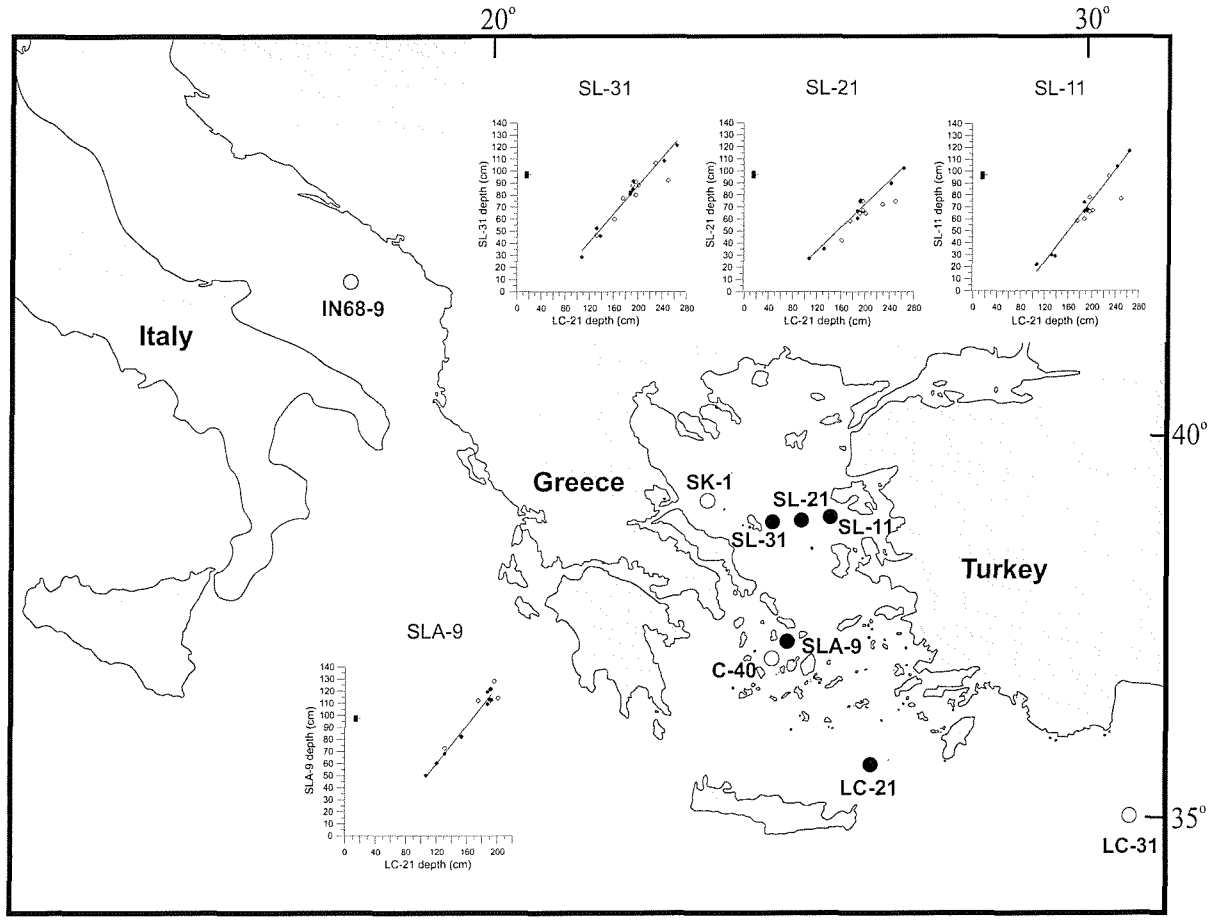

FIGURE 1. Core locations. Filled circles indicate cores presented in this study, open circles are core sites from the published literature (see text for references). Inset graphs show regressions of the depth occurrence (in cm down core) for primary events (filled diamonds) and ancillary events (open diamonds) detailed in this study. A 2 SE error bar is included for the x axis.

5.3 METHODS

We present results for three gravity cores on a transect through the Northern Aegean Basin (SL-11, SL-21 and SL-31), an additional gravity core (SLA-9) and a piston core (LC-21) from the Southern Aegean, and a further piston core (LC-31) from the Levantine Sea. All six cores consist of microfossil-rich hemipelagic ooze with a clearly defined darker band of sapropelic material. Core locations are shown in FIGURE 1, with their exact coordinates and water depth detailed in TABLE 1.

Core	Location	Depth	Regression coefficient (r^2)	No. of points	Equation
LC-21	35° 40' N 26° 35' E	1522 m	-	-	-
SL-11	39° 06' N 25° 48' E	258 m	0.9835	9	y = 0.64x – 52.27
SL-21	39° 01' N 25° 25' E	317 m	0.9661	8	y = 0.49x – 24.53
SL-31	38° 56' N 25° 00' E	430 m	0.9743	9	y = 0.58x – 28.11
SLA-9	37° 31' N 24° 33' E	260 m	0.9809	9	y = 0.81x – 36.65
LC-31	35° 00' N 31° 10' E	2298 m	0.9599	10	y = 0.71x – 28.96
IN68-9	41° 48' N 17° 55' E	1234 m	0.9590	7	y = 0.82x – 66.96
C-40	36° 56' N 24° 05' E	852 m	0.9792	6	y = 0.70x – 29.43
SK-1	39° 04' N 23° 94' E	~1000 m	0.9837	6	y = 2.67x – 39.17

TABLE 1. Location of cores and regression information.

Each core was sampled in a contiguous sequence; SL-21, SL-31 and SLA-9 at 0.5cm intervals; and LC-31 and LC-21 at 1cm intervals for faunal analysis. Cores SLA-9, LC-21 and LC-31 were also sampled at 1cm intervals for geochemical analysis. The faunal samples were freeze dried, weighed, and selected (weighed) sub-samples were disaggregated and wet sieved using demineralized water. The sieved fractions were collected on 600, 150, 125 and 63μm mesh sizes. The >150μm fractions were sub-divided using a random splitter to provide an aliquot of about 200 individual

planktonic foraminifera. These were then determined, sorted on Chapman slides, and counted. Results were recorded as absolute abundance in numbers g^{-1} and as relative abundance or percentages. Results are presented as percentages only, for brevity (FIGURE 2).

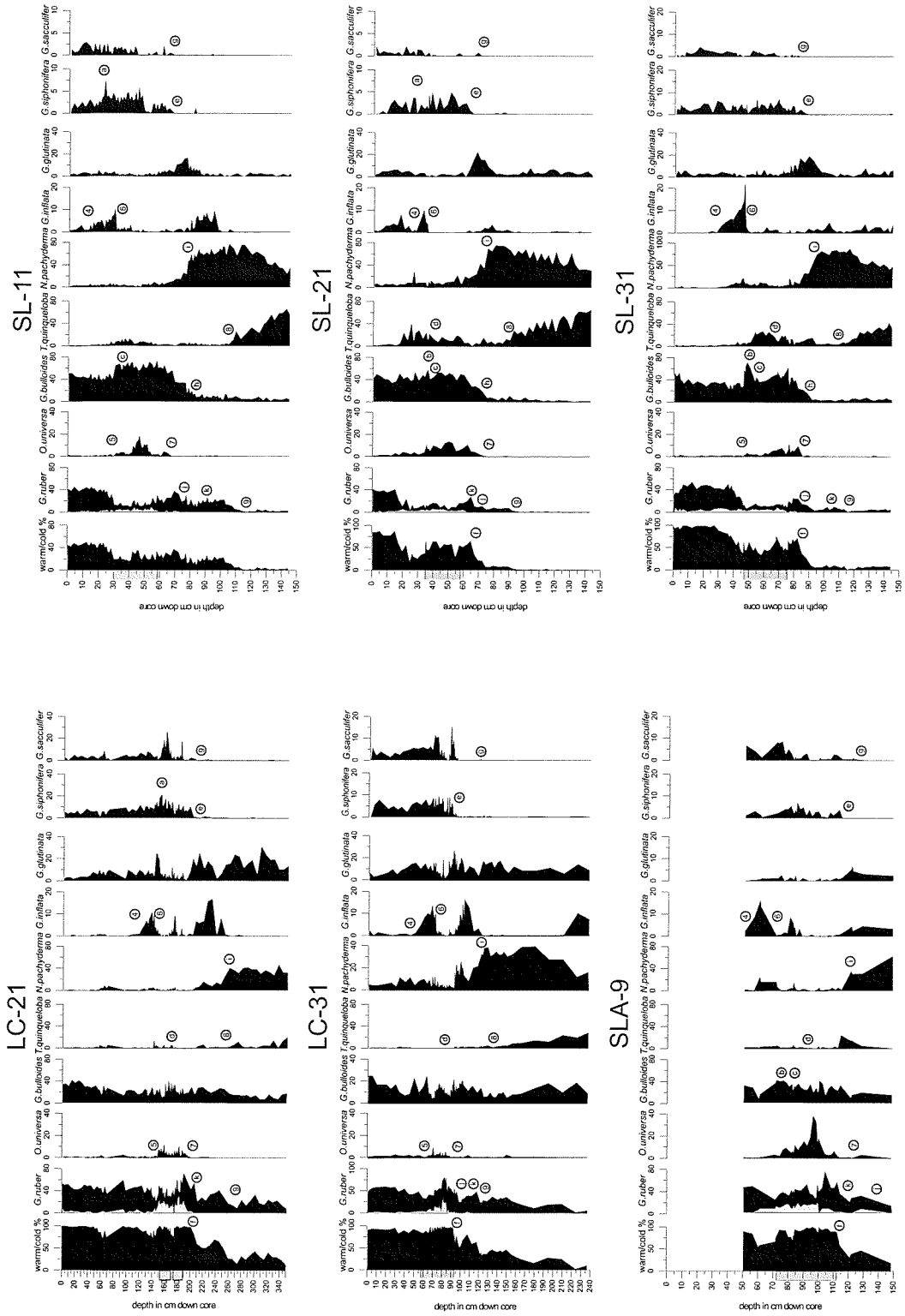

FIGURE 2. Relative abundance of selected planktonic foraminifera with depth, for cores presented in this study. Circled numbers locate occurrence of primary faunal events (detailed in TABLE 3) and circled letters show locations of ancillary events (detailed in TABLE 4).

AMS radiocarbon dates were obtained for cores LC-21, LC-31, SLA-9 and SL-31 using only handpicked clean planktonic foraminiferal tests with no evidence of pyritisation or overgrowth. The samples were too small for mono-specific dating, but no systematic differences would be expected for such dates relative to our results [cf. Jorissen et al., 1993]. The picked material was submitted for analysis at the NERC radiocarbon laboratory at SURRC (LC-21, LC-31) and at the Leibniz AMS Laboratory at Kiel (Germany) (SLA-9, SL-31). Datings for the other cores discussed here have been presented previously: core SK-1 [Zachariasse et al., 1997], IN68-9 [Jorissen et al 1993, Rohling et al., 1997], and C-40 [Geraga et al., 2000]. We present all datings as radiocarbon convention ages, (Table 2) and only use such ages. However for convenience, we also provide results for the calibration of these radiocarbon convention ages (TABLE 2), using the marine mode of the program Calib 4.2 [Stuiver and Reimer 1993] with an additional reservoir-age correction (ΔR) of 149 ± 30 years for the Aegean Sea [Facorellis et al., 1998].

True depth (cm)	Corrected depth (cm)	AMS lab. code	Uncorrected AMS^{14}C age from direct dating or dated horizon (ka BP)	cal. age (ka BP)	cal. age range (1σ) (ka BP)
LC-21					
50	50	CAMS-41314	3.35±0.06	3.20	3.11-3.27
95.5	85.5	CAMS-41313	4.29±0.06	4.40	4.32-4.45
137.75	127.75	CAMS-41311	5.59±0.06	5.95	5.90-6.03
161.5	151.5	CAMS-41315	7.48±0.06	7.90	7.94-7.84
174.25	164.25	CAMS-41312	8.12±0.06	8.52	8.59-8.44
179.5	169.5	AA-30364	9.01±0.07	9.54	9.22-9.86
209	199	AA-30365	11.77±0.08	13.14	12.77-13.51
252.5	242.5	CAMS-41316	14.45±0.06	16.85	16.96-16.74
LC-31					
28.5	28.5	CAMS-45864	3.45±0.05	3.33	3.26-3.36
60.5	60.5	CAMS-45863	6.12±0.05	6.54	6.47-6.62
87.5	82.5	CAMS-45861	8.74±0.05	9.38	9.34-9.43
96.5	91.5	CAMS-45862	8.50±0.05	9.06	8.98-9.19
131.5	126.5	CAMS-45860	12.04±0.05	13.57	13.47-13.69
247.5	242.5	CAMS-45859	32.96±0.05	35.96	
SL-31					
45.75	45.75	KIA9467	6.52±0.05	6.82	6.75-6.89
59.75	59.75	KIA9468	7.95±0.06	8.28	8.20-8.36
78.25	78.25	KIA9469	9.33±0.06	9.82	9.67-9.97
85	85	KIA9470	9.99±0.06	10.60	10.22-10.98
120.25	120.25	KIA9471	14.65±0.08	16.79	16.51-17.01
SLA-9					
60.5	60.5	KIA9472	5.95±0.05	6.21	6.16-6.26
71.5	71.5	KIA9473	6.45±0.05	6.74	6.67-6.81
83.25	83.25	KIA9474	7.90±0.05	8.19	8.12-8.26
99.5	99.5	KIA9475	8.40±0.05	8.77	8.65-8.89
120.5	120.5	KIA9476	11.91±0.07	13.17	12.82-13.52
C-40					
73.5	73.5	Beta-110420	6.83±0.11	7.30	7.20-7.39
82.5	82.5	Beta-110419	7.83±0.14	8.26	8.10-8.38
131	131	Beta-110418	12.35±0.16	13.93	13.72-14.16
SK-1					
143.5			3.81±0.10	3.56	3.50-3.62
284			6.58±0.07	6.90	6.85-6.95
524			9.64±0.08	10.27	10.21-10.33
690			13.43±0.13	15.42	15.39-15.45
IN-689					
11.5	7.5	UTC-500	3.16±0.12	2.93	2.78-3.10
54.5	38.5	UTC-1607	6.39±0.06	6.85	6.77-6.90
157.25	81.25	UTC-501	9.28±0.18	9.93	9.80-10.08
241.5	157.5	UTC-502	13.10±0.20	14.95	14.61-15.30
322.5	201.5	UTC-503	14.20±0.30	16.55	16.15-16.92
510.5	247.5	UTC-504	17.20±0.30	19.82	19.40-20.30

TABLE 2. Age control-points used in the present study, with true depths in the cores, and corrected depths (subtracting thickness of turbidites and ash-layers). Samples with codes starting CAM were prepared as graphite targets at the NERC radiocarbon laboratory and analysed at the Lawrence Livermore National Laboratory AMS facility. Sample codes AA were prepared at Scottish Universities Reactor Research Centre at East Kilbride and analysed at the Arizona Radiocarbon Facility. KIA sample codes indicate the Leibniz AMS Laboratory at Kiel. Radiocarbon convention ages were calibrated using marine mode of programme Calib4.2 [Stuiver and Reimer, 1993, 1998]. Cores LC-31, SL-31, SLA-9, C-40 and SK-1 datings include a local ΔR correction of 149 ± 39 years after [Facorellis et al., 1998]. Dates in LC-21 are after [Mercone et al., 1999] and in C-40 after [Geraga et al., 2000].

Detailed stable oxygen and carbon isotope records have been constructed for several individual planktonic foraminiferal species in cores LC-21, LC-31, SLA-9, SL-11, SL-21 and SL-31, with resolutions in the order of 1cm (FIGURE 3). The species selected here are; the shallow, surface-dwelling *Globigerinoides ruber*; and the deep-living species *Neogloboquadrina pachyderma* which has been associated with the Deep Chlorophyll Maximum at the base of the euphotic layer. This selection follows global and specific Mediterranean habitat descriptions [Hemleben et al 1989, Pujol and Vergnaud-Grazzini 1995, Rohling et al., 1993a, 1995, 1997, De Rijk et al., 1999 and Hayes et al., 1999], which are corroborated for the study area by isotopic evidence [Casford et al., 2001a, in press]. The stable isotope analyses were performed at two separate inter-calibrated facilities: at the Southampton Oceanography Centre (SOC) on a Europa Geo 20-20 with individual acid bath preparation; and at NERC Isotope Geoscience Laboratory (NIGL), Keyworth on the VG-Optima with a common acid bath preparation. Isotope results are reported in ‰ deviations from the Vienna Pee Dee Belemnite standard. Analytical errors are in the order of < 0.06 ‰ (std).

Geochemical samples were freeze-dried, providing approximately 5g of dried material for analysis in LC-31 and 3g in SLA-9 and LC-21. Samples from core LC-31 were analysed by X-Ray Fluorescence (XRF) at SOC. The dried sample was ground in an agate mortar, then 3g was pressed into disc shaped pellets. These pellets were analysed for minor elements. The remaining 2g of material was treated with a fluxing agent, then melted to form glass beads that were analysed for major elements. Cores SLA-9 and LC-21 [Mercone et al., 2000] were analyzed by ICP-AES.

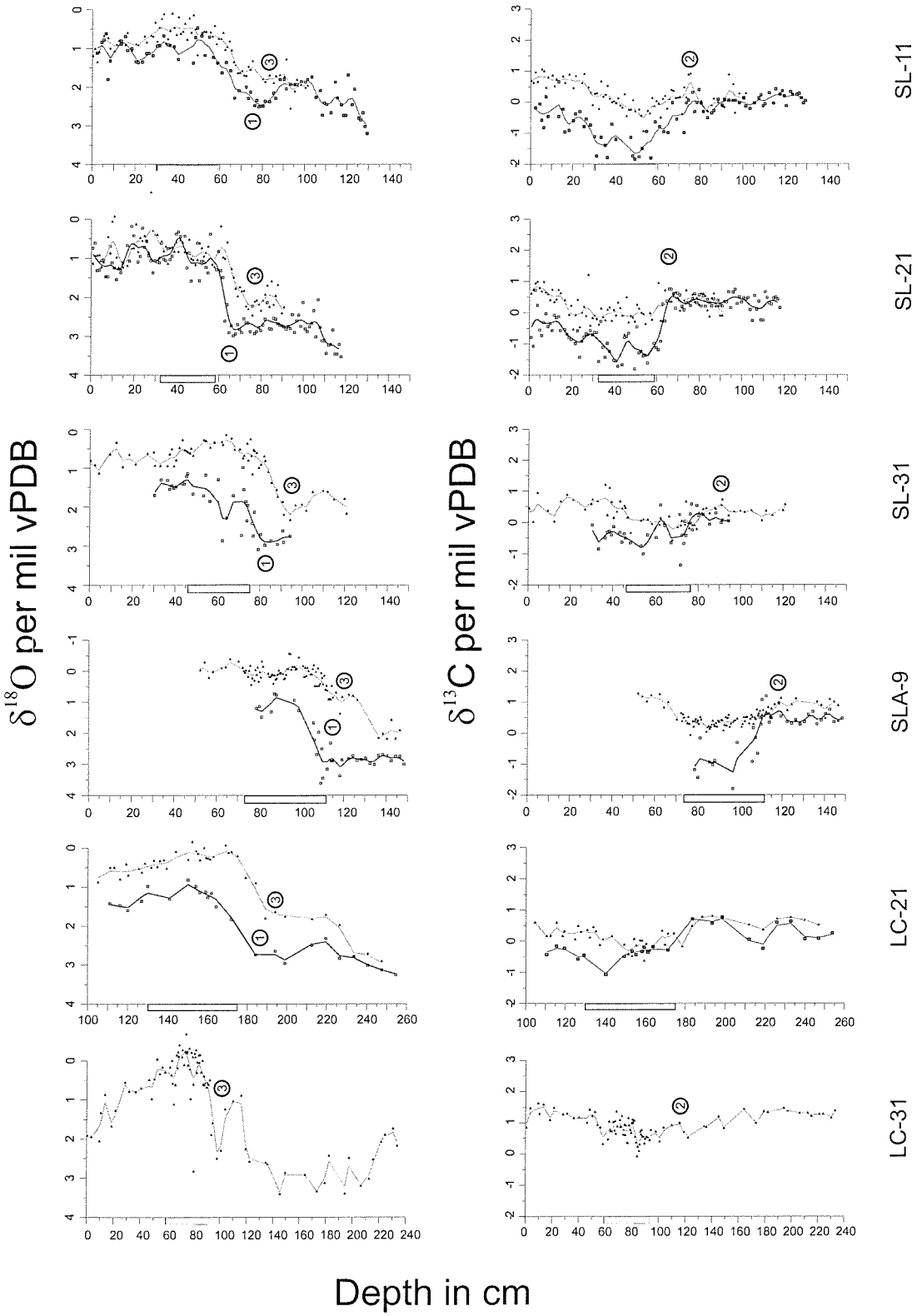

FIGURE 3. Stable isotope records for cores used in this study. (for LC-21 also see [Casford et al., 2001b and Rohling et al., 2001, both in press]). Circled numbers indicate locations of primary isotopic events detailed in TABLE 3.

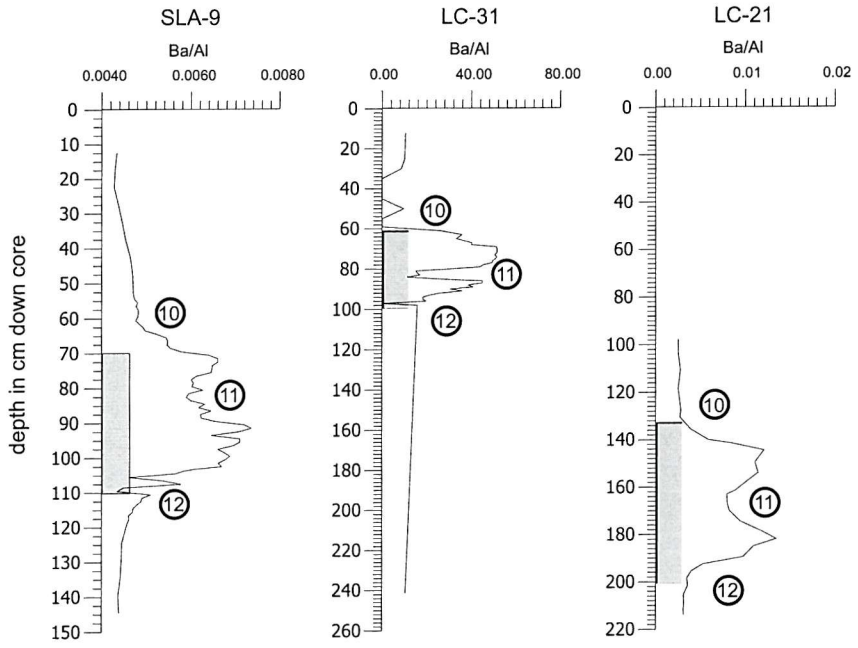

FIGURE 4. Concentration of Barium in bulk sediment, expressed as the ratio Ba/Al, for cores in this study (also see [Mercone et al., 2000] for LC-21). Circled numbers indicate primary geochemical events. (TABLE 3).

5.4 Results and Discussion

We identify and describe 24 faunal, isotopic and geochemical events. Each event is identified by either a sharp change in gradient with time or by alternations of presence and absence in the case of faunal changes. We divide these events into 12 primary and 12 ancillary events. The primary events are defined as occurring in all cores (analysis permitting) and appear to be basin wide. Secondary events (mostly faunal) are defined as those that occur only in some of the cores and/or those that may have the potential to give a local or asynchronous expression.

Primary events are sub-divided into isotopic, faunal and chemical. These are detailed, together with the depth of occurrence, by core, in Table 3.

The 3 primary isotopic events were defined as occurring at the point of inflection for the major gradient changes (see Figure 3). We recognize: (1) the inflection in the *N.pachyderma* $\delta^{18}O$ depletion immediately below base of the sapropel; (2) the high point at the shoulder of the $\delta^{13}C_{G.ruber}$ depletion sited around the onset of the sapropel. The final isotope based primary correlation event is: (3) the inflection in the $\delta^{18}O_{G.ruber}$, marking the start of the depletion sited immediately below base of the sapropel (T1b) similar in character to event (1) however, this appears to occur before the $\delta^{18}O_{N.pachyderma}$ inflection. For a more detailed look at the relative timings and interpretation of these events see Casford et al., [2001b].

Faunal events are identified on exits, entries and particularly strong inflections in the faunal record. Both absolute and relative abundance records were used to establish the exact levels of entries and exits. Inflections in the record were taken from relative abundance plots only and may reflect population shifts rather than changes in absolute numbers of the individual species listed. The primary faunal events (Figure 2 and Table 3) are: (4) the exit or low in *G.inflata* above peak at top of sapropel; (5) the first (near) absence of *O.universa* above the sapropel; and (6) the minimum or absence in *G.inflata* near the top of the sapropel, which is followed by a rapid increase in *G.inflata* on or shortly after the top of the darker sapropelic material. Next, we use (7) the last absence of *O.universa* before the sapropel; (8), the end of the ramping down in *T.quinqueloba* relative abundance below the sapropel, which often ramps down to zero abundance; and

(9) the first, rapid increase in *G.ruber* located below the sapropel, marking the shift from very low values or absence to the higher Holocene/sapropel levels. This population shift seems to be associated with the isotopic increase in $\delta^{18}O_{G.ruber}$ normally identified as Termination 1a [Casford et al 2001a]. This faunal point is constrained at the last low value in *G.ruber's* relative abundance before the increase.

Primary chemical events are identified by their deviation from background values, as shown in Figure 4: (10) the top of Ba/Al anomaly, where it returns to background values; (11) the lowest point in the saddle in the Ba/Al anomaly within the sapropel and; (12) the base of the barium anomaly, identified as point at which Ba/Al ratio appears to depart from background values.

#	Primary Events		LC21 (corr.)	SL11	SL21	SL31	SLA9	LC31	IN689	C-40	SK-1
	ISOTOPES										
1		$\delta^{18}O$ *N.pachyderma* inflection below sapropel.	186.5	66.75	66.75	82.75	109.25	-	-	-	-
2		$\delta^{13}C$ *G.ruber* high before depletion into sapropel.	186.5	74.25	60.75	82.25	119.25	106.5	-	-	-
3		$\delta^{18}O$ *G.ruber* inflection below sapropel.	191.5	68.25	75.75	91.75	112.75	101.5	86.5	-	-
	Fauna										
4		Exit/low in *G.inflata* above sapropel.	106.5	22.25	27.25	28.75	50.25	49.5	27.5	40	271
5		Exit/low in *O.universa* above sapropel.	137	29.25	-	46.25	-	59.5	37.5	65	300
6		Exit/low in *G.inflata* in the top of the sapropel.	131	30.25	35.25	52.75	68.25	71.75	47.5	70.5	293
7		Exit/low in *O.universa* below sapropel.	190.5	67.25	74.75	85.25	121.75	-	71.5	102.5	486
8		Exit/end of *T.quinqueloba* ramp-down.	242	104.25	89.75	108.75	-	134.5	141.5	131	622
9		Last distinct low in *G.ruber* (T1a?)	263	117.25	102.25	121.75	-	172.5	149.5	160.5	648
	Chemistry										
10		Top of Barium anomaly.	120.5	-	-	-	60.5	60	-	-	-
11		Lowest point in Barium saddle.	153	-	-	-	82.5	84	-	-	-
12		Base of Barium anomaly.	188.5	-	-	-	113.5	99	-	-	-

TABLE 3. Depth occurrence of primary events by core (in cm).

Ancillary events are identified in Table 4 and illustrated in Figures 2 and 3.

#	ANCILLARY EVENTS	LC21 (corr.)	SL11	SL21	SL31	SLA9	LC31	IN689	C-40	SK-1
a	Peak in *G.siphonifera.*	-	22.25	26.25	30.25	-				
b	*G.bulloides* peak in sapropel.	-	29.25	34.75	47.25	71.25			73	304.5
c	Low before *G.bulloides* peak.	-	34.25	37.25	53.25	80.25			76.5	314
d	Start of *T.quinqueloba* pick-up in sapropel.	160.5		42.25	60.25	-			89.5	402
e	Last exit of *G.siphonifera* before sapropel.	200.5	67.25	64.75	88.25	114.25			98.5	486
f	Drop in warm/cold plot below sapropel	190.5		64.75	88.25	112.25			95	520
g	Last exit of *G.sacculifer* below sapropel.	195.5	66.25	67.25	80.25	128.25			102.5	565
h	*G.bulloides* low	-	77.25	74.25	91.25	-			120.5	543
i	Shoulder of drop in *N.pachyderma.*	249	77.25	74.75	92.5	-			120.5	571
j	Last absence of *G.ruber rosa* below sapropel.	195.5	78.25	74.75	91.25	-			-	543
k	First occurrence of *G.ruber rosa* before sapropel.	228	96.25	72.25	106.75	-			-	555
l	Mid point of initial $\delta^{18}O$ *N.pachyderma* depletion (T1a)	-	105.75	108.5	120	-			-	-
	Top of dark layer	131	30.25	35.25	46.75	73				
	Base of dark layer	174.5	58.75	58.5	77.5	112.25				

Table 4. Depth occurrence of ancillary events by core (in cm).

Core LC-21 provides one of the best-dated and most understood records in the Eastern Mediterranean [Hayes et al., 1999, De Rijk et al 1999, Mercone et al., 2000, Mercone et al., 2001, Casford et al., 2001b, and Rohling et al., 2001]. Using this core as standard we plot the depth occurrence of the events in each individual core versus their depths in LC-21 (inset in Figure 1). The equations for the regressions of these cross-plots allow the intercomparison of the various records, with all cores standardized to LC-21 depth. The details of each regression are given in Table 1, and we show the ± 2 standard errors (SE) interval relevant for each regression on the plots (Figure 1).

Using the regression equations, we can project AMS ^{14}C datings from the various records (Table 2) onto the age-depth framework of LC-21. As we already have a well-constrained chronostratigraphic framework for LC-21 from its "own" AMS ^{14}C datings (Table 2), we can use the ages projected from other cores to assess the quality of our inter-core correlations. The 2 SE intervals help constraint the uncertainty in the assignment of a LC-21 equivalent depth. If this projection were poor, the dates from the other Aegean cores would be unlikely to fit within the established time framework. Having thus projected all datings into LC-21, the new joint dating framework can be compared against the framework based on the datings for LC-21 proper (Figure 5). As there is no statistical difference between these two frameworks, we conclude that our correlation model is robust. In addition, the age-depth model for LC-21 can thus be corroborated and further detailed by the addition of the projected datings from our correlated cores (also see Rohling et al., [2001], who relate this core to the GISP2 ice-core chronology).

We use the new Aegean time framework, based on our three dated Aegean cores (Figure 5), to examine other previously published, lower resolution records from the same region, SK-1 [Zachariasse et al., 1997] and C-40 [Geraga et al 2000]. These are located close to our existing cores (Figure 1) and provide good comparability with our records. The depth of each identified correlation level is listed in Table 3 and regressions for these cores are shown in Figure 6. The equations for standardizing depths to the LC-21 depth-scale are shown in Table 1, and these were used to calculate the LC-21 equivalent depths for the datings in cores SK-1 and C-40, reported in the source publications. Figure 6 then shows these dates against the Aegean "age versus LC-21 equivalent depth" framework, presented in Figure 5.

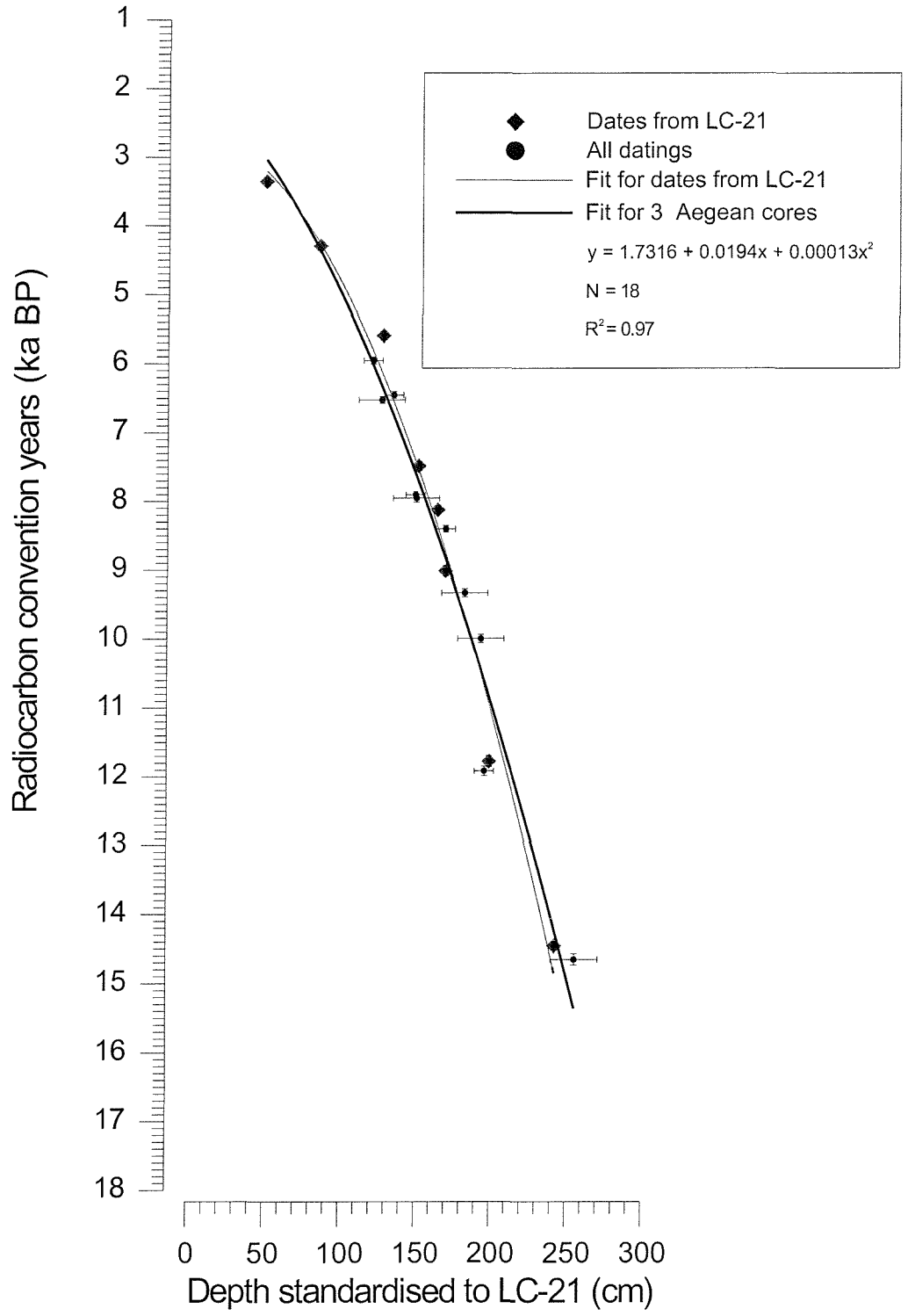

FIGURE 5. Chronostratigraphic framework for LC-21 and all dated Aegean cores from this study. Showing radiocarbon convention ages from our Aegean cores plotted versus a LC-21 equivalent depth. The narrow line indicates best fit regression for datings on LC-21 only, and the heavy line indicates the best-fit regression on our three Aegean Sea cores. Vertical error bars represent the machine errors quoted for the datings (see Table 2) and horizontal error bars equate to the 2 SE from our 'event occurrence versus depth' regressions, projected on a LC-21 equivalent depth scale. In addition, we detail the second order polynomial for all Aegean datings, shown within the legend.

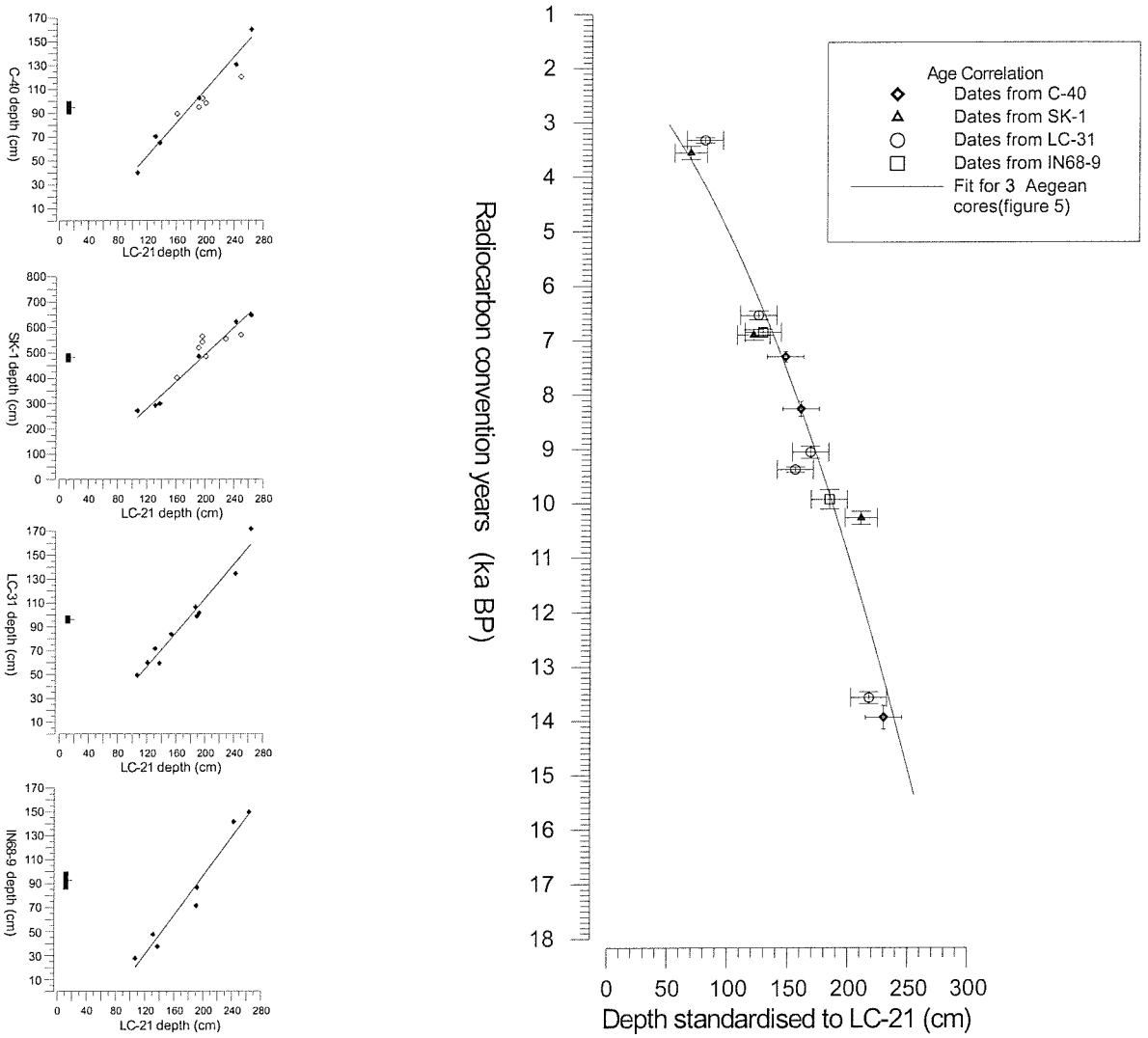

FIGURE 6. The extended, Eastern Mediterranean chronostratigraphic framework including the additional datings from C-40, Sk-1 LC-31 and IN68-9 against the regression for our three Aegean cores from FIGURE 5. Event occurrence regressions are included for to the right of the age correlation. With regressions of the depth occurrence (in cm down core) for primary events (filled diamonds) and ancillary events (open diamonds) and a 2 SE error bar on the x axis.

We also examine the potential use of our method in cores from outside the Aegean Sea. Two high-resolution cores were chosen LC-31 (Levantine/Eastern Mediterranean Sea; this study) and IN68-9 (Adriatic Sea, [Jorissen et al., 1993 and Rohling et al., 1997]). These cores were selected, as both possess multi-proxy records and AMS radiocarbon datings. The identified events are detailed in Table 2 and the regressions are shown in Figure 6 and itemized in Table 1. As with SK-1 and C-40, we plot these cores' AMS 14C datings versus LC-21 equivalent depth (based on the regressions), in comparison with our overall Aegean framework (Figure 5). The result provides strong endorsement of our new correlation method and of our overall Aegean chronostratigraphic framework, hence confirming that the framework is also applicable outside the Aegean Sea.

To evaluate the usefulness of our method and resultant overall chronostratigraphic framework (Figure 5), a critical quantitative assessment is needed. Using our chronostratigraphic framework an age can be predicted for each depth in LC-21, and therefore via the regressions, in any of the correlated cores. We can thus predict an age for all horizons at which AMS ^{14}C datings were preformed. In an ideal case the predicted and analyzed values would coincide perfectly, and a plot of one versus the other (Figure 7) would follow a 45° line through the origin. Since most conceivable mechanisms disturbing AMS based ages tend to impose shifts to too old values, we expect a proportion of the datings to fall off the isoline towards older ages (shades area). Figure 7 shows an excellent overall agreement between predicted and observed ages, even in datings that are entirely independent of the time-frame used for the predictions (ie those in LC-31, IN68-9, C-40 and SK-1).

Using the age in radiocarbon convention years, the isoline falls within 1 SE (~120 years) of the regression through all points (Figure 7). Within our ability to determine therefore, these lines appear to be identical. The framework must then approach the chronostratigraphic accuracy of the dating technique itself and the spread of datings around this line will reflect the total (analytical plus material-related) error of the individual AMS datings. This suggests that the total error for AMS 14C datings on this type of material is of the order of ± 240 (2 SE) in the Eastern Mediterranean.

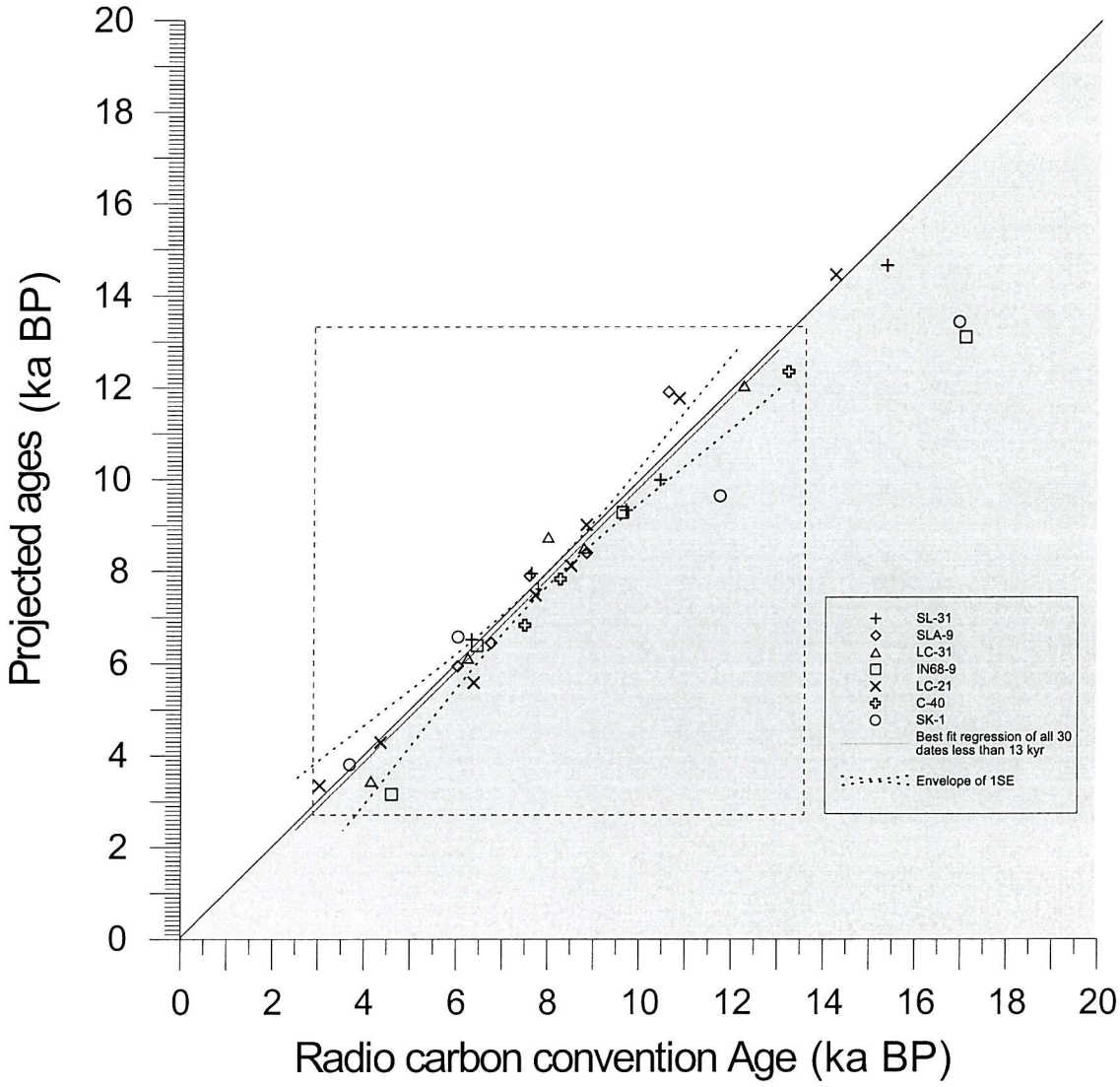

FIGURE 7. Evaluation of the overall time stratigraphic framework. Showing all AMS datings plotted versus their equivalent age, determined from their LC-21 standardized depth and projected on our three Aegean core chronostratigraphic framework. The dotted box shows the extent of the area constrained by our depth occurrence regressions and the shaded area indicates the 'fall' direction expected for older datings. The heavy line indicates the 'best fit' linear regression for all AMS datings younger than 14 ka BP (ie those that fall within our correlatable boundaries) and the lighter weight line shows our projected 45° ideal fit.

Most multi-proxy studies are commonly supported by up to 10 AMS 14C datings, for reasons of economy and practicality (ie availability of material). Some error reduction (relative to individual values) is achieved by these multiple datings, with the reduction proportional to $1/\sqrt{n}$ where n is the number of analyses. Analyzing 10 samples will thus only reduce the overall standard error to 31% of the error on the individual analyses. More than 30 datings are required to obtain an error reduction to 18% of the total spread of data (1 sigma is ± 650 years from this study) and more than 100 samples to reduce this to 10%. Beyond 30 samples, therefore, increasing numbers of datings results in only small and decreasing improvements in accuracy. Since we provide 30 datings inside our correlatable boundaries, relating a new core to our framework offers a cheap and easily applied tool to apply maximal error reduction for the time-stratigraphic framework of a newly added core. Every additional AMS dating correlated into our framework in addition helps to further improve its accuracy and usefulness. We emphasis that the main effort to improve the framework is best targeted at extending the upper and especially lower boundaries of the correlated interval.

5.5 Conclusions

Material used in individual marine AMS ^{14}C datings is normally a composite of both contemporaneous and allochthonous material. The present study provides a method to quantify the total statistical error resultant from this composite. Without error reduction individual AMS dates on planktonic foraminifera or other similar material need to account for the recorded variance. As shown both in the literature and by the 2 sigma (95% of variance) level in our study the errors to individual AMS datings are in the order of 1300 years. To optimize error reductions for the chronostratigraphic context of any single core, at least 30 data points are required, as standard error is proportional to $1/\sqrt{n}$.. Our method offers a standard E. Mediterranean framework with 30 datings already in place, and allows an optimum error reduction to the time frame of any correlated core, resulting in error values of ± 240 years (2SE). To achieve this accuracy we recommend that correlations are based on strict argument applied on events identified in records from multiple proxies, to reduce parameter specific bias. These records in addition require measurements to be on same/equivalent depth samples, to ensure similar

bioturbation effects etc. for all proxies in the core. Finally, the method works best if sampling resolution is better than ~200yrs ensuring accurate placement of events and hence dating accuracy.

Similar exercises could also be performed for other densely studied regions, such as the north Atlantic, which will ultimately help in the development of a better understanding of inter-core syn-/diachronieties and the limitations of chronostratigraphic precision.

CHAPTER 6

6. SYNTHESIS AND FURTHER WORK.

6.1. INTRODUCTION

6.2. ADVANCES IN UNDERSTANDING OF THE PALAEOCEANOGRAPHY OF THE LATE GLACIAL TO HOLOCENE AEGEAN SEA.

6.3. TIMING OF CIRCULATION CHANGE IN THE AEGEAN SEA

6.4. FURTHER WORK

6.1 Introduction

The stated aims of this study were,

1. To complete a high-resolution study of climatic change and palaeoceanography from marine cores.

2. To develop a time stratigraphic framework for the Late Glacial to Holocene in the Aegean Sea

3. To assess the influence of early diagenetic processes on marine sediments in the study region.

This Chapter assesses how the study has addressed these aims, identifying the advances in our understanding of the palaeoceanography of this region and highlighting the timing and sequence of the events revealed. It defines the questions these advances raise and finishes by looking forward to future avenues of research.

6.2 Advances in understanding of the Palaeoceanography of the Late Glacial to Holocene Aegean.

A high-resolution study of climatic change and palaeoceanography from marine cores

This study provides detailed multi-proxy records from six sediment cores in the Aegean Sea and Levantine Basin, including high-resolution (1 cm to 0.5 cm) faunal records of planktonic foraminifera; stable isotope data for oxygen and carbon based on the same samples; and inorganic geochemistry records for cores LC-21, LC-31, SLA-9 and MNB-3. In addition, preliminary data for two further cores (SPR-3 and MNB-3 from the Sporades Basin and Mount Athos Basin) were also produced (Appendix A). These records allow a high-resolution study of climatic change and palaeoceanography in the study region (chapters 2, 3 and 4).

Chapter 2 defined the essential palaeoceanographic changes leading to onset of sapropel S1 and the basin's recovery afterwards, detailing a previously unidentified lag in the isotopic signal of $\delta^{18}O_{N.pachyderma}$ relative to $\delta^{18}O_{G.ruber}$ at Termination 1b and proposing the isolation of deep/intermediate water ~1.5 kyr before the onset of S1. We suggest this is the result of increasing stratification in the water column and use this observation to posit a mechanism for nutrient accumulation. This provides a non-steady state concept to address one of the major problems in sapropel development, namely the source of nutrient supply required to sustain export productivity and hence sapropel accumulation.

Chapters 3 and 4 identify the occurrence of a distinct cycle of cold events previously only documented in the Atlantic. We infer these events are of a high latitude origin [O'Brien et al., 1995; Bond et al., 1997; Mayewski et al., 1997; Alley et al., 1997]. These are locally expressed as cooling associated with increased regional aridity and coincident with cultural reorganisation (Chapter 3). We compare the proxy record from the Aegean Sea with the GISP2 Greenland record (Chapter 4) to provide a more accurate time frame. This reveals a direct correlation between Aegean Sea surface temperature proxies and winter/spring intensities of the Siberian High. The study identifies a ~2300 year spacing in these cold events and equates this with the $\Delta^{14}C$ record, suggesting a solar modulation of the climate. This ~2300 cycle is also notably different from the ~1450 year cycle that dominates the glacial proxy records and may signal a shift from an ice dynamics modulated climate one to more directly related to solar variability.

The development of a high quality time frame in Chapter 4 also associates the onset of sapropel forming conditions with the start of the African Humid Period [deMenocal et al. 2000].

A TIME STRATIGRAPHIC FRAMEWORK FOR THE LATE GLACIAL TO HOLOCENE IN THE AEGEAN SEA

Chapters 4 and 5 provide a quality chronostratigraphy of the study region. We establish a well-dated time frame for LC-21, which was then tuned against the proxy records of the GISP2 ice core. Chapter 5 expands this time framework, initially to the rest of the Aegean Sea and later to the Eastern Mediterranean, by means of a multi-

proxy, event-based stratigraphy. Application of AMS dating in radiocarbon convention years within our event stratigraphy offers significant error reduction providing a well-dated framework from 13 ka BP to the present, with errors in the order of ± 250 years, for the eastern Mediterranean. By correlation with the event stratigraphic framework, it is possible to assign ages to all levels in all the cores in the study region for which a good proxy record is available. This represents the first 'master chronology' for the Late Glacial to Holocene in this region.

ASSESSING THE INFLUENCE OF EARLY DIAGENETIC PROCESSES ON MARINE SEDIMENTS.

Syn- and post- depositional processes appear to have a significant effect on the proxy record (assessed in chapters 2 and 4). The study identified a potential reorganization of the multi-species isotopic record (chapter 2, section 2.4) due to bioturbation. Using a simple model for bioturbational mixing, the homogenization of foraminifera sized particles was determined to be between 2.5 cm and 5 cm in sediments below the sapropel S1. This model suggests that the $\delta^{18}O$ profile would have shown more abrupt shifts than those preserved in the sedimentary record.

The 'reworking' by bioturbation also has significant implications for the dating of marine sediments. Chapter 4 identifies, and for the first time attempts to quantify the errors associated with AMS radiocarbon dating of planktonic foraminiferal material that has undergone such syn-/post-depositional processes (e.g. bioturbation, re-deposition and resuspension). The study demonstrates a confidence limit of the order of ± 250 years in radiocarbon convention ages, highlighting the need for of error reduction in radiocarbon-based time stratigraphic frameworks.

6.3 Timing of Circulation Change in the Aegean Sea

From the findings detailed previously, it is possible to develop a synthesis that interprets changes in palaeo-circulation as the result of climatic change, acting on several different time scales, combining glacial to inter-glacial warming, precession driven

monsoon variation and cooling events acting on the 1450 year and 2300 year cycles identified in Chapter 4. This is presented chronologically based on the Chapter 5 revised time frame, all figures quoted are in thousands of radiocarbon convention years before present (ka B.P.) and have a error of ± 0.25 ka B.P.

The datings of the base of the cores in this study falls outside the correlated limits of our master chronology. The palaeoceanography of the Aegean Sea at the base of our records is characterized by the presence of colder preferring species. It appears to have an isotopically homogenized water column with little isotopic differentiation between the shallow and deeper living species. This has been interpreted as typifying the 'glacial' conditions with a single, well-mixed water body throughout the year.

Termination 1a (T1a) is present in only a few of the cores shown here. Where it is seen we have identified the start of isotopic divergence between our shallow and Intermediate Water (I.W.) indicators (separation of $\delta^{18}O_{G.ruber}$ from $\delta 18O_{N.pachyderma}$, chapter 2). The faunal species present appear to indicate a warming trend into the Bölling Allerød, with an increase in *G.ruber* abundance. As T1a is known to be a period of rapid, global sea level rise, this was interpreted as marking the onset of thermal stratification and seasonal over-turn within the water column. This study also suggests that the timing of T1a may be linked with the flooding of the Aegean Continental shelf. Today this area is shallow (less than 200m), an important source of I.W. and the site of preconditioning for Deep-Water (D.W.) formation.

The Younger Dryas (Y.D.) is poorly defined in the isotope records of the Aegean and Eastern Mediterranean Seas, however it is immediately apparent in the warm/cold plots. Centered on 11.2-radiocarbon convention ka B.P. in our records, this has been associated with Heinrich-layer type cooling events [Bond et al. 1997 and 1999]. These appear to be linked to expansion in the Siberian High and outbreaks of orographically channeled polar air [Rohling et al.1998 and Chapter 4]. Rather than a return to full glacial conditions we interpret this as a shift in dominance from southerly 'Levantine type' conditions to a colder, more arid, northerly dominated regime. We see an increase in *G.inflata* our mixing/winter overturn indicator and no isotope homogenization that may provide evidence of year round mixing. These polar outbreaks occur even today but

are normally short-lived [Saaroni et al. 1996]. It is likely then that the time averaged proxy signal represents a more regular occurrence or a longer persistence of these conditions, as opposed to a jump to a different steady state.

With the ending of the Y.D. the deglacial warming trend is reasserted. Termination1b represents the second rapid rise in sea level from the Last Glacial Maximum, and the start of the Holocene. This period has also been identified with the start of an increase in fresh water input. Due to an increasing regional effect of both the African monsoon (African Humid Period [deMenocal et al. 2000]) and possibly the Indian monsoon [Rohling and Hilgen 1991, Rohling 1994]. This appears to be insolation driven, controlled by precessional orbital variation. In our cores this is characterized by a decrease in *G.inflata*, and a strong $\delta^{18}O$ depletion. This is interpreted as an increase in fresh water input that reduces buoyancy loss and hence further increases water column stability. The dissociation of the $\delta^{18}O$ depletion response between the surface living *G.ruber* and the deeper living *N.pachyderma* suggests that this increasing stability trend culminates in the year round stratification of the water column and the isolation of I.W. This represents the start of the process that will result in the deposition of sapropel S1 by 9.8 radiocarbon convention ka B.P.. Chapter 2 also identifies the isotopic signature of an incursion of 'foreign' I.W., and suggests that the source of this I.W. may be the Adriatic. The Adriatic shelf, is today a vital part of the Adriatic Deep Water (ADW) production, allowing for evaporative salinity increase and rapid winter cooling of surface waters. Flooding of Adriatic shelf would allow the start of such processes. Adriatic I.W. and ADW today are found in both the Aegean (via Rhodes Gyre) and Eastern Mediterranean. Isolation of this I.W. would reduce the concentration of dissolved O_2 as it travels farther from it's point of origin.

The presence of a low oxygen/euxinic intermediate water fits well with the model of sapropel anoxia evolving within the water column [Stratford et al.2000]. Nutrients accumulating in bottom waters are also isolated by this stratification of the water column. The accumulated nutrients may only be accessed by diffusive mixing. The 1/e fold mixing time of ~350 years, suggests that this equates well with timing of start of sapropel production, some 1000 years after the isolation of the I.W. With anoxic I.W. and the

development of anoxia in the sediment [Higgs et al. 1994. Thomson et al.1995], even occasional bottom water ventilation attested to by the presence of benthic foraminifera, would not stop the accumulation of C_{org}. Bottom water anoxia could be quickly re-established, up from the sediment and down the water column as soon as the ventilation stopped.

Occasional ventilation increases again around 8.4 ka B.P. with the first of the Holocene 2300-year recurrent cooling events (Chapter 4), interrupting sapropel deposition. Again, we see the 'Levantine' background conditions replaced with the dominance of a northerly regime, linked to Siberian High expansion. This change in regime may also reduce any direct monsoon influence within the Aegean. However as there is little or no change in background conditions (i.e. warm/wet), as the cool interval ends, we return to sapropel producing conditions. This raises the question; are the proxy signals giving a typical averaged background record, or are they recording the influence of occasional abnormal events?

As the AHP reduces in intensity around 6.2 ka B.P. the sapropel also finishes. This is identified in the records by a sharp rise in *G.inflata* abundance. This is coincident with the next cooling event seen in the warm/cold plots. The coincidence of the polar excursion probably brings to an end the S1 rather earlier than would otherwise have occurred. As this cold event in turn finishes, we see the establishment of what appear to be the modern faunal assemblage and conditions in the Aegean Sea. These continue only interrupted by the next of the 2300-year spaced events. This one centered on 3.6 radiocarbon convention ka B.P.

To summarize, the palaeoceanography of the study region is controlled by three orders of climatic change. A long-term warming from the Last Glacial Maximum, causing a two staged rise in sea level. The warming increases stability in the water column and the increase in sea level expands the surface area of the basins allowing greater evaporation and increases exposure to winter cooling. A precessional timed, insolation driven alteration of monsoonal paths increasing precipitation and runoff in the region, acting to further increase water column stability and reduce buoyancy loss. Finally a recurrent cooling cycle, an ice moderated 1450 years cycle during the Last Glaciation and up to

the Younger Dryas, which is replaced (develops into) a 2300 years event spacing through the Holocene. These produce short lived (~200year) coolings that reduce water column stability and promote buoyancy loss. Further, the evidence suggests that these are not continuous conditions but rather a shift in the balance of normal climatic variability. Coolings for example are simply the product of an increased occurrence of known polar excursions. Sapropel conditions may be the result of an increase in the number of years where increased fresh water input reduces deep-water formation. While this may isolate the bottom waters in most years, it need not necessarily completely prevent ventilation during sapropel deposition.

One implication of the reconstructed stratification of the water column and the incursion of foreign intermediate water would also be that the intermediate water at the onset of the sapropel should give older dates than the surface water. This is open to testing, by the mono-specific dating of foraminifera associated with the two water bodies. *N.pachyderma* appears to give the low variability signal and heavier $\delta^{18}O$ values associated with deeper waters, and would be a suitable candidate to date the intermediate water. *G.ruber* shows considerable isotopic variability, but is known to dwell very shallowly so is probably the best surface-water species. This approach offers an opportunity to confirm the presence of an aging water body and to possibly reveal the source of this intermediate water, by a regional dating program on this horizon. Coring of the Adriatic and Aegean shelves to identify and date flooding horizons would be required to confirm ideas in Chapter 2 linking local intermediate water production to increasing stratification, both at T1a and T1b.

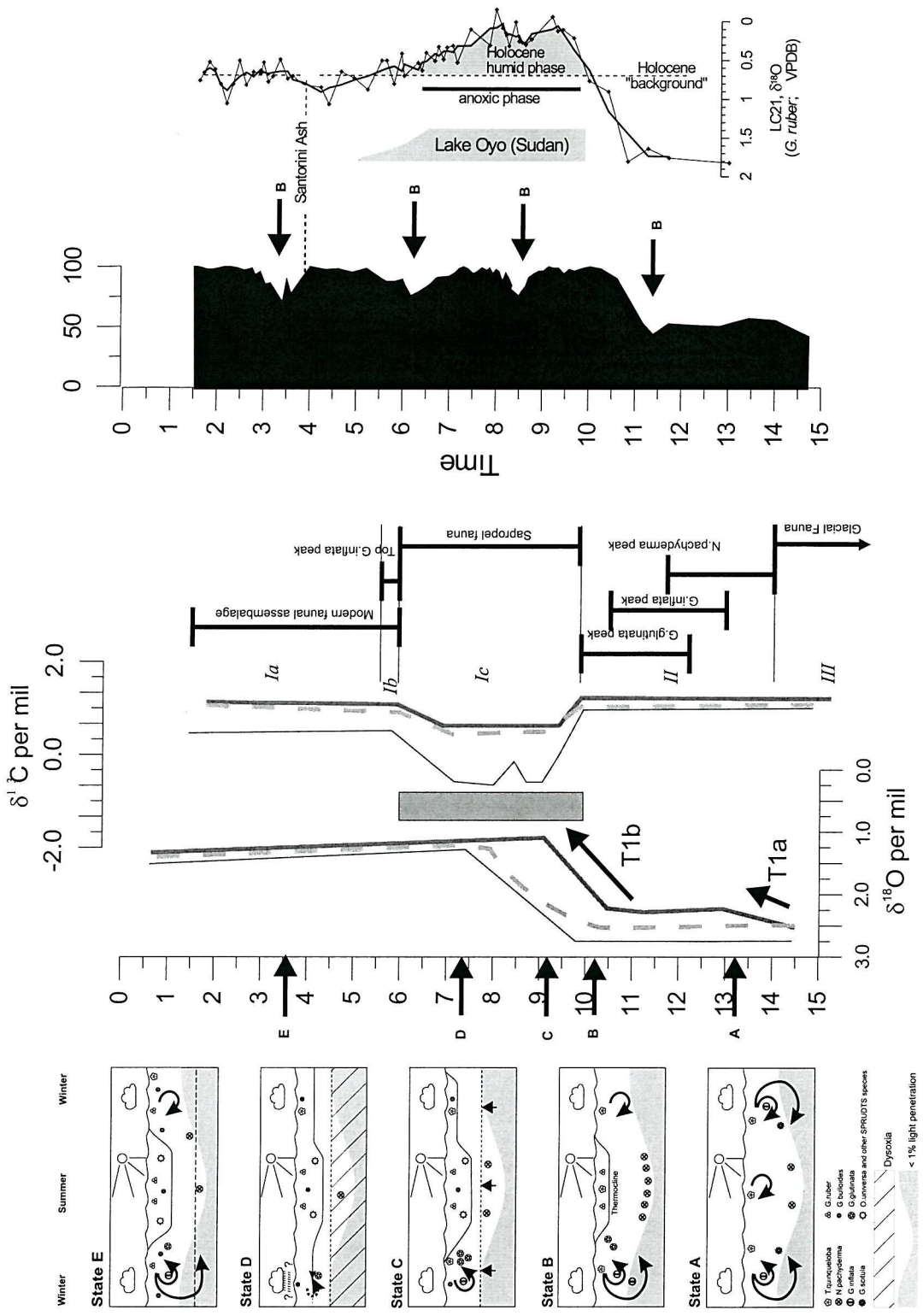

FIGURE 1. Timeline for the Aegean Sea, Late Glacial to Holocene. Based on figures 5 and 6 from Chapter 2 and figure 1 from Chapter 5, this is derived from the most complete core, LC-21. This core also has a timeframe statistically indistinguishable from that developed in Chapter 5. Recurrent cold events are shown to the right of a stylized warm/ cold plot, as a reoccurrence of state B described in Chapter 2. In addition, the extent of the African Humid Phase is shown against an isotope plot of *G.ruber* in LC-21. The interval of presence of Lake Oyo (N.W. Sudan) marks the early Holocene Monsoonal Maximum [Ritchie et al. 1985].

6.4 Further Work

This study clearly illustrates the usefulness of high resolution, multi-proxy studies, revealing a wealth of detail and providing insight into the mechanism of environmental change. As we have seen this in turn raises more questions.

Having highlighted the presence of foreign intermediate water at the base of the sapropel, we next need to determine the source of this water. A regional program of dating *N.pachyderma* and *G.ruber* from the base of the sapropel may highlight the direction of aging of intermediate water throughout the region. In addition, coring of the Aegean and Adriatic shelves would provide evidence of regional flooding of the continental shelf. The dating of these flood horizons may provide insight into the timing of crucial topographic development in areas known to be sources of intermediate water and hence too possible timing of the regional onsets of Deep/Intermediate water formation.

Further studies of sapropel and black shale development are also needed to determine if the mechanisms posited in this study are typical of these deposits or restricted to the Mediterranean. These studies need to cover both temporal and spatial distribution, to assess whether similar mechanisms apply in older sapropels and in the organic rich deposits of the Red Sea, Sea of Japan and other marginal basins. These also provide the potential to unearth additional insights into global and regionally linked climatic systems. Marginal basins are ideal for such studies, giving large amplitude, detailed records of climatic change.

Our records also highlight the shift from a possible ice modulated forcing of climate to direct solar forcing (Chapter 4). This clearly requires further study, involving an in-depth multi-disciplinary (i.e. modeling, climatological and palaeoceanographic) assessment of solar modulation on centennial scales.

Another avenue that would benefit from further investigation, is the possible effect of nutrient concentrations on the applicability of simple warm/cold interpretation and transfer functions for temperature. An understanding of the limits to the faunal reconstruction of sea surface temperature is required to derive accurate information from

these techniques. Clearly, a detailed statistically supported study of these effects would be of great use.

The development of the time frame in this study also raises the potential for further study. Extension of the time framework into the wider Mediterranean, i.e. Ionian and Western Mediterranean would be of use. In addition, local application of this technique hold the potential to accurately correlation between adjacent cores, and defining local limits in AMS dating of microfaunal material from around the globe.

One question not considered in this study concerns the timing and effect of Black Sea outflow. The transect SL-11 to SL-31 was deliberately chosen as it lies across the modern salinity gradient that defines this out-flow. However, there appears to be little evidence of the catastrophic connection proposed by Ryan et al. [1997]. The rapid flooding of the Black Sea and the consequent flushing of the lake that predates it should give a clearly identifiable signal. Why do we not see it in this material? Given the detail in these records it ought to be possible to resolve this question. An earlier connection with the Black Sea may help to explaining the records. Several recent studies have questioned the scenario proposed by Ryan et al. [1997], suggesting a more gradual connection between the Aegean and Black Sea. The start of fresh water influx from the Black Sea into the Aegean has been placed as early as ~12 ka B.P. [Cağatay et al. 2000 Görür et al. 2001, and Algan et al. 2001]. This has considerable potential for further work.

UNDERLYING ASSUMPTIONS

This study has used ecological and taxonomial assumptions from the literature however, this study and other recent work questions several of these assumptions.

Modern habitats of foraminifera appear poorly understood. Due to the variability in the hydrology with time seen in the Aegean, is it safe to assume that all foraminifera are restricted to a single environmental niche and hence a single position in the water column? Is this niche the same as that identified in the present Aegean Sea? These questions require answering. Two linked approaches are required to answer this. 1) A program, of direct identification of foraminifera, the habitat they are discovered in and measurement of the isotopic signal of live tests and the water mass they inhabit. This

approach in needed both in the region of study and the laboratory. 2) The detailed modeling of hydrographic change in the region determining the isotopic composition of the water and relating it to a multi-species determination of actual isotopic values, through a period of known hydrographic change, e.g. a sapropel. A comparison of these two signals may go some way to determining the position individual species prefers in the water column and their degree of variability.

It is also necessary to address why some signals show considerable noise while others in the same sample do not. This may be a function of the individual species favored position in the water column, with surface waters subject to greater variation in temperature and salinity than hence giving a more variable $\delta^{18}O$ record than deeper waters. Equally, it may reflect a shifting niche for the species. To resolve this question we need to understand the composition of the samples that make up our analyses. Are they product of a simple time averaging by deposition or are they weighted to rarer, extreme events, producing large numbers of particular species? A statistically validated study of test composition based on individual forams may address this question.

Recent advances in DNA profiling suggest that many of the morphotypes considered as individual species may in fact be made up of several genetically distinct species [Darling et al. 1996,1997 and 1999]. Direct analysis of the isotopic signals of these genetically determined species and ecological data of their prefer habitat is vital to determining the validity of the signals obtained from the palaeo-record. We need to determine whether individual identifiable species, or groupings of species, can give a representative signal of particular habitats/water masses.

In summary, key to progress seems to lie in concerted efforts involving intensive isotopic analyses on fossil as well as living foraminifera. In addition, this data needs to be placed in sedimentary, ecological and hydrological context.

REFERENCES

ALLEY, R.B., MAYEWSKI, P.A., SOWERS, T., STUIVER, M., TAYLOR, K.C. & CLARCK, P.U. Holocene climatic instability: a prominent, widespread event 8200 yr ago, *Geology* 25, 483-486, 1997.

ASKU, A.E., T. ABRAJANO, P.J. MUDIE AND D. YAŞAR, Organic geochemical and palynological evidence for the terrigeneous origin of the organic matter in Aegean Sea sapropel S1. *Marine Geol.,* 153, 303-318, 1999.

BARD, E., (2001) Paleoceanographic implications of the difference in deep-sea sediment mixing between large and fine particles, *Paleoceanography* 16(3), 235-239, 2001.

BAR-MATTHEWS, M., AYALON, A., KAUFMAN, A. & WASSERBURG, G.J. The eastern Mediterranean paleoclimate as a reflection of regional events: Soreq cave, Israel, *Earth and Planetary Science letters* 166, 85-95, 1999.

BEER, J., MENDE, W., and STELLMACHER, R., The role of the sun in climate forcing, *Quat. Sci. Rev., 19*, 403-415, 2000.

BETHOUX, J.P., B. GENTILI, P. MORIN, E. NICHOLAS, C. PIERRE and D. RUIZ-PINO The Mediterranean Sea: a miniature ocean for climatic and environmental studies and a key for climatic functioning of the North Atlantic. *Prog. Oceangr.* 44, 131-146, 1999.

BÉTHOUX, J.P. & GENTILLI, B. The Mediterranean Sea, coastal and deep-sea signatures of climatic and environmental changes, *Journal of Marine Systems* 7, 383-394, 1996.

BÉTHOUX, J.P., GENTILLI, B., RAUNET, J. & TAILLEZ, D. Warming trend in the western Mediterranean deep water, *Nature* 347, 660-662, 1990.

BIANCHI, G.G., AND MCCAVE, I.N., Holocene periodicity in North Atlantic climate and deep-ocean flow south of Iceland, *Nature, 397*, 515-517, 1999.

BIJMA, J., W.W. FABER JR., CH. HEMLEBEN, Temperature and salinity limits for growths and survival of some planktonic foraminifers in laboratory cultures. *J. Foram. Res.*, 20, 95-116, 1990a

BIJMA, J., J. EREZ and CH. HEMLEBEN Lunar and semi lunar reproductive cycles in some spinose planktonic foraminifera. *J. Foram. Res.*, 20, 117-127, 1990b

BISCAYE, P.E., GROUSSET, F.E., REVEL, M., VAN DER GAAST, S., ZIELINSKI, G.A., VAARS, A. AND KUKLA, G. Asian provenance of glacial dust (stage 2) in the Greenland Ice Sheet Project 2 ice core, Summit, Greenland. *J. Geophys. Res., 102*, 26765-26782, 1997.

BLANCHON, P., AND SHAW, J., Reef drowning during the last deglaciation: evidence for catastrophic sea-level rise and ice-sheet collapse, *Geology, 23*, 4-8, 1995.

BOND, G., SHOWERS, W., CHESEBY, M., LOTTI, R., ALMASI, P., DEMENOCAL, P., PRIORE, P., CULLEN, H., HAJDAS, I., AND BONANI, G., A pervasive millenial-scale cycle in North Atlantic Holocene and Glacial climates, *Science, 278*, 1257-1266, 1997.

BOND, G.C., SHOWERS, W., ELLIOT, M., EVANS, M., LOTTI, R., HAJDAS, I., BONANI, G., AND JOHNSON, S., The North Atlantic's 1-2 kyr climate rhythm: relation to Heinrich events, dansgaard/Oeschger cycles and the little ice age, in Clark, P.U., Webb, R.S., and Keigwin, L.D. (eds.) Mechanisms of global climate change at millenial time scales, *AGU Geophys. Monogr., 112*, pp. 35-58, American Geophysical Union, Washington DC, 1999

BOYLE, E.A., Characteristics of the deep ocean carbon system during the past 150,000 years: ΣCO_2 distributions, deep water flow patterns, and abrupt climate change, *Proc. Natl., Acad. Sci. USA, 94*, 8300-8307, 1997.

BROECKER, W.S., Abrupt climate change: causal constraints provided by the paleoclimate record, *Earth-Sci. Rev., 51*, 137-154, 2000.

BRUCE, J.G., AND H. CHARNOCK, Studies of winter sinking of cold water in the Aegean Sea. *Rapports Comm. Int. Mer. Médit.*, 18, 773-778, 1965.

BRUINS, H.J., AND VAN DER PLICHT, J., The exodus enigma, *Nature, 382*, 213-214, 1996.

BRYDEN, H.L., & WEBB, D.J. A perspective on the need to build a dam across the Strait of Gibraltar, *Newsletter European Geophysical Society* 69, 1-3, 1998.

BURMAN, I. AND O.H. OREN, Water outflow close to the bottom from the Aegean. *Cahiers Océanographique*, 22, 775-780, 1970.

CACHO, I., GRIMALT, J.O., CANALS, M., SBAFFI, L., SHACKLETON, N.J., SCHÖNFELD, J., AND ZAHN, R., Variability of the western Mediterranean Sea surface temperatures during the last 25,000 years and its connection with the northern hemisphere climatic changes, *Paleoceanography, 16*, 40-52, 2001.

CACHO, I., GRIMALT, J.O., SIERRO, F.J., SHACKLETON, N.J., AND CANALS, M., Evidence of enhanced Mediterranean thermohaline circulation during rapid climate coolings, *Earth Planet. Sci. Lett., 183*, 417-429, 2000.

CACHO, I., GRIMALT, J.O., PELEJERO, C., CANALS, M., SIERRO, F.J., FLORES, J.A., AND SHACKLETON, N., Dansgaard-Oeschger and Heinrich event imprints in Alboran Sea paleotemperatures, *Paleoceanography, 14*, 698-705, 1999.

CAMPBELL, I.D., CAMPBELL, C., APPS, M.J., RUTTER, N.W. & BUSH, A.B.G. Late Holocene: 1500 yr climatic periodicities and their implications, *Geology* 26, 471-473 (1998).

CAPOTONDI, L., BORSETTI, A.M. & MORIGI, C. Foraminiferal ecozones, a high-resolution proxy for the late Quaternary biochronology in the central Mediterranean Sea, *Marine Geology* 153, 253-274 1999.

CASFORD J.S.L., E.J. ROHLING, R. ABU-ZIED, S. COOKE, C. FONTANIER, M. LENG, AND V. LYKOUSIS Circulation changes and nutrient concentrations in the Late Quaternary Aegean Sea: A non-steady state concept for sapropel formation *Paleoceanography*, in press, 2001a

CASFORD, J.S.L., R. ABU-ZIED, E.J. ROHLING, S. COOKE, K.P. BOESSENKOOL, H. BRINKHUIS, C. DE VRIES, G. WEFER, M. GERAGA, G. PAPATHEODOROU, I. CROUDACE, J. THOMSON, V. LYKOUSIS, Mediterranean climate variability during the Holocene *Mediterranean Marine Science,* in press, 2001b.

CITA, M.B., VERGNAUD-GRAZZINI, C., ROBERT, C., CHAMLEY, H., CIARANFI, N. & D'ONOFRIO, S. Paleoclimatic record of a long deep sea core from the eastern Mediterranean. *Quaternary Research* 8, 205-235, 1977.

CRAMP, A. & G. O'SULLIVAN, Neogene sapropels in the Mediterranean: a review., *Marine Geology*, 153, 11-28, 1999.

CRAMP, A., & M. COLLINS, A Late Pleistocene-Holocene sapropel layer in the N.W. Aegean Sea eastern Mediterranean., *Geo-Mar. Letts.*, 8, 19-23, 1988.

CRAMP, A., M. COLLINS and R. WEST, Late Pleistocene-Holocene sedimentation in the NW Aegean Sea: A palaeoclimatic palaeoceanographic reconstruction. *Paleogeogr., Paleoclimat., Paleoecol.,* 68, 61-77, 1988.

CRISPI, G., A. CRISE and E. MAURI , A seasonal three-dimensional study of the nitrogen cycle in the Mediterranean Sea: Part II verification of the energy constrianed trophic model. *J. Mar. Sys.*,20, 357-379, 1999.

DARLING, K.F., C.M. WADE, I.A. STEWART, D. KROON, R. DINGLE, A.J.L. BROWN, Molecular evidence for genetic mixing of Arctic and Antarctic subpolar populations of planktonic foraminifers. Nature, 405(6782), 43-47, 2000

DARLING, K.F., D. KROON, C.M. WADE, & A.J.L. BROWN, Molecular phylogeny of the planktic foraminifera. *Journal of Foraminiferal Research,* 26(4) 324-330, 1996

DARLING, K.F., C.M. WADE, D. KROON, A.J.L. BROWN, Planktic foraminiferal molecular evolution and their polyphyletic origins from benthic taxa. *Marine Micropaleontology*, 30(4), 251-266, 1997.

DE LANGE, G.J., J.J. MIDDELBURG, C.H. VAN DER WEIJDEN, G. CATALANO, G.W. LUTHER III, D.J. HYDES, J.R.W. WOITTIEZ and G.P. KLINKHAMMER , Composition of anoxic hypersaline brines in the Tyro and Bannock Basin, eastern Mediterranean., *Mar. Chem.*, 31, 63-88, 1990.

DE RIJK, S., ROHLING, E.J., and HAYES, A. Onset of climatic deterioration in the eastern Mediterranean around 7 ky BP; micropalaeontological data from Mediterranean sapropel interruptions. *Mar. Geol.*,153, 337-3432, 1999.

DEMENOCAL P., J. ORTIZ, T. GUILDERSON, J. ADKINS, M.SARNTHEIN, L. BAKER and M. YARUSINSKY Abrupt onset and termination of the African Humid Period: rapid climate responses to gradual insolation forcing. *Quat. Sci. Reveiws*, 19, 347-361, 2000.

DENTON, G.H., AND KARLEN, W., Holocene climatic variations – Their pattern and possible cause, *Quat. Res., 3*, 155-205, 1973.

EDMUNDS, W.M., E.FELLMAN and I.B. GONI Lakes, groundwate and palaeohydrology in the Sahel of NE Nigeria: evidence from hydrogeochemistry. *J. Geol. Soc. London*, 156, 345-355, 1999.

FACORELLIS, Y., MANIATIS, Y., AND KROMER, B., Apparent ^{14}C ages of marine mollusc shells from a Greek island: calculation of the marine reservoir effect in the Aegean Sea, *Radiocarbon, 40*, 963-973, 1998.

FINKEL, R.C., AND NISHIIZUMI, K., Beryllium 10 concentrations in the Greenland Ice Sheet Project 2 ice core from 3-40 ka. J. Geophys. Res., 102, 26699-26706, 1997.

FONTANIER, C. Successions ecologiques dea foraminiferes benthiques et planctaniques durant les derniers 13.000 ans en mer Egee. Unpublished dissertation, Bordeaux University, 2000.

FONTUGNE, M.R., M. PATERNE, S.E. CALVERT, A. MURAT, F. GUICHARD and M. ARNOLD Adriatic deep water formation during the Holocene; implications for the reoxygenation of the deep Mediterranean Sea. *Paleoceanography*, 4, 199-206, 1989.

GASSE, F., FONTES, J.CH., VAN CAMPO, E. & WEI, K. Holocene environmental changes in Bangong Co basin (western Tibet). Part 4: Discussion and conclusions, *Palaeogeography, Palaeoclimatology, Palaeoecology* 120, 79-92, 1996.

GERAGA M., ST. TSAILA-MONOPOLIS, C. IOAKIM, G. PAPATHEODOROU AND G. FERENTINOS Evaluation of palaeoenvironmental changes during the last 18,000 years in the Myrtoon basin, SW Aegean Sea. *Palaeo., Paleo., Paleo.*, 156, 1-1714, 1999.

HAIGH, J.D., The impact of solar variability on climate, *Science, 272*, 981-984, 1996.

HASSAN, F.A. Holocene climatic change and riverine dynamics in the Nile Valley, in *Before food production in North Africa, Union Internationale de Sciences Prehistoriques et protohistoriques, XIII world congress, Forli, 1996* (eds di Lernia, S. & Manzi, G.), 43-51 (A.B.A.C.O Edizioni, Rome), 1998.

HASSAN, F.A., Abrupt Holocene climatic events in Africa, in *Aspects of African Archaeology* (eds Pwiti, G. & Soper, R.), 83-89. (University of Zimbabwe, Harare), 1996.

HASSAN, F.A., Desert environment and origins of agriculture in Egypt, *Norwegian Archaeological Review* 19, 63-76 1986.

HASSAN, F.A., Holocene palaeoclimates of Africa, *African Archaeological Review* 14, 213-230, 1997.

HASSAN, F.A., Nile Floods and political disorder in early Egypt, in *Third millenium BC climate change and old world collapse* (eds Nüzhet Dalfes, H., Kukla, G. & Weiss, H.), *NATO ASI Series* I 49, 1-23 (Springer-Verlag, Berlin), 1997.

HAYES, A., E.J. ROHLING, S. DE RIJK, D. KROON AND W.J. ZACHARIASSE, Mediterranean planktonic foraminifera faunas during the last glacial cycle, *Mar. Geol.,* 153, 239-252, 1999.

HECHT, A., Abrupt changes in the characteristics of Atlantic and Levantine intermediate waters in the southeastern Levantine basin, *Oceanol. Acta, 15*, 25-42, 1992.

HEMLEBEN, C., M. SPINDLER AND O.R. ANDERSON *Modern Planktonic Foraminifera* Publ. Springer, New York, 363pp. 1989.

HIGGS, N.C., J. THOMSON, T.R.S. WILSON, CROUDACE I.W. Modification and complete removal of eastern mediterranean sapropels by postdepositional oxidation. *Geology* 22 (5), 423-426, 1994.

HILGEN, H.J. Astronomical calibration of Gauss to Matuyama sapropels in the Mediterranean and implication for the geomagnetic polarity time scale. *Earth Planet. Sci. Lett.*. 104, 226-244, 1991.

HILL, A.E., & MITCHELSON-JACOB, E.G. Observations of a poleward-flowing saline core on the continental slope west of Scotland, *Deep-Sea Research* 40, 1521-1527, 1993.

HUANG, T.C. and D.J. STANLEY Western Alboran Sea; Sediment Dispersal, Ponding and Reversal of Currents. In THE MEDITERRANEAN SEA; A NATURAL SEDIMENTATION LABORATORY published by Dowden, Hutchinson & Ross, Stroudsburg, Pennsylvania. 521-559, 1972.

INDERMÜHLE A., STOCKER, T.F., JOOS, F., FISCHER, H., SMITH, H.J., WAHLEN, M., DECK, B., MASTROIANNI, D., TSCHUMI, J., BLUNIER, T., MEYER, R., AND STAUFFER, B., Holocene carbon-cycle dynamics based on CO2 trapped in ice at Taylor Dome, Antarctica. *Nature, 398*, 121-126, 1999.

JENKINS, J.A., AND D.F. WILLIAMS Nile water as a cause of eastern Mediterranean sapropel formation; evidence for and against. *Mar. Micropaleontol.*, 9, 521-534, 1983.

JORISSEN, F.J., A. ASIOLI, A.M. BORSETTI, L.CAPOTONDI, J.P. DE VISSER, F.J. HILGEN, E.J. ROHLING, K. VAN DER BORG, C. VERGNAUD GRAZZINI, and W.J. ZACHARIASSE Late Quaternary central Mediterranean biochronology. *Mar. Micropaleontol.,* 21, 169-189, 1993.

KALLEL, N., M. PATERNE, J.C. DUPLESSY, C. VERGNAUD-GRAZZINI, C. PUJOL, L. LABEYRIE, M. ARNOLD, M. FONTUGNE and C.PIERRE. Enhanced rainfall in the Mediterranean region during the last sapropel event. *Oceanol. Acta*, 20, 697-712, 1997

KLEIN, B., ROETHER, W., MANCA, B.B., BREGANT, D., BEITZEL, V., KOVACEVIC, V., AND LUCHETTA, A., The large deep water transient in the eastern Mediterranean, *Deep-Sea Res., 46*, 371-414, 1999.

KUNIHOLM, P.I., KROMER, B., MANNING, S.W., NEWTON, M., LATINI, C.E. & BRUCE, M J. Anatolian tree rings and the absolute chronology of the eastern Mediterranean, 2220-718 BP, *Nature* 381, 780-783, 1996.

LACOMBE, H., P. TCHERNIA and G. BENOIST Contribution à 'étude hydrologique de la Mer Egée en période d'été. *Bull. Inf. COEC*, 8, 454-468. 1958.

LAMB, H.H., *Climate; past, present and future* 1, 613 pp. (Methuen & Co, London, 1972).

LASCARATOS, A. Hydrology of the Aegean Sea. *Reports in Meteorology and Oceanography*, 40 vol I., 313-431, 1989.

LASCARATOS, A., W. ROETHER, K. NITTIS, and B. KLEIN Recent changes in deep water formation and spreading in the eastern Mediterranean Sea: a review. *Progress in Oceanography* 44(1/3)5-36, 1999

LEAMAN, K.D. & SCHOTT, F.A. Hydrographic structure of the convection regime in the Gulf of Lions: Winter 1987, *Journal of Physical Oceanography* 21, 575-598, 1991.

LEGRAND, M. AND MAYEWSKI, P.A., Glaciochemistry of polar ice cores: A review. *Rev. Geophys.,*35, 219-143, 1997.

LOURENS, L.J.A., F.J. ANTONARAKOU, F.J. HILGEN, A.A.M. VAN HOOF, C. VERGNAUD-GRAZZINI and W.J. ZACHARIASSE Evaluation of the Plio-Pleistocene astronomical timescale. *Paleoceanography*, 11, 391-431. 1996.

LÖWEMARK L. and F. WERNER Dating errors in high-resolution stratigraphy: a detailed X-ray radiograph and AMS-14C study of *Zoophycos* burrows. *Mar. Geol.*, 177, 191-198, 2001.

MAGNY, M., Solar influences on Holocene climatic changes illustrated by correlations between past lake-level fluctuations and the atmospheric 14C record, *Quat. Res., 40*, 1-9, 1993.

MARIOLOPOULOS, E.G. An outline of the climate of Greece, *Publications of the Meteorological Institute of the University of Athens* 6, 51 pp. 1961.

MAYEWSKI, P.A., MEEKER, L.D., TWICKLER, M.S., WHITLOW, S., YANG, Q., LYONS, W.B. & PRENTICE, M. MAJOR features and forcing of high-latitude northern hemisphere atmospheric circulation using a 110,000-year-long glaciochemical series, *Journal of Geophysical Research* 102, 26345-26366, 1997.

MCKIM MALVILLE, J., WENDORF, F., MAZAR, A.A. & SCHILD, R. Megaliths and Neolithic astronomy in southern Egypt, *Nature* 392, 488-491, 1998.

MEEKER, L.D. AND MAYEWSKI, P.A. A 1400 year long record of atmospheric circulation over the North Atlantic and Asia, *Holocene*, in press.

MERCONE, D., J. THOMSON, I.W. CROUDACE, G. SIANI, M. PATERNE & S. TROELSTRA. Duration of S1, the most recent sapropel in the Mediterranean Sea, as indicated by accelerator mass spectroscopy radiocarbon and geochemical evidence. *Paleoceanography* 15, 336-347, 2000.

MERCONE, D., THOMSON, J., ABU-ZIED, R.H., CROUDACE, I.W., AND ROHLING, E.J., High-resolution
geochemical and micropalaeontological profiling of the most recent eastern Mediterranean sapropel, *Mar. Geol., 177*, 25-44, 2001.

MILLER, A.R. Physical Oceanography of the Mediterranean Sea: A discourse. *Rapp. Comm.Int. Mer Médit.*, 17, 857-871, 1963.

MYERS, P., HAINES, K., AND ROHLING, E.J., Modelling the paleo-circulation of the Mediterranean: The last glacial maximum and the Holocene with emphasis on the formation of sapropel S1. *Paleoceanography, 13*, 586-606, 1998.

MYERS, P.G., AND ROHLING, E.J. Modelling a 200 year interruption of the Holocene sapropel S1, *Quat. Res., 53*, 98-104, 2000.

O'BRIEN, S.R., MAYEWSKI, P.A., MEEKER, L.D., MEESE, D.A., TWICKLER, M.S., AND WHITLOW, S.I., Complexity of Holocene climate as reconstructed from a Greenland ice core. *Science* 270, 1962 – 1964, 1995.

ORTIZ, J.D. & MIX, A.C. Comparison of Imbrie-Kipp transfer function and modern analog temperature estimates using sediment trap and core top foraminiferal faunas, *Paleoceanography* 12, 175-190, 1997.

PARISI, E. Carbon and Oxygen isotope composition of *Globerinoides ruber* in two deep sea cores from the Levantine Basin (eastern Mediterranean). *Mar. Geol.* 75, 201-219, 1987.

PATERNE, M., KALLEL, N., LABEYRIE, L., VAUTRAVERS, M., DUPLESSY, J-C., ROSSIGNOL-STRICK, M., CORTIJO, E., ARNOLD, M., AND FONTUGNE, M., Hydrological relationship between the North Atlantic ocean and the Mediterranean during the past 15-75 kyr, *Paleoceanography, 14*, 626-638, 1999.

PERISSORATIS, C. and J.W. PIPER Age, Regional Variation, and Shallowest Occurrence of S1 Sapropel in the Northern Aegean Sea, *Geo-Marine Letters*, 12, 49-53, 1992.

PFLAUMANN, U., DUPRAT, J., PUJOL, C. & LABEYRIE, L.D. SIMMAX: a modern analog technique to deduce Atlantic sea surface temperatures from planktonic foraminifera in deep-sea sediments, *Paleoceanography* 11, 15-35, 1996.

POULOS, S.E., DRAKOPOULOS, P.G. & COLLINS, M.B. Seasonal variability in sea surface oceanographic conditions in the Aegean Sea (eastern Mediterranean): an overview, *Journal of Marine Systems* 13, 225-244, 1997.

PUJOL, A. and C. VERGNAUD GRAZZINI Distribution patterns of live planktic foraminifera as related to regional hydrography and productive systems of the Mediterranean Sea., *Mar. Micropaleontol.*, 25, 187-217, 1995.

REID, J.L. On the contribution of the Mediterranean outflow to the Norwegian-Greenland Sea, *Deep-Sea Research* 26, 1199-1223, 1979.

REISS, Z., HALICZ, E., AND LUZ, B., Late-Holocene foraminifera from the SE Levantine Basin, *Isr. J. Earth Sci., 48*, 1-27, 2000.

RITCHIE, J.C., EYLES, C.H., AND HAYNES, C.V., Sediment and pollen evidence for an early to mid-Holocene humid period in the eastern Sahara, *Nature, 314*, 352-355, 1985.

ROETHER, W. H., MANCA, B. B., KLEIN, B., BREGANT, D., GEORGOPOULOS, D., BEITZEL, V., KOVACEVIC, V. & LUCHETTA, A. Recent changes in eastern Mediterranean deep waters. *Science, 271*, 333-335, 1996.

ROHLING, E.J., P.A. MAYEWSKI, R.H. ABU-ZIED, J.S.L. CASFORD and A. HAYES Holocene atmosphere-ocean interactions: records from Greenland and The Aegean Sea. *Climate Dynamics,* in press 2001.

ROHLING, E.J. Paleosalinity: confidence limits and future applications. *Mar. Geol.*,163, 1-11, 2000.

ROHLING, E.J., and S. DE RIJK Holocene climate optimum and the Last Glacial Maximum in the Mediterranean: the marine oxygen isotope record. *Mar. Geol.*, 153, 57-75. 1999a.

ROHLING, E.J., (1999b). Environmental controls on salinity and $\delta^{18}O$ in the Mediterranean. *Paleoceanography*, 14, 706-715, 1999b.

ROHLING, E.J., HAYES, A., KROON, D., DE RIJK, S. & ZACHARIASSE, W.J. Abrupt cold spells in the NW Mediterranean. *Paleoceanography* 13, 316-322, 1998.

ROHLING, E.J., F.J. JORISSEN and H.C. DE STIGTER 200 year interruption of Holocene sapropel formation in the Adriatic Sea. *J. Micropaleontol.*, 16, 97-108, 1997.

ROHLING, E.J., DEN DULK, M., PUJOL, C., and VERGNAUD-GRAZZINI, C., Abrupt hydrographic change in the Alboran Sea (western Mediterranean) around 8000 yrs BP, *Deep-Sea Research,* 42; 1609-1619, 1995.

ROHLING, E.J. Review and new aspects concerning the formation of eastern Mediterranean sapropels. *Mar. Geol.*, 122, 1-28, 1994.

ROHLING, E.J., JORISSEN, F.J., VERGNAUD-GRAZZINI, C., AND ZACHARIASSE, W.J., Northern

Levantine and Adriatic Quaternary planktic foraminifera; Reconstruction of paleoenvironmental gradients. *Mar. Micropaleontol., 21*, 191-218, 1993a.

ROHLING, E.J., H.C. DE STIGTER, C. VERGNAUD-GRAZZINI and R. ZAALBERG Temporary repopulation by low oxygen tolerant benthic foraminifera within an Upper Pliocene sapropel: Evidence for the role of oxygen depletion in the formation of sapropels. *Mar. Micropaleontol.*, 22, 207-219, 1993b.

ROHLING, E.J. & BRYDEN, H.L. Man-induced salinity and temperature increases in Western Mediterranean Deep Water. *Journal of Geophysical Research* 97, 11191-11198, 1992.

ROHLING, E.J. and F.J. HILGEN The eastern Mediterranean climate at times of sapropel formation: a review. *Geologie en Mijnbouw*, 70, 253-264. 1991.

ROHLING, E.J. and W.W.C. GIESKES Late Quaternary changes in Mediterranean intermediate water density and formation rate. *Paleoceanography* 4, 531-545, 1989.

ROSSIGNOL-STRICK, M. The Holocene climatic optimum and pollen records of Sapropel 1 in the eastern Mediterranean, 9000-6000 BP. Quaternary Science Review, 18, 515-530, 1999.

ROSSIGNOL-STRICK, M.. Paléoclimat de la Méditerranée orientale et de l Asie du Sud-Ouest de 15 000 à 6 000 BP, *Paléorient* 23, 175-186, 1998.

ROSSIGNOL-STRICK, M. Sea-land correlation of pollen records in the eastern Mediterranean for glacial-interglacial transition: biostratigraphy versus radiometric time-scale. *Quaternary Science Review*, 14, 893-915. 1995.

ROSSIGNOL-STRICK, M. Late Quaternary climate in the eastern Mediterranean. *Paléorient*, 19(1), 135-152. 1993.

ROSSIGNOL-STRICK, M. Rainy periods and bottom water stagnation initiating brine concentrations, 1. The Late Quaternary. *Paleoceanography*, 2, 330-360, 1987.

ROSSIGNOL-STRICK, M. Mediterranean Quaternary sapropels: an immediate response of the African monsoon to variation of insolation. *Palaeogeogr., Palaeoclimatol., Palaeocol.*, 49, 237-265, 1985.

ROSSIGNOL-STRICK, M. African monsoons, an immediate response to orbital insolation. *Nature* 304, 46-49, 1983.

ROSSIGNOL-STRICK, M., W. NESTEROFF, P. OLIVE and C. VERGNAUD-GRAZZINI After the deluge: Mediterranean stagnation and sapropel formation. *Nature*, 295, 105-110. 1982.

RYAN, W.B.F., and M.B. CITA Ignorance concerning episodes of ocean-wide stagnation. *Mar. Geol.*, 23, 193-215, 1977.

SAARONI, H., A. BITAN, P. ALPERT & B. ZIV, Continental Polar outbreaks into the Levant and Eastern Mediterranean. *International Journal of Climatology*, 16, 1175-1191, 1996.

SAMUEL, S., K. HAINES, S. JOSEY and P.G. MYERS Response of the Mediterranean Sea Thermohaline circulation to observed changes in the winter wind stress field in the period 1980-1993. *J. Geophys. Res.*, 104(C4), 7771-7784, 1999.

SARNTHEIN, M., KENNET, J.P., CHAPPELL, J., CROWLEY, T., CURRY, W., DUPLESSY, J.C., GROOTES, P., HENDY, I., LAJ, C., NEGENDANK, J., SCHULZ, M., SHACKLETON, N.J., VOELKER, A., and ZOLITSCHKA, B., Exploring late Pleistocene climate variations. *EOS* 81(51), 625-630, 2000.

SHAW, H.F., and G. EVANS The nature, distribution and origin of a sapropelic layer in sediments of the Cilicia Basin, northeastern Mediterranean. *Mar. Geol.,* 61, 1-12. 1984.

SMITH, H.J., FISCHER, H., MASTROIANNI, D., DECK, B. AND WAHLEN, M., Dual modes of the carbon cycle since the Last Glacial Maximum, *Nature 400*, 248-250, 1999.

STANLEY D.J., Mud redepositional processes as a major influence on Mediterranean margin-basin sedimentation. In *Geological Evolution of the Mediterranean Basin*, Ed. D.J.STANLEY and F-C. WEZEL publ. Springer-Verlag, 377-413. 1985.

STANLEY, D.J., AND HAIT, A.K., Deltas, radiocarbon dating, and measurements of sediment storage and subsidence, *Geology, 28*, 295-298, 2000.

STRATFORD, K., R.G. WILLIAMS AND P.G. MYERS. Impact of the circulation on sapropel formation in the eastern Mediterranean. *Global Biogeochemical Cycles*, 14(2), 683-695. 2000.

STUIVER, M., AND BRAZIUNAS, T.F., Atmospheric 14C and century-scale solar oscillations, *Nature, 338*, 405-408, 1989.

STUIVER, M., AND BRAZIUNAS, T.F., Sun, ocean, climate and atmospheric $^{14}CO_2$: an evaluation of causal and spectral relationships, *Holocene, 3*, 289-305, 1993.

STUIVER, M., AND REIMER, P.J., Extended ^{14}C data base and revised Calib 3.0 ^{14}C age calibration program, *Radiocarbon, 35*, 215-230, 1993.

STUIVER, M., P.J. REIMER, E. BARD, J.W. BECK, G.S. BURR, K.A. HUGEN, B. KROMER, F.G. MCCORMAC, J. PLICHT and M. SPURK INTCAL98 radiocarbon age calibration, 24,000-0 cal BP. *Radiocarbon* 40, 1041-1083, 1998.

STUIVER, M., P.M. GROOTES, AND T.F. BRAZIUNAS, The GISP2 18O climate record of the past 16,500 years and the role of the sun, ocean and volcanoes, *Quat. Res. 44*, 341-354, 1995.

STUIVER, M., REIMER, P.J., BARD, E., BECK, J.W., BURR, G.S., HUGHEN, K.A., KROMER, B., MCCORMAC, F.G., VAN DER PLICHT, J., AND SPURK, M., INTCAL98 Radiocarbon Age Calibration, 24,000-0 cal BP, *Radiocarbon, 40*, 1041-1083, 1998.

STUIVER, M.,and P.J. REIMER Extended 14C data base and revised CALIB 3.0 14C age calibration program, *Radiocarbon* 35, 215-230, 1993.

TARGARONA, J. Climatic and Oceanographic evolution of the Mediterranean region over the last glacial-interglacial transition; a palynological approach, *LPP Contributions* 7, 155 pp. 1997.

TARGARONA, J., BOESSEKOOL, K., BRINKHUIS, H., VISSCHER, H., AND ZONNEVELD, K. Land-Sea correlation of events in relation to the onset and ending of sapropel S1: a palynological approach. In TARGARONA, J. (ed) *Climatic and Oceanographic evolution of the Mediterranean region over the last glacial-interglacial transition: a palynological approach, LPP Contributions Series, 7*, Febo, Utrecht, NL, 87-112, 1997.

THEOCHARIS, A., AND GEORGOPOULOS, D., Dense water formation over the Samothraki and Limnos Plateaux in the north Aegean Sea (eastern Mediterranean Sea), *Cont. Shelf Res., 13*, 919-939, 1993.

THEOCHARIS, A., Deep water formation and circulation in the Aegean Sea. *Reports in Meteorology and Oceanography*, H. CHARNOCK (Ed.), 40(I), 335-359, 1989.

THOMSON, J., N.C. HIGGS, T.R.S. WILSON, I.W. CROUDACE, G.J. DE LANGE, P.J.M. VAN SANTVOORT Redistribution and geochemical behaviour of redox-sensitive elements around S1, the most recent eastern Mediterranean sapropel., *Geochim. Cosmochim. Acta*, 59, 3487-3501, 1995.

THUNELL, R.C. and D.F. WILLIAMS Glacial-Holocene salinity changes in the Mediterranean Sea: hydrographic and depositional effects. *Nature*, 338, 493-496, 1989.

THUNELL, R.C., D.F. WILLIAMS and M. HOWELL Atlantic-Mediterranean water exchange during the Late Neogene. *Paleoceanography*, 2, 661-678, 1987.

THUNELL, R.C., Eastern Mediterranean Sea during the last glacial maximum; an 18,000 year BP reconstruction, *Quat. Res., 11*, 353-372, 1979.

THUNELL, R.C. Distribution of recent planktonic foraminifera in surface sediments of the Mediterranean Sea. *Mar. Micropaleontol.*, 3, 147-173, 1978.

THUNELL, R.C., WILLIAMS, D.F., & KENNETT, J.P. Late Quaternary paleoclimatology, stratigraphy, and sapropel history in eastern mediterranean deep-sea sediments. *Marine Micropaleontology* 2, 371-388, 1977.

TRENBERTH, K.E. AND PAOLINO, D.A. JR., The northern hemisphere sea level pressure data set: trends, errors and discontinuities, *Monthly Weather Rev., 106*, 855-872, 1980.

TZEDAKIS, P.C. The last climatic cycle at Kopais, Central Greece. *J. Geol. Soc. London,* 156, 425-434, 1999.

VAN GEEL, B., RASPOPOV, O.M., RENSSEN, H., VAN DER PLICHT, J., DERGACHEV, V.A., AND MEIJER, H..A.J., The role of solar forcing upon climate change, *Quat. Sci. Rev., 18*, 331-338, 1999.

WILLIAMS, D.F., R.C. THUNELL and J.P. KENNET Periodic fresh-water flooding and stagnation of the eastern Mediterranean Sea during the late Quaternary *Science*, 201, 252-254, 1978.

WÜST, G. On the vertical circulation of the Mediterranean Sea. *J. Geophys. Res.*, 66(10), 3261-3271, 1961.

YÜCE, H. North Aegean Water Masses. *Estuarine, Coastal and Shelf Science*, 41, 325-343, 1995.

ZACHARIASSE, W J., JORISSEN, F.J., PERISSORATIS, C., ROHLING, E.J. & TSAPRALIS, V. Late Quaternary foraminiferal changes and the nature of sapropel S1 in Skopelos Basin. *Proceedings 5th Hellenic symposium on Oceanography and Fisheries, Kavalla, Greece, 15-18 April 1997* 1, 391-394, 1997.

ZHANG, H.C., MA, Y.Z., WÜNNEMANN, B., AND PACHUR, H J., A Holocene climatic record from arid northwestern China, *Palaeogeogr. Palaeoclimatol., Palaeoecol., 162*, 389-401, 2000.

ZHANG, X.Y., ARIMOTO, R., AN, Z.S., CHEN, T., ZHANG, G.Y., SHU, G. AND WANG, X.F., Atmospheric trace elements over source regions of Chinese dust: Concentrations, sources and atmospheric input to the Loess plateau, *Atmospheric Environment, 27A*, 2051-2067, 1993.

ZIELINSKI, G., AND GERMANI, M.S., New ice-core evidence challenges the 1620s BC age for the Santorini (Minoan) eruption, *J. Archaeol. Sci., 25*, 279-289, 1998.

Other publication in the same field, not submitted for examination

ROHLING, E.J., CASFORD, J., ABU-ZIED, R., COOKE, S., MERCONE, D., THOMSON, J., CROUDACE, I., JORISSEN, F.J., BRINKHUIS, H., KALLMEYER, J., AND WEFER, G., Rapid Holocene climate changes in the eastern Mediterranean, in F. Hassan (ed.) Droughts, Food and Culture: Ecological Change and Food Security in Africa's Later Prehistory, Plenum Press, London, in press 2001.